



NRL/MR/6180--20-10,062

# Surfactant Monolayers at Heptane-water Interfaces

XIAOHONG ZHUANG

RAMAGOPAL ANANTH

*Naval Technology Center for Safety and Survivability Branch  
Chemistry Division*

May 26, 2020

# REPORT DOCUMENTATION PAGE

*Form Approved*  
*OMB No. 0704-0188*

Public reporting burden for this collection of information is estimated to average 1 hour per response, including the time for reviewing instructions, searching existing data sources, gathering and maintaining the data needed, and completing and reviewing this collection of information. Send comments regarding this burden estimate or any other aspect of this collection of information, including suggestions for reducing this burden to Department of Defense, Washington Headquarters Services, Directorate for Information Operations and Reports (0704-0188), 1215 Jefferson Davis Highway, Suite 1204, Arlington, VA 22202-4302. Respondents should be aware that notwithstanding any other provision of law, no person shall be subject to any penalty for failing to comply with a collection of information if it does not display a currently valid OMB control number. **PLEASE DO NOT RETURN YOUR FORM TO THE ABOVE ADDRESS.**

<b>1. REPORT DATE (DD-MM-YYYY)</b> 26-05-2020			<b>2. REPORT TYPE</b> NRL Memorandum Report			<b>3. DATES COVERED (From - To)</b> 21-02-2018 – 20-02-2020		
<b>4. TITLE AND SUBTITLE</b>  Surfactant Monolayers at Heptane-water Interfaces						<b>5a. CONTRACT NUMBER</b>		
						<b>5b. GRANT NUMBER</b>		
						<b>5c. PROGRAM ELEMENT NUMBER</b>		
<b>6. AUTHOR(S)</b>  Xiaohong Zhuang and Ramagopal Ananth						<b>5d. PROJECT NUMBER</b>		
						<b>5e. TASK NUMBER</b>		
						<b>5f. WORK UNIT NUMBER</b> 6A70/1P02		
<b>7. PERFORMING ORGANIZATION NAME(S) AND ADDRESS(ES)</b>  Naval Research Laboratory 4555 Overlook Avenue, SW Washington, DC 20375-5320						<b>8. PERFORMING ORGANIZATION REPORT NUMBER</b>  NRL/MR/6180--20-10,062		
<b>9. SPONSORING / MONITORING AGENCY NAME(S) AND ADDRESS(ES)</b>  Office of Naval Research One Liberty Center 875 N. Randolph Street, Suite 1425 Arlington, VA 22203-1995						<b>10. SPONSOR / MONITOR'S ACRONYM(S)</b>  ONR/SERDP		
						<b>11. SPONSOR / MONITOR'S REPORT NUMBER(S)</b>		
<b>12. DISTRIBUTION / AVAILABILITY STATEMENT</b>  <b>DISTRIBUTION STATEMENT A:</b> Approved for public release; distribution is unlimited.								
<b>13. SUPPLEMENTARY NOTES</b>								
<b>14. ABSTRACT</b>  To develop fluorine-free aqueous foam for effective fire suppression, molecular dynamics (MD) simulations are performed to study the effect of structure of surfactants on the surfactant monolayer properties at the heptane/water interfaces. The results show that the hydroxyl-capped trisiloxane is a better candidate than methoxyl-capped trisiloxane; the alkylglucoside with hydrocarbon length of 8 or 9 may be best candidate; the $\beta$ - and ( $\alpha$ , $\beta$ -1>4)-alkyl glucoside are much better candidate than the $\alpha$ - and ( $\alpha$ , $\beta$ -1>6)-alkyl glucoside; the neutral charged hydrocarbon surfactants have lower heptane transport rate (less heptane in the interface region) than that of the charged hydrocarbon. Two Glucopon-based hydrocarbon surfactants g215 and g225 have very similar interface properties; trisiloxane with oxyethylene length of 7 or 8 have lower heptane transport rate than the length of 11.								
<b>15. SUBJECT TERMS</b>  Molecular dynamics      Surfactant monolayer Oxyethylene length      Hydrocarbon length								
<b>16. SECURITY CLASSIFICATION OF:</b>				<b>17. LIMITATION OF ABSTRACT</b>	<b>18. NUMBER OF PAGES</b>	<b>19a. NAME OF RESPONSIBLE PERSON</b> Ramagopal Ananth		
<b>a. REPORT</b> Unclassified Unlimited	<b>b. ABSTRACT</b> Unclassified Unlimited	<b>c. THIS PAGE</b> Unclassified Unlimited		Unclassified Unlimited	67	<b>19b. TELEPHONE NUMBER (include area code)</b> (202) 767-3197		

This page intentionally left blank.

## CONTENTS

EXECUTIVE SUMMARY .....	vii
<b>0. SYMBOLS</b> .....	1
<b>1. INTRODUCTION</b> .....	1
<b>2. ABJECTIVE</b> .....	2
<b>3. APPROACH</b> .....	2
<b>4. RESULTS</b> .....	3
<b>4.1 Polyoxyethylenated Trisiloxane with Varied Oxyethylene Unit Length</b> .....	4
4.1.1 Surfactant Chemical Structure .....	4
4.1.2 Surface Area per Molecule ( $A$ ) .....	5
4.1.3 Interfacial Thickness of Water ( $d_w$ ) and Heptane ( $d_h$ ).....	5
4.1.4 Heptane to Surfactant Ratio ( $hsr$ ) and Heptane Surface Number Density ( $hsnd$ ).....	7
4.1.5 Volumetric Number Densities ( $msnd^{-1}$ and $hvnd$ ).....	8
4.1.6 Intermolecular Hydrogen Bond .....	9
<b>4.2 Polyoxyethylenated Trisiloxane with Varied Types of Head Terminal Group</b> .....	10
4.2.1 Surfactant Chemical Structure .....	11
4.2.2 Surface Area per Molecule ( $A$ ) .....	11
4.2.3 Interfacial Thickness of Water ( $d_w$ ) and Heptane ( $d_h$ ).....	11
4.2.4 Heptane to Surfactant Ratio ( $hsr$ ) and Heptane Surface Number Density ( $hsnd$ ).....	12
4.2.5 Volumetric Number Densities ( $msnd^{-1}$ and $hvnd$ ).....	13
4.2.6 Intermolecular Hydrogen Bonds.....	14
<b>4.3 Polyalkylglucoside with Varied Hydrocarbon Unit Length Dependence</b> .....	15
4.3.1 Surfactant Chemical Structure .....	15
4.3.2 Surface Area per Molecule ( $A$ ) .....	15
4.3.3 Interfacial Thickness of Water ( $d_w$ ) and Heptane ( $d_h$ ).....	16
4.3.4 Heptane to Surfactant Ratio ( $hsr$ ) and Heptane Surface Number Density ( $hsnd$ ).....	17
4.3.5 Volumetric Number Densities ( $msnd^{-1}$ and $hvnd$ ).....	18
4.3.6 Intermolecular Hydrogen Bonds.....	18
<b>4.4 Alkylglucoside Configuration and Linkage Dependence</b> .....	19
4.4.1 Surfactant Chemical Structure .....	19
4.4.2 Surface Area per Molecule ( $A$ ) and Interfacial Thicknesses ( $d_w, d_h$ ) .....	20
4.4.3 Heptane to Surfactant Ratio ( $hsr$ ) and Number Densities ( $hsnd, msnd^{-1}, hvnd$ ) .....	20
4.4.4 Intermolecular Hydrogen Bonds.....	21

<b>4.5 Siloxane with Varied Head and Tail Group</b> .....	21
4.5.1 Surfactant Chemical Structure .....	21
4.5.2 Surface Area per Molecule ( $A$ ) and Interfacial Thicknesses ( $d_w, d_h$ ) .....	23
4.5.3 Heptane to Surfactant Ratio ( $hsr$ ) and Number Densities ( $hsnd, msnd^{-1}, hvnd$ ) .....	23
4.5.4 Intermolecular Hydrogen Bonds .....	24
<b>4.6 Pure Hydrocarbon surfactant with varied charged head groups</b> .....	24
4.6.1 Surfactant Chemical Structure .....	24
4.6.2 Surface Area per Molecule ( $A$ ) and Interfacial Thicknesses ( $d_w, d_h$ ) .....	25
4.6.3 Heptane to Surfactant Ratio ( $hsr$ ) and Heptane Surface Number Density ( $hsnd$ ) .....	26
4.6.4 Volumetric Number Densities ( $msnd^{-1}$ and $hvnd$ ) .....	27
<b>4.7 Surfactant Mixtures with Varied Molecular (Molar) Fraction</b> .....	27
4.7.1 Surfactant Chemical Structure .....	27
4.7.2 Surface Area per Molecule ( $A$ ) .....	28
4.7.3 Interfacial Thicknesses ( $d_w, d_h$ ) .....	29
4.7.4 Heptane to Surfactant Ratio ( $hsr$ ) and Heptane Surface Number Density ( $hsnd$ ) .....	30
4.7.5 Volumetric Number Densities ( $msnd^{-1}$ and $hvnd$ ) .....	30
4.7.6 Intermolecular Hydrogen Bonds .....	31
<b>4.8 Commercial Surfactants</b> .....	32
4.8.1 Surfactant Chemical Structure .....	32
4.8.2 Surface Area per Molecule ( $A$ ) .....	33
4.8.3 Interfacial Thicknesses ( $d_w, d_h$ ) .....	34
4.8.4 Heptane to Surfactant Ratio ( $hsr$ ) and Heptane Surface Number Density ( $hsnd$ ) .....	35
4.8.5 Comparison of $msnd^{-1}$ and $hvnd$ to Experimental Heptane Diffusion Coefficient .....	36
4.8.6 Comparison of Surfactants Packing .....	39
<b>5. CONCLUSION</b> .....	40
<b>6. FUTURE WORK</b> .....	42
<b>7. ACKNOWLEDGEMENTS</b> .....	42
<b>8. PERSONNEL</b> .....	42
<b>9. REFERENCES</b> .....	42
<b>10. APPENDIX A</b> .....	43

## FIGURES

Fig. 1 .....	3
Fig. 2 .....	4
Fig. 3 .....	5
Fig. 4 .....	6
Fig. 5 .....	7
Fig. 6 .....	8
Fig. 7 .....	8
Fig. 8 .....	9
Fig. 9 .....	10
Fig. 10 .....	11
Fig. 11 .....	12
Fig. 12 .....	13
Fig. 13 .....	14
Fig. 14 .....	15
Fig. 15 .....	15
Fig. 16 .....	16
Fig. 17 .....	17
Fig. 18 .....	17
Fig. 19 .....	18
Fig. 20 .....	19
Fig. 21 .....	19
Fig. 22 .....	20
Fig. 23 .....	21
Fig. 24 .....	21
Fig. 25 .....	22
Fig. 26 .....	23
Fig. 27 .....	24
Fig. 28 .....	24
Fig. 29 .....	25
Fig. 30 .....	26
Fig. 31 .....	26
Fig. 32 .....	27
Fig. 33 .....	28
Fig. 34 .....	28
Fig. 35 .....	29
Fig. 36 .....	30
Fig. 37 .....	31
Fig. 38 .....	32
Fig. 39 .....	34
Fig. 40 .....	35
Fig. 41 .....	36
Fig. 42 .....	38
Fig. 43 .....	39
Fig. 44 .....	40

This page intentionally left blank.

## EXECUTIVE SUMMARY

The molecular dynamics (MD) simulations are performed to study the effect of structure of surfactants on the surfactant monolayer properties at the heptane/water interfaces. We varied the structure of surfactants and compare the interfacial properties in order to search possible good candidate that can be effective enough for fire suppression and be MilSpec-qualified. From the MD simulations, the interfacial properties such as the surface area per molecule ( $A$ ), interfacial thicknesses of water ( $d_w$ ) and heptane ( $d_h$ ), the heptane to surfactant ratio ( $hsr$ ), the heptane surface number density ( $hsnd$ ), the inverse of maximum surfactant number density ( $msnd^{-1}$ ), the heptane volumetric number density ( $hvnd$ ), hydrogen bond number per molecule ( $hbnm$ ) and hydrogen bond number per  $\text{\AA}^2$  ( $hbna$ ) are calculated. The  $d_w$  and  $hbnm$  are the properties of the hydrophilic head group, and  $d_h$ ,  $hsr$ ,  $msnd^{-1}$ , and  $hvnd$  are the properties of the hydrophobic tail. The  $hbnm$  is related to stability of the head group, while the  $hsr$ ,  $msnd^{-1}$  and  $hvnd$  are related to heptane transport rate in the tail.

The key aspects of variation of structures that we are interested are tested, and the detail results are presented in this report. The key conclusions are that hydroxyl-capped trisiloxane have smaller heptane to surfactant ratio ( $hsr$ ) and inverse of maximum surfactants number density ( $msnd^{-1}$ ) than methoxyl-capped trisiloxane, which suggests that hydroxyl-capped trisiloxane is a better candidate. By varying the alkyl glucoside length  $n$ , the result that the alkyl glucoside with  $n \geq 9$  would have lower  $msnd^{-1}$  and  $hvnd$ , and also higher  $hbnm$ , which make  $n \geq 9$  good candidate. The  $\beta$ - and ( $\alpha, \beta$ -1 $\rightarrow$ 4)-alkylglucoside have significantly smaller  $hsr$ ,  $hvnd$ , thus better candidate than the ones with  $\alpha$ - and ( $\alpha, \beta$ -1 $\rightarrow$ 6) linkage. The 2k3s and 2k3t have smaller  $hvnd$  and greater  $hbnm$  than other siloxanes which make them good candidate. The neutral charged or zwitterionic hydrocarbon surfactants have lower heptane number density than that of the charged ones. By studying the commercial surfactants, we conclude that two GlucoPON-based hydrocarbon surfactants g215 and g225 have very similar interface properties. Among the commercial surfactant, capstone and capstone/g215e have the minimum  $hvnd$  which agrees with the experimental heptane diffusion rate of AFFF. Among the pure trisiloxane and trisiloxane/alkylglucoside studied, the H8 and H8/g225 have the minimum  $d_h$ ,  $hsr$  and also  $msnd^{-1}$  and  $hvnd$ .

This page intentionally left blank.

# Surfactant Monolayers at Heptane-Water Interface

## 0. SYMBOLS

Surface Area per Molecule ( $A$ )

Interfacial Thickness of Water ( $d_w$ )

Interfacial Thickness of Heptane ( $d_h$ )

Heptane to Surfactant Ratio ( $hsr$ ), i.e., number of heptane molecule per surfactant molecule

Heptane Surface Number Density per Angstrom square ( $hsnd$ , where  $hsnd=hsr/A$ )

Maximum Surfactants volumetric Number Density ( $msnd$ )

Inverse of the Maximum Surfactants volumetric Number Density ( $msnd^{-1}$ )

Heptane Volumetric Number Density ( $hvnd$ ) at  $msnd$

Hydrogen Bond Number per Molecule between surfactants ( $hbnm$ )

Hydrogen Bond Number per Angstrom square between surfactants ( $hbna$ , where  $hbna=hbnm/A$ )

## 1. INTRODUCTION

To develop fluorine-free surfactants for effective fire suppression, molecular dynamics (MD) simulations are performed to study the effect of surfactant structure on the properties of monolayers at the heptane/water interface. The polyoxyethylenated nonionic surfactants in the form of  $R(OC_2H_4)_nX$ , where R is hydrophobic tail, X is the capping terminal group of hydrophilic head, and  $n$  is number of oxyethylene unit, have been extensively studied and widely used. However, there are quite limited information on the characterization of interfacial properties of the monodispersed surfactants due to the difficulty of the purification to obtain a single oxyethylene chain length during synthesis. Experiment results from our lab showed that the mixture of the commercial polyoxyethylenated trisiloxane surfactant 502W (mixture with unknown oxyethylene lengths and ratio) and GlucoPON 225 (mixture with 1 and 2 glucoside and hydrocarbon length about 8~10) with ratio 2:3 can suppress heptane fire reasonably effective, but still not able to be MilSpec-qualified.

Therefore, we varied the structures of surfactants and compare the interfacial properties in order to search possible good candidate that can be effective enough for fire suppression and be MilSpec-qualified. **Firstly**, we are interested on how the variation of oxyethylene chain length of trisiloxane surfactant impact the interfacial properties of surfactant monolayer. By applying the simulation method that we developed previously, we simulate the surfactant monolayer of pure polyoxyethylenated trisiloxane, trisiloxane/1g9, trisiloxane/2g9, trisiloxane /1g9/2g9 with varied oxyethylene chain length ( $n=2\sim 20$ ). **Secondly**, by comparing the hydroxyl-capped and methoxyl-capped trisiloxane, we simulate the surfactant monolayer of pure hydroxyl-capped and methoxyl-capped polyoxyethylenated trisiloxane, trisiloxane /1g9, and trisiloxane /2g9 with varied oxyethylene chain length ( $n=6\sim 13$ ). **Thirdly**, the experiment also shows that the hydrocarbon length of glucoside may affect the aqueous foam stability and fuel transport rate, therefore, the effect of the hydrocarbon length of glucoside on the interfacial properties of surfactant monolayer

are also studied. We simulate the surfactant monolayer of pure glucoside and trisiloxane(X=OH,  $n=11$ )/glucoside with varied hydrocarbon chain length ( $n=5\sim 12$ ). **Fourthly**, we test the effect of configuration ( $\alpha$ ,  $\beta$ ) and linkage of glucoside ( $1\rightarrow 4$ ,  $1\rightarrow 6$ ). **Fifthly**, the different head and tail group of siloxane surfactant, by comparing the linear carbohydrate and ring-structured glucoside head group, and also linear and branched siloxane tail group. **Sixthly**, the hydrocarbon with varied charged head group are simulated to study the charge effect, which including nonionic, negative and positive charged hydrocarbon surfactants. **Seventhly**, we study the fraction effect on capstone/alkylglucoside and trisiloxane H10/alkylglucoside (1g9, 2g9) by varying the fraction of capstone and trisiloxane (0.0, 0.2, 0.4, 0.5, 0.6, 0.8, and 1.0). **Eighthly**, by studying the commercial surfactants, we compare the interfacial properties of pure perfluorocarbon surfactants (pfoa and capstone), trisiloxane surfactants (M7, M8, H7, H8, H11), and GlucoPON-based (mimicking) hydrocarbon surfactants (g215 and g225). Moreover, the capstone/g215 and trisiloxane/g225 and trisiloxane/g225 mixture are also simulated. The calculated  $msnd^{-1}$  and  $hvn d$  of surfactants are compared to experimental heptane diffusion coefficient.

## 2. OBJECTIVE

To develop fluorine-free aqueous foam for effective fire suppression, molecular dynamics (MD) simulations are performed to study the effect of structure of surfactants on the surfactant monolayer properties at the heptane/water interfaces. From the MD simulations, the interfacial properties such as the surface area per molecule ( $A$ ), interfacial thicknesses of water ( $d_w$ ) and heptane ( $d_h$ ), the heptane to surfactant ratio ( $hsr$ ), the heptane surface number density ( $hsnd$ ), the inverse of maximum surfactant volumetric number density ( $msnd^{-1}$ ), the heptane volumetric number density ( $hvn d$ ), hydrogen bond number per molecule ( $hbnm$ ) and hydrogen bond number per  $\text{\AA}^2$  ( $hbna$ ) are calculated. The  $d_w$  and  $hbnm$  are the properties of the hydrophilic head group, and  $d_h$ ,  $hsr$ ,  $msnd^{-1}$ , and  $hvn d$  are the properties of the hydrophobic tail, while the  $hsnd$  and  $hbna$  are the additional cross-sectional unit area properties calculated to compare to unit molecule properties ( $hsr$  and  $hbnm$ ), respectively. The  $hbnm$  is related to stability of the head group, while the  $msnd^{-1}$  and  $hvn d$  are related to heptane transport rate in the tail. The  $hsr$  is related to both stability and heptane transport rate in the tail.

## 3. APPROACH

MD simulations are performed on the heptane/surfactant-monolayer/water interface (**Fig. 1**) with constant number of molecules, pressure and temperature ( $NPT$ ) ensemble using an orthorhombic box ( $\alpha=\beta=\gamma=90.0^\circ$ ,  $L_x\neq L_y\neq L_z$ ) with a hexagonal close packing as initial conditions. The initial set up is generated from a fixed total number of surfactant molecules,  $N_s=36$  (6 by 6 array). The initial values of the area per surfactant molecule  $A_i$  are given. (The area per molecule will change with time and reach a steady-state value for  $A$  at the end of simulation.) We then take the water and heptane layer from the large pure systems with dimensions the same as the surfactant monolayer ( $L_x$  and  $L_y$ ). We appended the water and heptane layers in such a way that half of the head and tail groups of the surfactants overlapped with the water and heptane layers respectively. The thickness of the water and heptane layers are selected so that the tail end of the surfactant monolayers do not interact with each other. The total thickness  $L_{zi}$  is the summation of the initial water layer thickness  $L_{wi}$  and the initial heptane thickness  $L_{hi}$ , and the half of the surfactant length,

i.e.  $Lz_i = Lw_i + 2Lh_i + L_s/2$ . For each run, we start with 10000 steps of energy minimization, and then equilibrate with  $NVT$  ensemble for 0.05 ns with the time step of 1.0 fs, followed by another equilibration with  $NPT$  ensemble for 0.6 ns with the time step 2.0 fs. Eventually, we run MD simulations with  $NPT$  ensemble for 100.0 ns with the time step of 2.0 fs at 25°C and 60°C. Each simulation is run with three replicates to obtain average and standard deviation of each properties calculated. For two-component and three-component surfactant monolayer, the distribution of components are random in each replicate to get a good statistics.

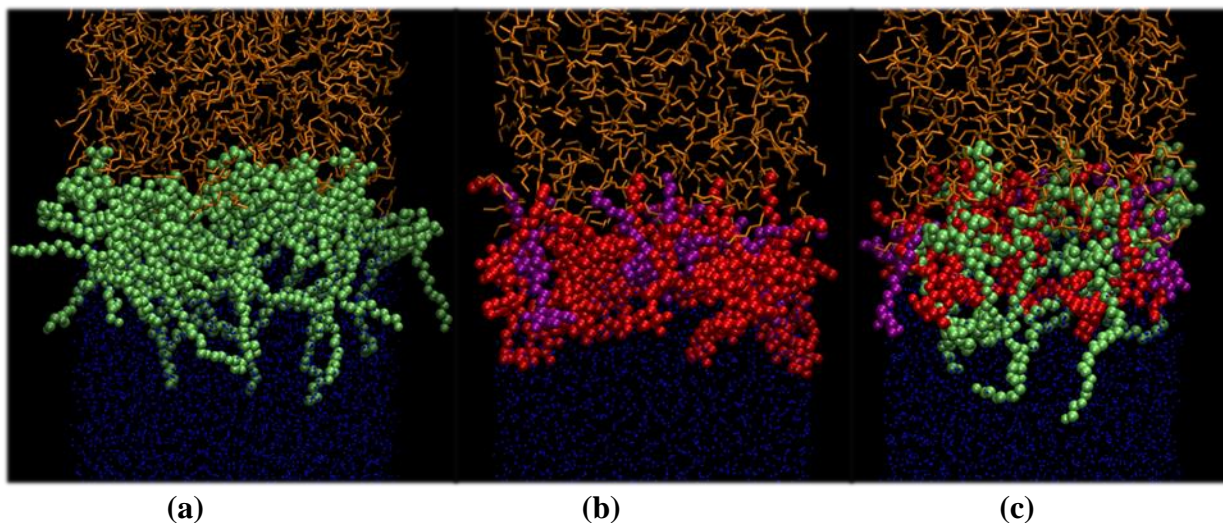


Fig. 1

(a) The pure polyoxyethyleneated trisiloxane ( $X=OH$ ,  $n=8$ ) (b) the 1g9/2g9 two-component surfactant monolayer with ration 3:7 (c) trisiloxane ( $X=OH$ ,  $n=8$ )/1g9/2g9 three-component surfactant monolayer at the heptane/water interface system at the end of the MD simulations, respectively. (Water is not shown for image clarity, heptane as orange lines, and trisiloxane surfactant are shown in cyan spheres.) 1g9 are shown in purple spheres, and 2g9 are shown in red spheres. Only the top half in the  $z$  direction of the simulation setup are shown, the bottom half is nearly a mirror image of the top one.

#### 4. RESULTS

**Note:** There is a hypothesis that the calculated property such as  $hbnm$  is related to stability of the surfactant monolayer; the higher  $hbnm$ , the more stable the surfactant monolayer in the head group region. The properties  $msnd^{-1}$  and  $hvnd$  are related to heptane transport rate; the lower  $msnd^{-1}$  and  $hvnd$ , the lower the heptane transport rate. The  $hsr$  may be related to both the stability and heptane transport rate; the higher the  $hsr$ , the lower the stability, and the higher the heptane transport rate. The  $msnd^{-1}$  determines the transport channel size, and  $hsr$  determine the heptane source in the monolayer tail region. Therefore, in order to have low heptane transport rate, either the low  $msnd^{-1}$  or low  $hsr$  is needed. The  $hbnm$  describes the stability in the head region, while the  $hsr$  is related to the stability in the tail region. Therefore, in order to have high stability, both the high  $hbnm$  and low  $hsr$  are needed. The  $hvnd$  directly describes the heptane transport rate, however, it is a smaller value with higher fluctuation compared to  $msnd^{-1}$  and  $hsr$ . Therefore, the  $hvnd$  is a more direct but

potential a less reliable/accurate reference to describe heptane transport rate. The properties  $A$ ,  $d_w$ ,  $d_h$ , are the properties that indicating the overall molecular size, the strength of hydrogen bonding in the head group and hydrophobic interaction strength in the tail, and the water and heptane penetration distance. The  $hbna$  and  $hsnd$  are the cross-sectional unit area properties may also be related to monolayer stability and heptane transport.

## 4.1 Polyoxyethylenated Trisiloxane with Varied Oxyethylene Unit Length

### 4.1.1 Surfactant Chemical Structure

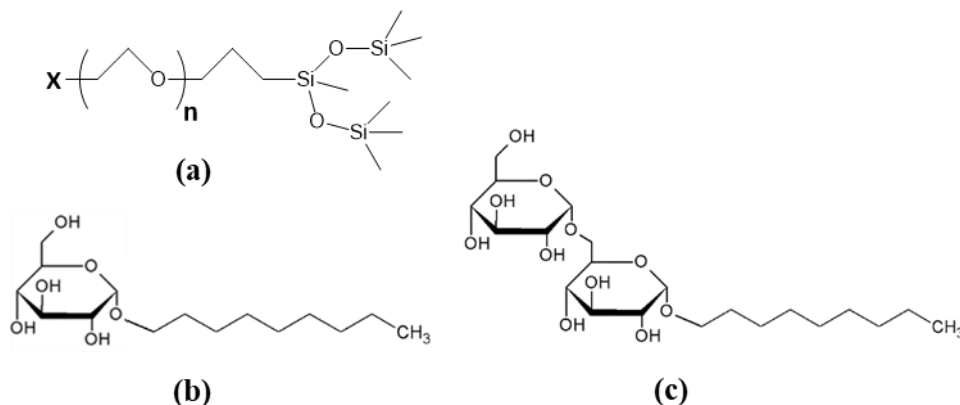


Fig. 2

(a) Chemical Structure of polyoxyethylenated trisiloxane (existing in commercial trisiloxane 502W), X is OH,  $n$  is oxyethylene length in the range between 2 to 20 (b) alkylglucoside 1g9 (existing in commercial Glucopon) with one glucoside head group and hydrocarbon length of 9 and (c) alkyl glucoside 2g9 (also existing in commercial Glucopon) with two glucosides head group 1→6 glucoside linkage and hydrocarbon length of 9.

The chemical structure of polyoxyethylenated trisiloxane surfactant and hydrocarbon surfactant with one and two glucoside head group are shown in **Fig. 2**. Three types of monolayer systems with total of 36 molecules per monolayer are simulated. **Firstly**, pure trisiloxane with a terminal hydroxyl (OH) group and varied oxyethylene length ( $n=3\sim 20$  at 25 °C, and  $n=4\sim 20$  at 60 °C). **Secondly**, two-component trisiloxane/1g9 and trisiloxane/2g9 systems with varied oxyethylene length of trisiloxane ( $n=2\sim 20$  at 25 °C). **Thirdly**, three-component trisiloxane/1g9/2g9 systems with varied oxyethylene length of trisiloxane ( $n=2\sim 20$  at 60 °C). The experimental measurement shows that the fire suppression performance is best when the ratio of trisiloxane to Glucopon is 2:3, which is applied in the simulations. In the two-component systems, the molecular number ratio of trisiloxane:1g9 and trisiloxane:2g9 is 2:3, i.e. in each monolayer, there are 14 trisiloxane, and 22 1g9 or 22 2g9. Glucopon 225 is a commercial Glucopon with one and two glucoside head, and hydrocarbon tail ranges from 8~10, the averaged value 9 is used in our simulation. The average number of glucosides in Glucopon 225 is 1.7, which gives ratio of 1g9:2g9=3:7. Therefore, to mimic Glucopon 225 behavior in the three-component systems, in each monolayer, the numbers of trisiloxane, 1g9, and 2g9 are 14, 7, and 15, respectively. Also,

1g9:2g9=1:1 for Glucopton 215, in each monolayer of the three-component systems, the numbers of trisiloxane, 1g9, and 2g9 are 14, 11, and 11, respectively.

#### 4.1.2 Surface Area per Molecule ( $A$ )

The surface area per molecule is calculated by dividing total cross-sectional area by the total number of surfactant 36, i.e.  $A = A_{tot}/36$ . Previous studies reported that the ratio of surface area per molecule of polyoxyethylenated surfactant ( $A$ ) and the square root of oxyethylene unit number ( $\sqrt{n}$ ) is constant, i.e., there is the correlation  $A = k \times \sqrt{n}$  for specific type of surfactant at air/water interface [1-3]. For an example, the value of  $k$  for a polyoxyethylenated hydrocarbon surfactant  $C_{12}H_{25}(OC_2H_4)_nOH$  is between 21.7-24.8 at 25 °C [3]. As shown in **Fig. 3a**, for hydroxyl-capped polyoxyethylenated trisiloxane at heptane/water interface, there is a similar linear correlation that  $A = k \times \sqrt{n} + b$ , where  $k$  and  $b$  values are  $9.2 \pm 0.1$  and  $48.4 \pm 0.5$  at 25 °C, and they are  $10.6 \pm 0.3$  and  $47.3 \pm 1.0$  at 60 °C, respectively. Moreover, with the same oxyethylene unit number  $n$ , the surface areas of pure trisiloxane at 60 °C are generally greater than the values at 25 °C due to more atomic movement at higher temperature. The differences are slightly greater at high oxyethylene length. The surface area per molecule  $A$  of pure trisiloxane increases as  $n$  increases, while for trisiloxane/1g9 and trisiloxane/2g9, the  $A$  increase slightly and then level off. The  $A$  of pure trisiloxane are much greater than the values of trisiloxane/1g9 and trisiloxane/2g9, and the difference is greater at large  $n$  at 25 °C (**Fig. 3b**). Similar trend is observed in pure trisiloxane and three-component trisiloxane/1g9/2g9 systems at 60 °C (**Fig. A1**). It suggests that pure trisiloxane is much more sensitive to oxyethylene length than the mixture systems when  $n$  is large.

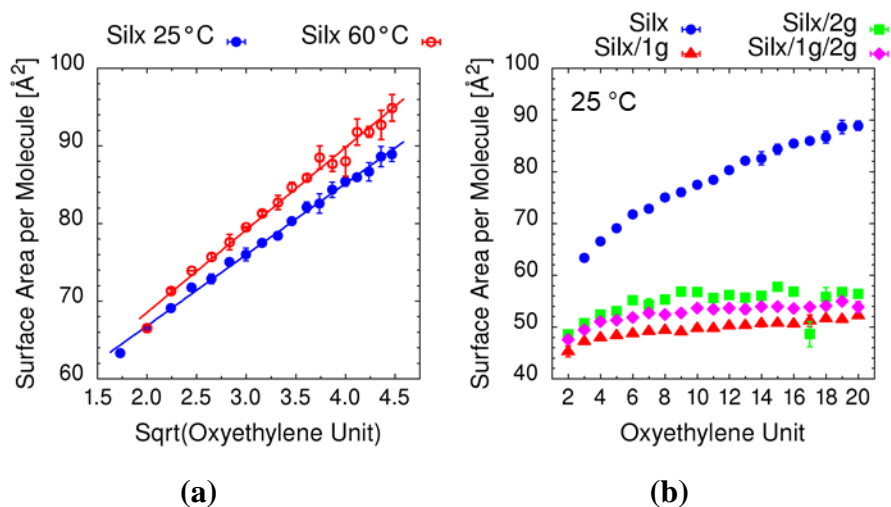


Fig. 3

(a) The surface area per molecule of pure trisiloxane at 25 °C and 60 °C as function of square root of oxyethylene length. (b) The surface area per molecule of pure trisiloxane, trisiloxane/1g9, trisiloxane/2g9, and trisiloxane/1g9/2g9 at the heptane/surfactant-monolayer/water interface at 25 °C as function of trisiloxane oxyethylene length.

#### 4.1.3 Interfacial Thickness of Water ( $d_w$ ) and Heptane ( $d_h$ )

**Mass Density Profile** Mass density profile of each component (trisiloxane, alkylglucoside, water, and heptane) is calculated based on atomic number density of each individual atoms. The heptane/surfactant-monolayer/water system in the normal  $z$  direction are divided into small bins with bin size  $0.2 \text{ \AA}$ , and then add up the bins of same molecule to obtain the atomic number density of each component. Based on atomic mass, the mass density profile for each component are obtained as shown in **Fig. 4a**. Then, the interfacial thicknesses of water ( $d_w$ ) and heptane ( $d_h$ ), and also the heptane to surfactant ratio in the interface ( $hsr$ ) are calculated based on the mass density profile. Interfacial thickness of water  $d_w$  is defined as the distance between the 10% to 90% mass density of water. Interfacial thickness of heptane  $d_h$  is defined as the distance between the 10% to 90% mass density of heptane, as shown in **Fig. 4b**. The  $hsr$  is the ratio of number of heptane molecule to number of surfactant molecule in the interface, which is the region between 90% and 90% of the bulk heptane density.

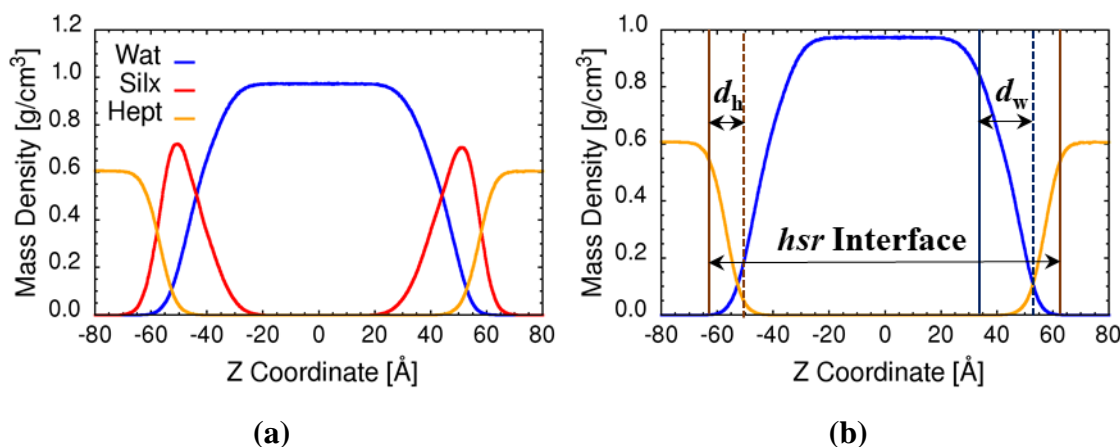


Fig. 4

(a) Mass density profile, and the interface used to calculate interfacial thicknesses and heptane to surfactant ratio ( $hsr$ ) of trisiloxane H8 at  $60 \text{ }^\circ\text{C}$  (b) Schematic plots indicating the definition of interfacial thicknesses of water, heptane and  $hsr$  interface, respectively.

The interfacial thickness of water  $d_w$  increases as trisiloxane oxyethylene  $n$  increases as expected at both  $25 \text{ }^\circ\text{C}$  (**Fig. 5a**) and  $60 \text{ }^\circ\text{C}$  (**Fig. A2a**). The  $d_w$  of pure trisiloxane are very similar at  $25 \text{ }^\circ\text{C}$  and  $60 \text{ }^\circ\text{C}$  which indicate weak temperature dependence. The pure trisiloxane have the greatest  $d_w$ , while the two-component trisiloxane/1g9 and trisiloxane/2g9 and the three-component trisiloxane/1g9/2g9 have similar and smaller  $d_w$ . Generally, the interfacial thickness of heptane  $d_h$  of all systems increases slightly with  $n$  when  $n \geq 9$ , but the  $n$  dependence is weak. Unlike the  $d_w$ , the  $d_h$  of pure trisiloxane are smaller at  $25 \text{ }^\circ\text{C}$  than  $60 \text{ }^\circ\text{C}$  which indicate strong temperature dependence. The pure trisiloxane have generally smaller  $d_h$  than trisiloxane/1g9, trisiloxane/2g9, and trisiloxane/1g9/2g9 at large  $n$  (**Fig. 5b**, **Fig. A2b**), the difference is greater at 2g9 at  $60 \text{ }^\circ\text{C}$ .

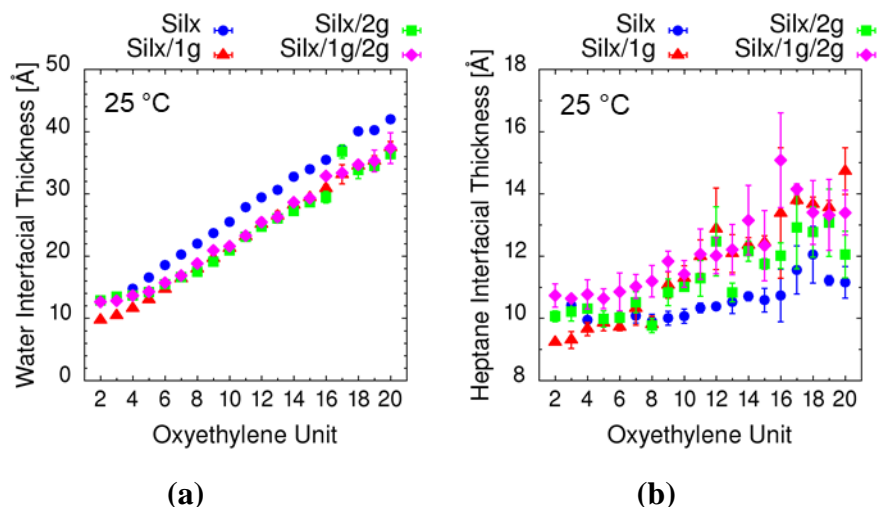


Fig. 5

The interfacial thickness of (a) water (b) heptane of pure trisiloxane, trisiloxane/1g9, trisiloxane/2g9, and trisiloxane/1g9/2g9 at 25 °C as function of trisiloxane oxyethylene length.

#### 4.1.4 Heptane to Surfactant Ratio ( $hsr$ ) and Heptane Surface Number Density ( $hsnd$ )

The region between 90% and 90 % of the bulk heptane density is used to calculate heptane to the surfactant ratio ( $hsr$ ). The  $hsr$  is the ratio of number of heptane molecule to number of surfactant molecule (72 for all systems in this report) in the interface, i.e. it is the number of heptane molecule per surfactant molecule. The heptane surface number density ( $hsnd$ ) is the number of heptane molecule per unit area ( $\text{Angstrom}^2$ ), and it is calculated by  $hsnd = hsr/A$ , where  $A$  is the surface area per surfactant molecule.

As shown in **Fig. 6a** and **Fig. A3a**, generally, the  $hsr$  increases as  $n$  increase for all systems. The  $hsr$  of pure trisiloxane is greater than two- and three-component mixtures. The  $hsr$  of pure trisiloxane at 60 °C is significantly greater than the value of 25 °C, which suggests strong temperature dependence of  $hsr$ . The  $hsnd$  values of trisiloxane/1g9 and trisiloxane/2g9 are slightly higher when  $n \geq 9$  at 25 °C (**Fig. 6b**), while the  $hsnd$  of pure trisiloxane are nearly  $n$  independent, and trisiloxane/1g9/2g9 are slightly increases when  $n \geq 4$  at 60 °C (**Fig. A3b**),

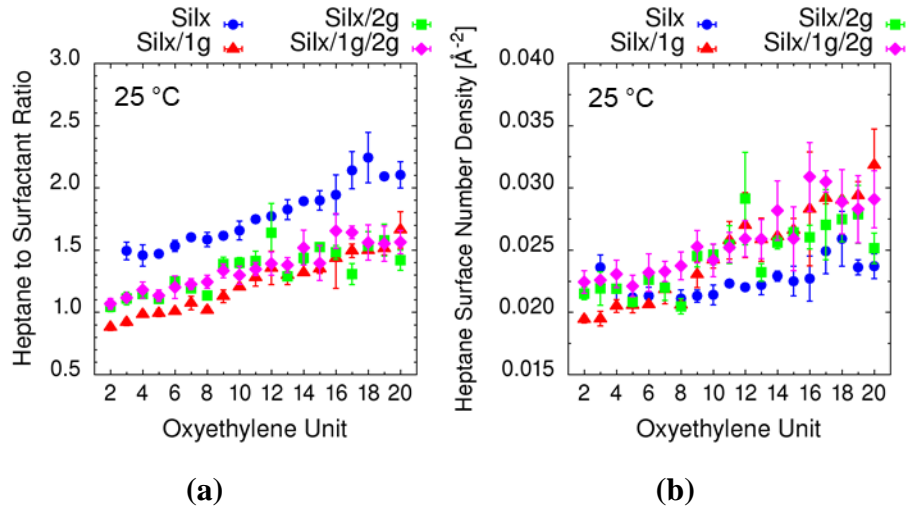


Fig. 6

(a) Heptane to surfactant ratio of pure trisiloxane, trisiloxane/1g9, trisiloxane/2g9, and trisiloxane/1g9/2g9 at the interface and (b) the heptane surface number density at 25 °C as function of trisiloxane oxyethylene length.

#### 4.1.5 Volumetric Number Densities ( $msnd^{-1}$ and $hvnd$ )

Atomic number density profile of each component (type of molecule) can also be calculated based on atomic number density of each individual atoms. Then the maximum surfactant volumetric number density ( $msnd$ ) and the heptane volumetric number density ( $hvnd$ ) at  $msnd$  are calculated based on molecular/group number density. The  $msnd$  is the atomic number density of surfactant is at its maximum, and the  $hvnd$  is the atomic number density of heptane where the atomic number density of surfactant is at its maximum, as shown in **Fig. 7**. The  $msnd$  and  $hvnd$  are calculated because they can be used to describe the smallest channel size and the minimum (limit) heptane concentration that can pass through the surfactant monolayer. In this report, the inverse of  $msnd$ , i.e.  $msnd^{-1}$  is used instead of  $msnd$  in order to correlate it to  $hvnd$  trend directly. The  $msnd^{-1}$  is the channel size of the narrowest region in the surfactant monolayer. Generally we expect high  $hvnd$  when  $msnd^{-1}$  is high.

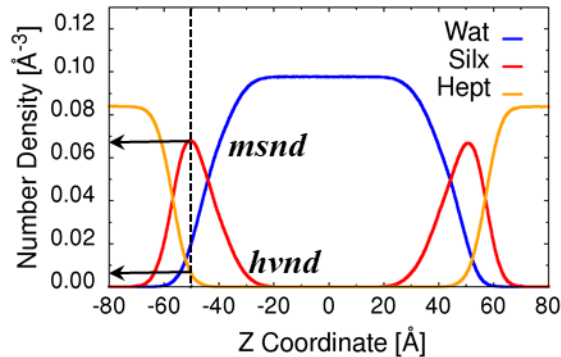


Fig. 7

Atomic number density profile of each component in trisiloxane H8 system. The lines indicates the definition of the maximum surfactant volumetric number density ( $msnd$ ) and the heptane volumetric number density ( $hvnd$ ) at the  $msnd$ .

As shown in **Fig. 8a** and **Fig. A4a**, the  $msnd$  of pure trisiloxane at 25 °C is slightly greater than the values at 60 °C. The  $msnd^{-1}$  of trisiloxane/1g9 and trisiloxane/2g9 are smaller than pure trisiloxane (**Fig. 8a**), and the trisiloxane/1g9/2g9 have the smallest  $msnd^{-1}$  values (**Fig. A4a**). As  $n$  increase,  $msnd^{-1}$  of trisiloxane/1g9, trisiloxane/2g9 and trisiloxane/1g9/2g9 do not show  $n$  dependence. As  $n$  increase, the  $hvnd$  of pure trisiloxane increases slightly, while the  $hvnd$  of all mixtures increases more significantly. The  $hvnd$  of pure trisiloxane are greater than trisiloxane/1g9 and trisiloxane/2g9 when  $n$  is small ( $n \leq 11$ ). However, the  $hvnd$  of trisiloxane/1g9 increases so fast that the values get very close to pure trisiloxane at 25 °C (**Fig. 8b**), similar trend is also observed in the  $hvnd$  of trisiloxane/1g9/2g9 which is likely due to the presence of 1g9 (**Fig. A4b**).

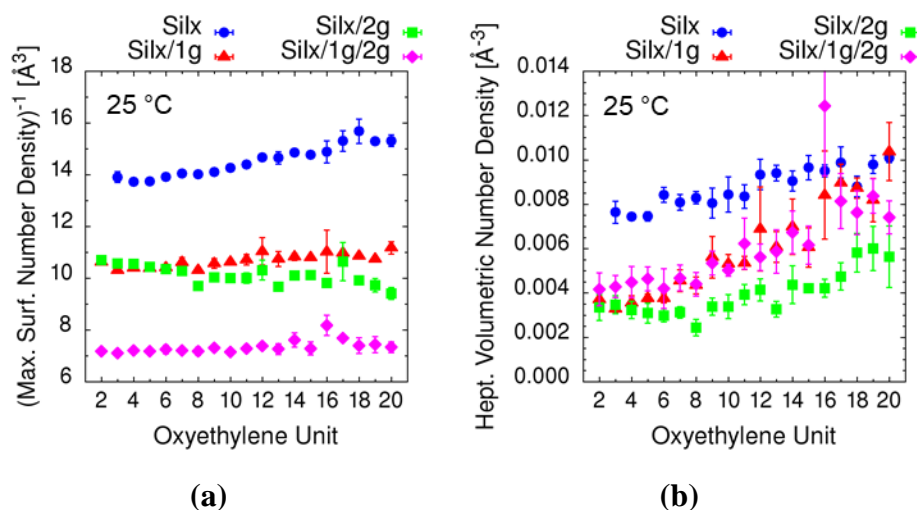


Fig. 8

(a) Inverse of the maximum surfactant volumetric number density ( $msnd^{-1}$ ) and (b) the heptane volumetric number density ( $hvnd$ ) at  $msnd$  at 25 °C as function of trisiloxane oxyethylene length.

#### 4.1.6 Intermolecular Hydrogen Bond

The number of hydrogen bond is calculated based on the condition that the distance of proton-donor and proton-acceptor pair is less than 2.4 Å, and the angle between them is greater than 150°. The intermolecular hydrogen bond is the hydrogen bond formed between different surfactant molecules, while the intramolecular hydrogen bond is the hydrogen bond formed within the same molecule, which involves bending of proton-donor and proton-acceptor group. The more the intermolecular hydrogen bond, and the less intramolecular hydrogen bond, the more stable the surfactant monolayer head group region. The intramolecular hydrogen bond numbers are generally very small, therefore, the data are not presented in this report. However, it is considered in the intermolecular hydrogen bond calculation for higher accuracy. The number of the intermolecular hydrogen bond is calculated by subtracting the number of intramolecular hydrogen bond from the total number of hydrogen bond, i.e.  $N_{inter} = N_{tot} - N_{intra}$ .

The (intermolecular) hydrogen bond number per molecule (*hbnm*) of pure trisiloxane at 60 °C are slightly smaller than the ones at 25 °C (**Fig. 9a**), which agree with the slightly greater surface area at 60 °C (**Fig. 3a**). As *n* increases, the *hbna* of pure trisiloxane decreases (**Fig. 9b**) while the *hbna* of mixture decrease and level off (and may have a minimum between  $9 \leq n \leq 12$ ) (**Fig. 9d**). The opposite trend of *hbnm* and *hbna* indicate that besides the stability of the monolayer, the *hbna* as a cross-sectional unit area properties, may be related to the heptane transport rate. The *hbnm* of trisiloxane/2g9 are much greater trisiloxane/1g9, and the pure trisiloxane have the least *hbnm* and *hbna* due to the number of glucoside in the system (**Fig. 9c, 9d**). As *n* increases, the *hbnm* of trisiloxane/1g9 increases when  $n \leq 11$ , and then level off. The *hbnm* of trisiloxane/2g9 when  $n \geq 13$  are generally greater than smaller *n*. However, both the *hbnm* and *hbna* of trisiloxane/2g9 data are quite scattered at 25 °C.

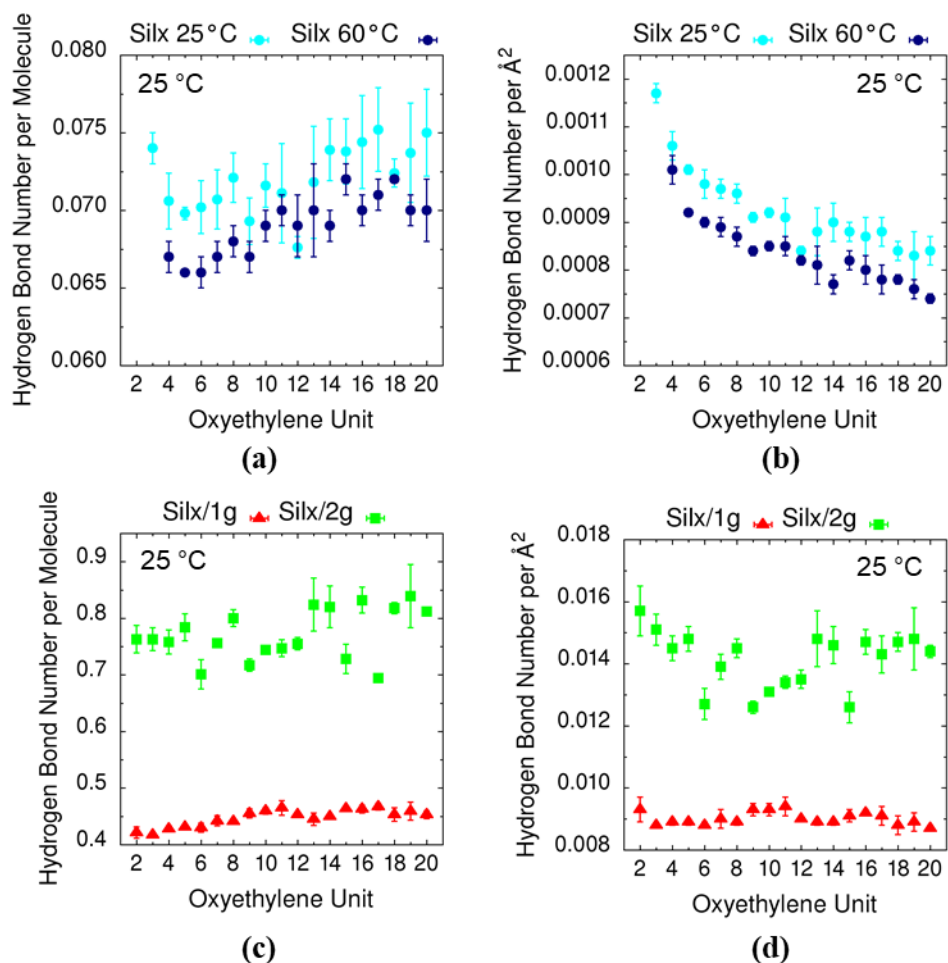


Fig. 9

Intermolecular hydrogen bond number per molecule and intermolecular hydrogen bond number per Å<sup>2</sup> of (a-b) pure trisiloxane at 25 °C and 60 °C, and (c-d) mixed trisiloxane/1g9, and trisiloxane/2g9 at 25 °C as function of trisiloxane oxyethylene length.

#### 4.2 Polyoxyethylenated Trisiloxane with Varied Types of Head Terminal Group

#### 4.2.1 Surfactant Chemical Structure

The chemical structure of general polyoxyethylenated trisiloxane surfactant is shown in **Fig. 2a**. The hydrophilic polyoxyethylene of the trisiloxane can be capped by either hydroxyl ( $X=OH$ , which exist in commercial trisiloxane surfactant 502W) or methoxyl ( $X=OCH_3$ , which exist in commercial trisiloxane surfactant 501W). The hydroxyl-capped (denoted as H in Figures) methoxyl-capped (denoted as M in Figures) polyoxyethylenated trisiloxane surfactant are simulated and compared to study the effect of the head capping terminal group on the interfacial properties of surfactant monolayer at heptane/water interface. Please note that except in this section, the polyoxyethylenated trisiloxane without explicitly specifying the capping group are actually hydroxyl-capped.

#### 4.2.2 Surface Area per Molecule ( $A$ )

As shown in **Fig. 10a**, similar to the hydroxyl-capped trisiloxane, the surface areas per molecule  $A$  of methoxyl-capped polyoxyethylenated surfactants and the square root of oxyethylene unit number ( $\sqrt{n}$ ) also have a linear correlation that  $A = k \times \sqrt{n} + b$ , where  $k$  and  $b$  values are  $8.3 \pm 0.6$  and  $53.2 \pm 1.8$  at  $25^\circ\text{C}$ , and they are  $10.9 \pm 0.5$  and  $48.2 \pm 1.5$  at  $60^\circ\text{C}$ , respectively. With the same temperature and oxyethylene length, the  $A$  of methoxyl-capped polyoxyethylenated trisiloxane are slightly larger than hydroxyl-capped ones (**Fig. 10**). The difference is greater in pure trisiloxane than in trisiloxane/alkylglucoside mixture. The  $A$  are greater at  $60^\circ\text{C}$  than  $25^\circ\text{C}$  as expected (**Fig. A5**).

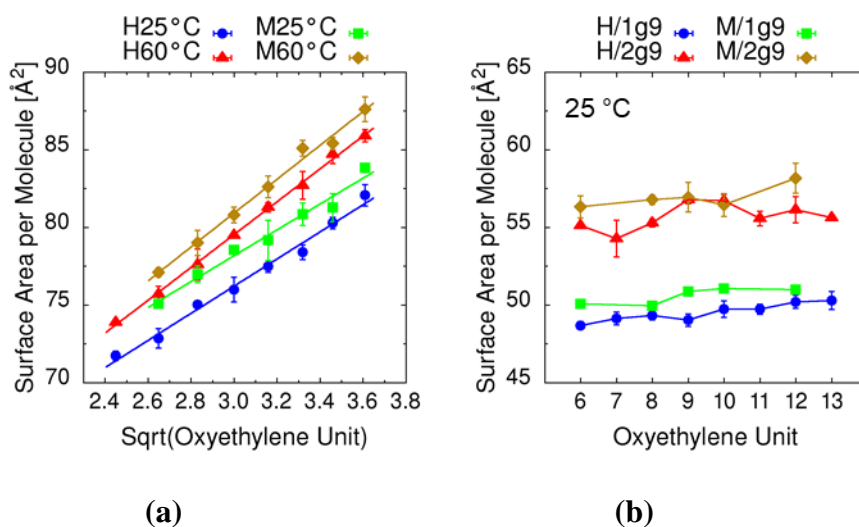


Fig. 10

(a) The surface area per molecule of pure hydroxyl-capped (H) and methoxyl-capped (M) trisiloxane at  $25^\circ\text{C}$  and  $60^\circ\text{C}$  as function of square root of oxyethylene length. (b) The surface area per molecule of trisiloxane/1g9 and trisiloxane/2g9 at  $25^\circ\text{C}$  as function of trisiloxane oxyethylene length.

#### 4.2.3 Interfacial Thickness of Water ( $d_w$ ) and Heptane ( $d_h$ )

The water interfacial thickness  $d_w$  of pure hydroxyl-capped (H) and methoxyl-capped (M) trisiloxane and trisiloxane/alkyl glucoside are very close at same temperature (**Fig. 11a-b**). The  $d_w$  of pure trisiloxane are slightly greater at 25 °C than the ones at 60 °C. The heptane interfacial thickness  $d_h$  of pure methoxyl-capped (M) trisiloxane are greater than the  $d_h$  of hydroxyl-capped (H) trisiloxane (**Fig. 11c**). The  $d_h$  of pure trisiloxane are greater at 60 °C than the ones at 25 °C. When oxyethylene unit length  $n < 9$ , the M/2g9 have greater  $d_h$ . The  $d_h$  of trisiloxane/1g9 and trisiloxane/2g9 at 25 °C are generally very similar (**Fig. 11d**).

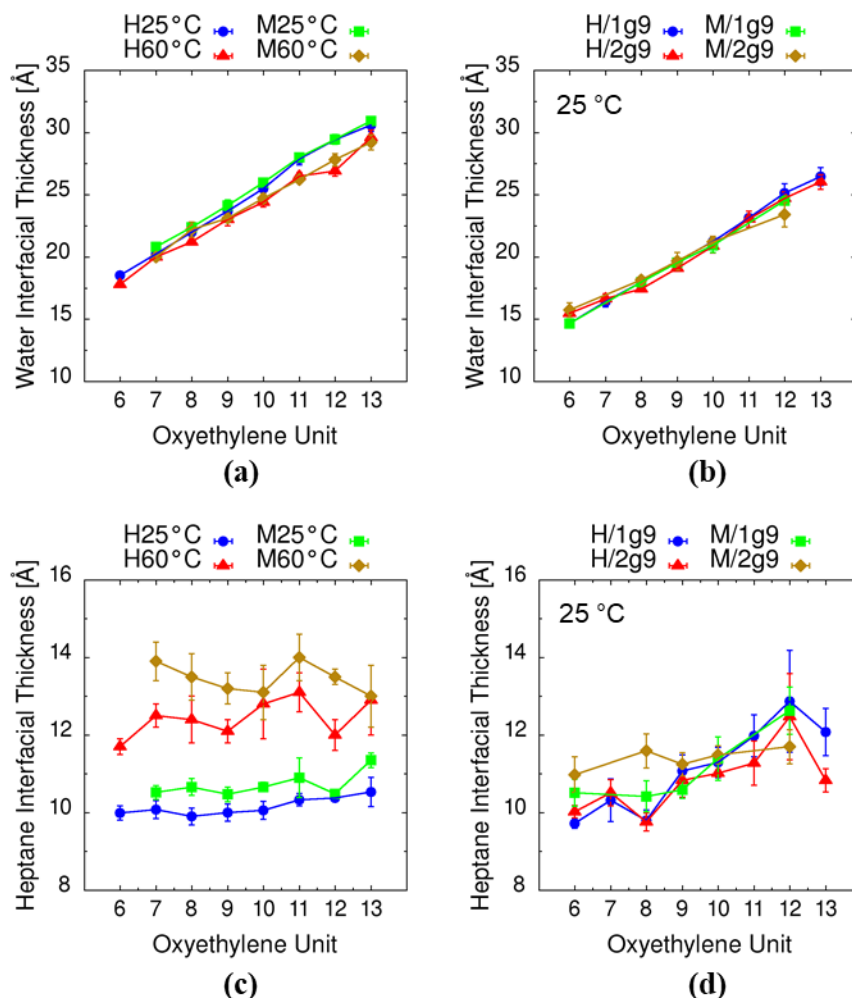


Fig. 11

The water interfacial thickness of (a) pure hydroxyl-capped (H) and methoxyl-capped (M) trisiloxane at 25 °C and 60 °C and (b) trisiloxane/1g9 and trisiloxane/2g9 at 25 °C as function of trisiloxane oxyethylene length. The heptane interfacial thickness of (c) pure hydroxyl-capped (H) and methoxyl-capped (M) trisiloxane at 25 °C and 60 °C and (d) trisiloxane/1g9 and trisiloxane/2g9 at 25 °C as function of trisiloxane oxyethylene length.

#### 4.2.4 Heptane to Surfactant Ratio ( $hsr$ ) and Heptane Surface Number Density ( $hsnd$ )

The heptane to surfactant ratios ( $hsr$ ) of methoxyl-capped (M) trisiloxane are generally higher than hydroxyl-capped (H) trisiloxane for both pure trisiloxane and trisiloxane/alkylglucoside, (**Fig.**

12). The difference of pure trisiloxane is greater at 60 °C than 25 °C, and the difference of trisiloxane/alkylglucoside is greater when oxyethylene length  $n < 9$  and alkylglucoside is 2g9. The heptane surface number density ( $hsnd$ ) demonstrate similar trend as  $hsr$  (Fig. A6).

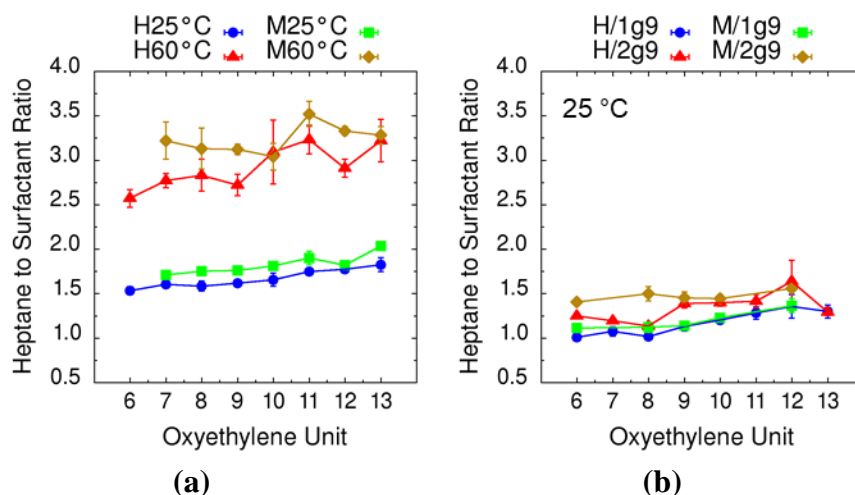


Fig. 12

Heptane to surfactant ratio of (a) pure hydroxyl-capped (H) and methoxyl-capped (M) trisiloxane at 25 °C and 60 °C and (b) trisiloxane/1g9 and trisiloxane/2g9 at 25 °C as function of trisiloxane oxyethylene length.

#### 4.2.5 Volumetric Number Densities ( $msnd^{-1}$ and $hvnd$ )

The inverse of maximum surfactants volumetric number density ( $msnd^{-1}$ ) of hydroxyl-capped (H) trisiloxane are generally lower than methoxyl-capped (M) trisiloxane for pure trisiloxane. The  $msnd^{-1}$  of pure trisiloxane is higher at 60 °C than 25 °C. The  $msnd^{-1}$  of trisiloxane/2g9 is lower than trisiloxane/1g9 (Fig. 13a-b). Unlike the  $msnd^{-1}$ , the heptane volumetric number density ( $hvnd$ ) of pure hydroxyl-capped (H) and methoxyl-capped (M) trisiloxane does not show clear difference. The  $hvnd$  of pure trisiloxane is slightly lower at 60 °C than 25 °C when  $n \geq 9$ . The  $hvnd$  of the trisiloxane/2g9 is lower than trisiloxane/1g9 (Fig. 13c-d). Both  $msnd^{-1}$  and  $hvnd$  data suggest that trisiloxane/2g9 has lower heptane transport rate than trisiloxane/1g9. The heptane transport rate of the hydroxyl-capped trisiloxane/2g9 is lower than or methoxyl-capped trisiloxane/2g9 when  $n \leq 10$ .

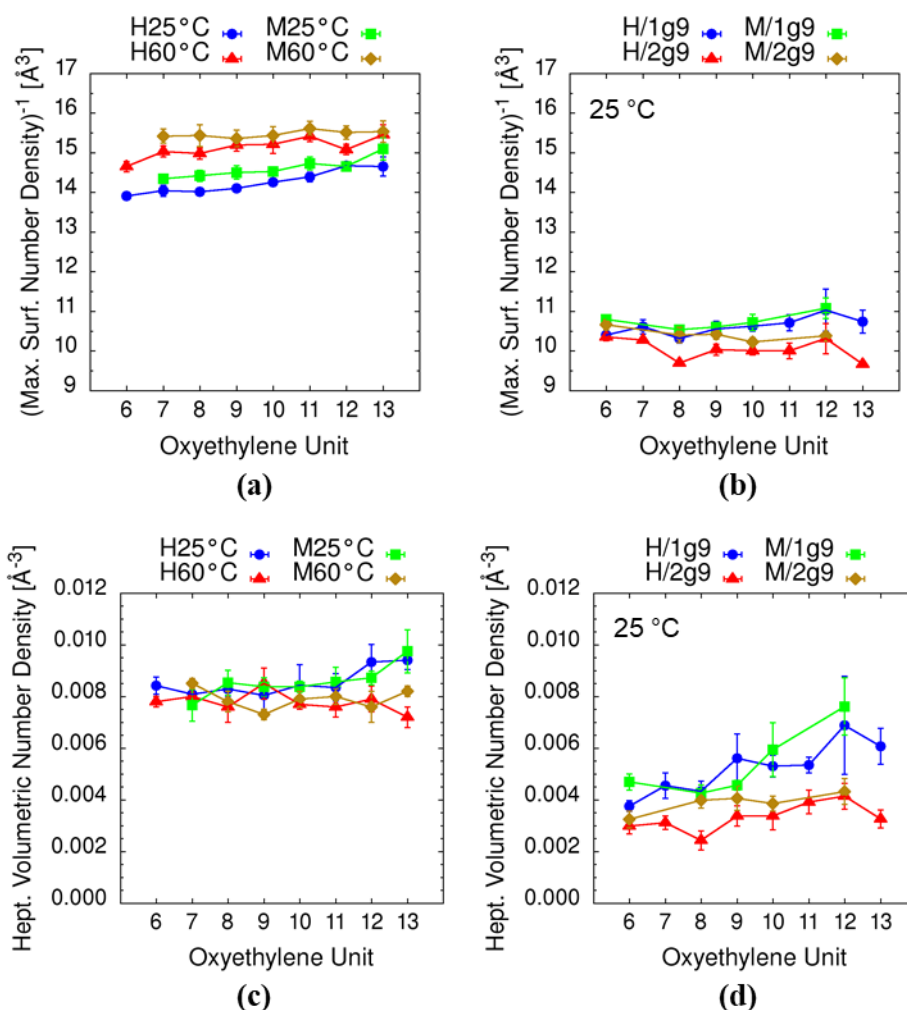


Fig. 13

Inverse of the maximum surfactant number density ( $msnd^{-1}$ ) of (a) pure hydroxyl-capped (H) and methoxyl-capped (M) trisiloxane at 25 °C and 60 °C and (b) trisiloxane/1g9 and trisiloxane/2g9 at 25 °C as function of trisiloxane oxyethylene length. The heptane volumetric number density ( $hvnd$ ) at  $msnd$  of (c) pure hydroxyl-capped (H) and methoxyl-capped (M) trisiloxane at 25 °C and 60 °C and (d) trisiloxane/1g9 and trisiloxane/2g9 at 25 °C as function of trisiloxane oxyethylene length.

#### 4.2.6 Intermolecular Hydrogen Bonds

The hydrogen bond number per molecule ( $hbnm$ ) of trisiloxane/2g9 are much greater than trisiloxane/1g9 due to additional glucoside in the head group. The  $hbnm$  of hydroxyl-capped (H) trisiloxane/2g9 is higher than methoxyl-capped (M) trisiloxane/2g9 at 25 °C, while the  $hbnm$  of hydroxyl-capped (H) trisiloxane/1g9 and methoxyl-capped (M) trisiloxane/1g9 are very similar (Fig. 14). The trend of  $hbna$  is very similar to the trend of  $hbnm$  (Fig. A7).

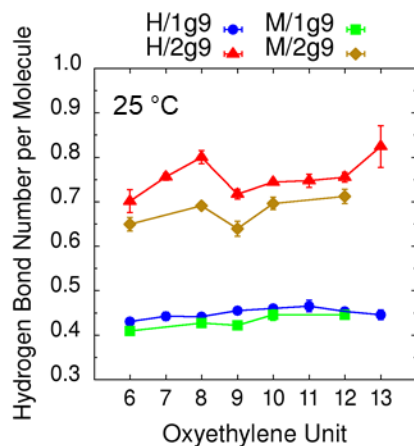


Fig. 14

The intermolecular hydrogen bond number per molecule of hydroxyl-capped (H) trisiloxane/alkylglucoside and methoxyl-capped (M) trisiloxane/alkylglucoside at 25 °C as function of trisiloxane oxyethylene length.

### 4.3 Polyalkylglucoside with Varied Hydrocarbon Unit Length Dependence

#### 4.3.1 Surfactant Chemical Structure

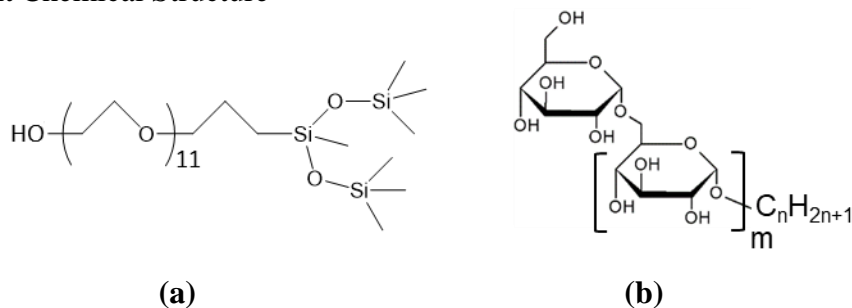


Fig. 15

(a) Chemical Structure of trisiloxane with OH as polar terminal group and oxyethylene length of 11. (b)  $\alpha$ -alkylglucoside and ( $\alpha$ ,  $\alpha$ -1 $\rightarrow$ 6)-alkylglucoside (existing in Glucopon 225) with varied number of glucoside head group ( $m=0, 1$ ) and varied number of hydrocarbon tail length ( $n=5\sim 12$ ).

The chemical structure of polyoxyethylenated trisiloxane and alkyl glucoside surfactant are shown in **Fig. 15**. The MD simulations are performed on two types of surfactant monolayer systems. **Firstly**, pure alkylglucoside with varied number of glucoside head group ( $m=0, 1$ ) and varied number of hydrocarbon tail length ( $n=7\sim 12$  at 25 °C and 60 °C). **Secondly**, two-component system containing H-capped polyoxyethylenated trisiloxane with oxyethylene length of 11 ( $X=OH$ ,  $n=11$ ) and alkylglucoside. The trisiloxane/alkylglucoside (H11/1g and H11/2g) systems with varied hydrocarbon unit length of alkyl glucoside ( $n=5\sim 12$  at 25 °C and 60 °C).

#### 4.3.2 Surface Area per Molecule (A)

The surface area per molecule  $A$  of pure alkyl glucoside, trisiloxane/1g and trisiloxane/2g are shown in **Fig. 16** and **Fig. A8**. Generally, the surface area per molecule at 25 °C is 4~6 Å<sup>2</sup> smaller than 60 °C, which is similar to the change of  $A$  of the pure trisiloxane. The  $A$  of trisiloxane/1g and trisiloxane/2g mixture are greater than the pure alkyl glucoside. Also, the  $A$  of trisiloxane/2g is similar to pure 2g when  $n=11$  and 12. As the alkyl glucoside hydrocarbon length increase, the  $A$  increase first and then level off at  $n$  around 9 for both 25 °C and 60 °C.

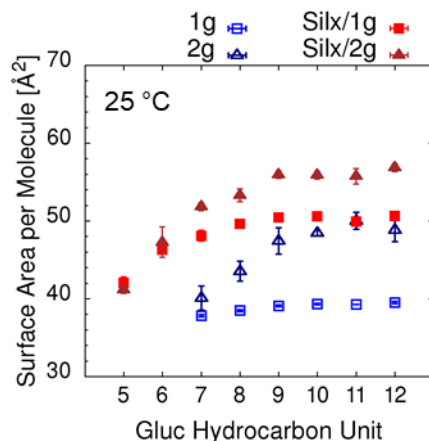


Fig. 16

The surface area per molecule of pure glucoside, trisiloxane/alkylglucoside (H11/1g and H11/2g) at 25 °C as function of alkyl glucoside hydrocarbon (CH<sub>2</sub>) length.

#### 4.3.3 Interfacial Thickness of Water ( $d_w$ ) and Heptane ( $d_h$ )

As the alkylglucoside hydrocarbon length  $n$  increases, the interfacial thickness of water  $d_w$  of pure alkylglucoside, trisiloxane/alkylglucoside (H11/1g and H11/2g) decreases first and then level off (**Fig. 17a**, **Fig. A9a**). The  $d_w$  of the mixture are generally between the pure alkyl glucoside. As the alkylglucoside hydrocarbon length  $n$  increases, the interfacial thickness of heptane  $d_h$  of H11/1g and H11/2g also decreases first and then level off, however, pure alkylglucoside demonstrate a minimum around  $n=9$  (**Fig. 17b**, **Fig. A9b**). The  $d_h$  of the mixture are much smaller than the pure alkyl glucoside. When  $n \leq 7$ , the  $d_w$  and the  $d_h$  of H11/2g are greater than H11/1g. However, when  $n \geq 8$ , the  $d_w$  and the  $d_h$  are very similar for H11/1g and H11/2g even though they have very different surface area per molecule. Moreover, the  $d_w$  and the  $d_h$  at 60 °C are slightly greater than the ones at 25 °C. However, the overall difference is small, which suggest that temperature does not have the strong effect on the overall packing of surfactant monolayer.

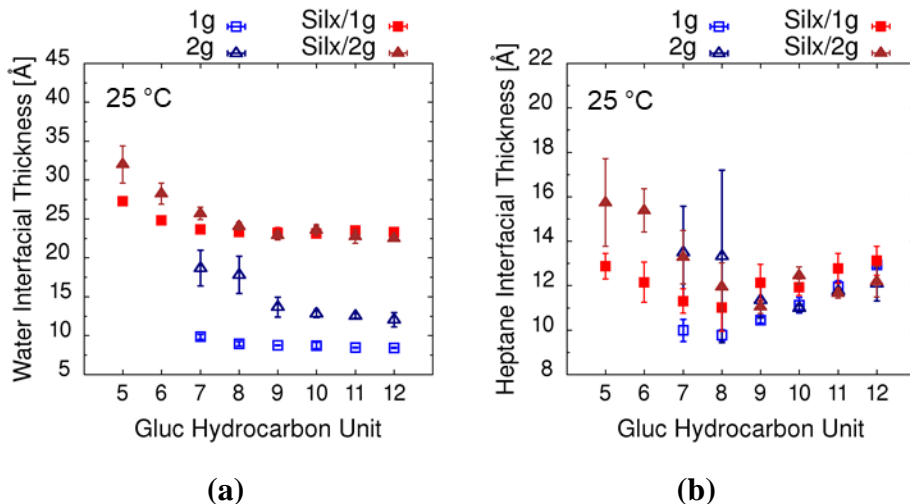


Fig. 17

(a) The interfacial thickness of water and (b) heptane of pure alkylglucoside, trisiloxane/alkylglucoside (H11/1g and H11/2g) at 25 °C as function of alkylglucoside hydrocarbon length.

#### 4.3.4 Heptane to Surfactant Ratio (*hsr*) and Heptane Surface Number Density (*hsnd*)

The heptane to surfactant ratio *hsr* does not show clear hydrocarbon length *n* dependence. The *hsr* of the mixture are greater than pure alkylglucoside (Fig. 18a and Fig. A10a). The heptane surface number density *hsnd* for  $n \leq 6$  are greater than the values for  $n \geq 7$  (Fig. 18b and Fig. A10b). It shows a possible minimum at *n* around 8 for 25 °C.

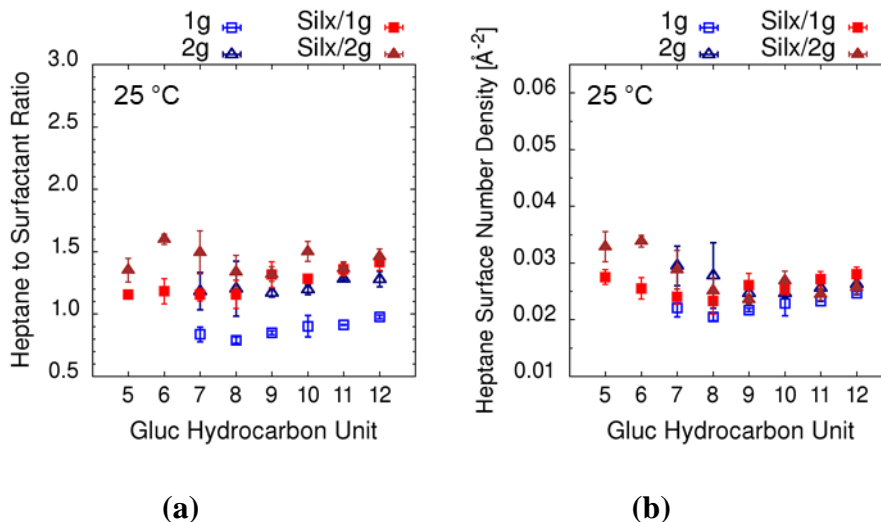


Fig. 18

(a) Heptane to surfactant ratio and (b) the heptane surface number density of pure glucoside, trisiloxane/alkylglucoside (H11/1g and H11/2g) at 25 °C as function of alkylglucoside hydrocarbon length.

#### 4.3.5 Volumetric Number Densities ( $msnd^{-1}$ and $hvnd$ )

As the alkylglucoside hydrocarbon length  $n$  increases, the inverse of maximum surfactants volumetric number density  $msnd^{-1}$  decrease first and then level off at  $n=9$  (**Fig. 19a** and **Fig. A11a**), and the heptane volumetric number density ( $hvnd$ ) at  $msnd$  also decrease and level off (**Fig. 19b** and **Fig. A11b**). As  $msnd^{-1}$  and  $hvnd$  may be related to heptane transport rate as both describe the limiting channel size and the transport rate that that heptane can pass through the surfactant monolayer. To minimize the heptane transport rate, we would prefer low  $msnd^{-1}$  and  $hvnd$ , according to which, the alkylglucoside with hydrocarbon length  $n \geq 9$  is a better choice.

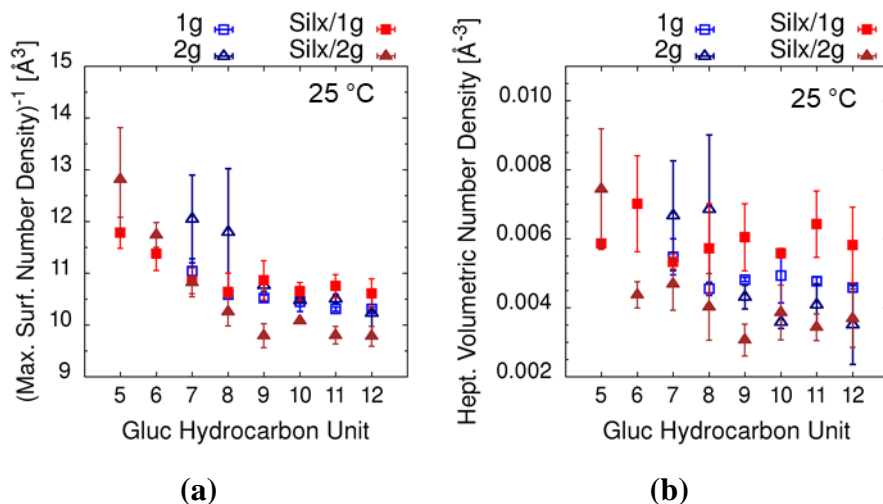
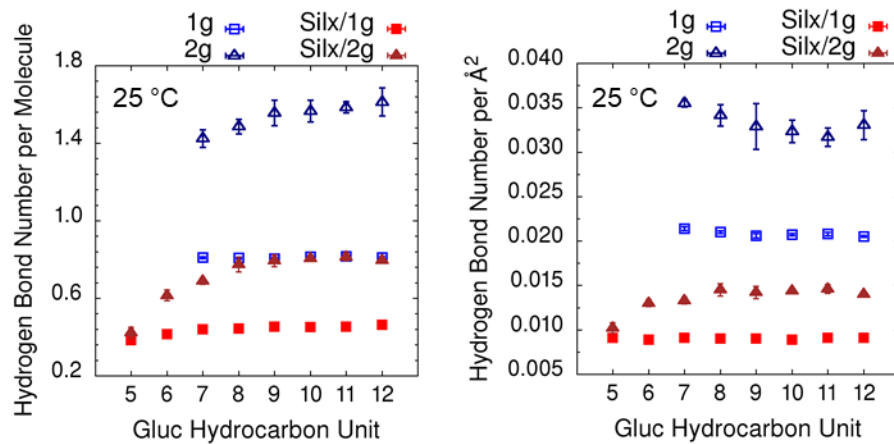


Fig. 19

(a) Inverse of the maximum surfactant volumetric number density ( $msnd^{-1}$ ) and (b) heptane volumetric number density at maximum surfactant number density of pure alkylglucoside, trisiloxane/alkylglucoside (H11/1g and H11/2g) at 25 °C as function of alkylglucoside hydrocarbon length.

#### 4.3.6 Intermolecular Hydrogen Bonds

The results show that as the alkyl glucoside hydrocarbon length  $n$  increases, hydrogen bond number per molecule ( $hbnm$ ) and the hydrogen bond number per angstrom ( $hbna$ ) of the mixture increase first at low  $n$  and then immediately level off at  $n$  around 7~9, while the pure alkyl glucoside does not show clear  $n$  dependence (**Fig. 20** and **Fig. A12**). As  $hbnm$  and  $hbna$  may be related to stability of the surfactant monolayer in the hydrophilic region. To maximize stability, we would prefer high  $hbnm$  and  $hbna$ . Therefore, the alkyl glucoside with  $n \geq 8$  is a better choice.



(a) (b)

Fig. 20

(a) Intermolecular hydrogen bond number per molecule and (b) intermolecular hydrogen bond number per Å<sup>2</sup> of pure glucoside, trisiloxane/alkylglucoside (H11/1g and H11/2g) at 25 °C as function of alkyl glucoside hydrocarbon length.

#### 4.4 Alkylglucoside Configuration and Linkage Dependence

##### 4.4.1 Surfactant Chemical Structure

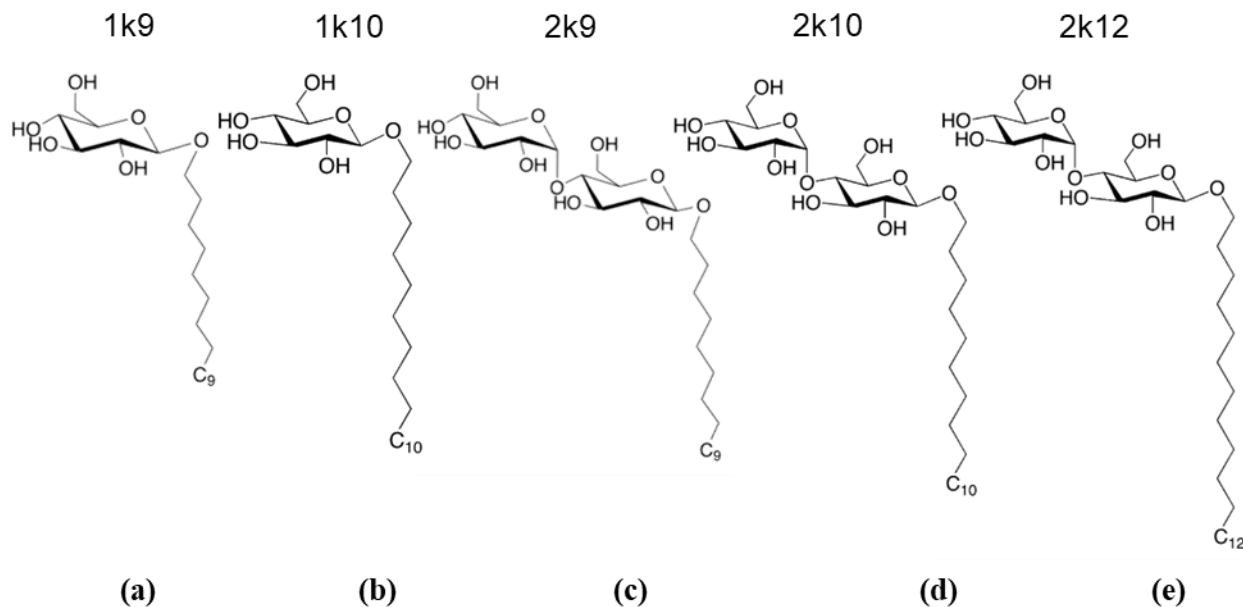


Fig. 21

Chemical Structure of  $\beta$ -alkylglucoside and  $(\alpha, \beta$ -1 $\rightarrow$ 4)-alkylglucoside with varied hydrocarbon tail length

The chemical structure of  $\beta$ -alkylglucoside and ( $\alpha$ ,  $\beta$ -1 $\rightarrow$ 4)-alkylglucoside surfactant are shown in **Fig. 21**, as compared to  $\alpha$ -alkylglucoside and ( $\alpha$ ,  $\alpha$ -1 $\rightarrow$ 6)-alkylglucoside (in Glucopon 225) shown in the previous section (**Fig. 15**). The MD simulations are performed on the pure alkylglucoside with varied number of glucoside head group ( $m=0, 1$ ) and varied number of hydrocarbon tail length ( $n=9, 10, \text{ and } 12$  at 25 °C and 60 °C).

#### 4.4.2 Surface Area per Molecule ( $A$ ) and Interfacial Thicknesses ( $d_w, d_h$ )

As shown in **Fig. 22a** and **Fig. A13a**, with the same hydrocarbon length, the  $\beta$ - and ( $\alpha$ ,  $\beta$ -1 $\rightarrow$ 4)-alkylglucoside (represented by  $mkn$ ) have significantly smaller surface area per molecule  $A$  and tighter packing than  $\alpha$ - and ( $\alpha$ ,  $\alpha$ -1 $\rightarrow$ 6)-alkylglucoside (represented by  $mgn$ ). The hydrocarbon length  $n$  (whether  $n=9, 10, \text{ or } 12$ ) does not show clear effect on the  $A$  of  $mkn$  alkyl glucoside. Unlike the  $A$ , The  $d_w$  and  $d_h$  do not demonstrate dependence on the glucoside linkage. With the same hydrocarbon length, the difference of the interfacial thicknesses due to the configuration and linkage are all within the standard deviation (**Fig. 22b** and **Fig. A13b**).

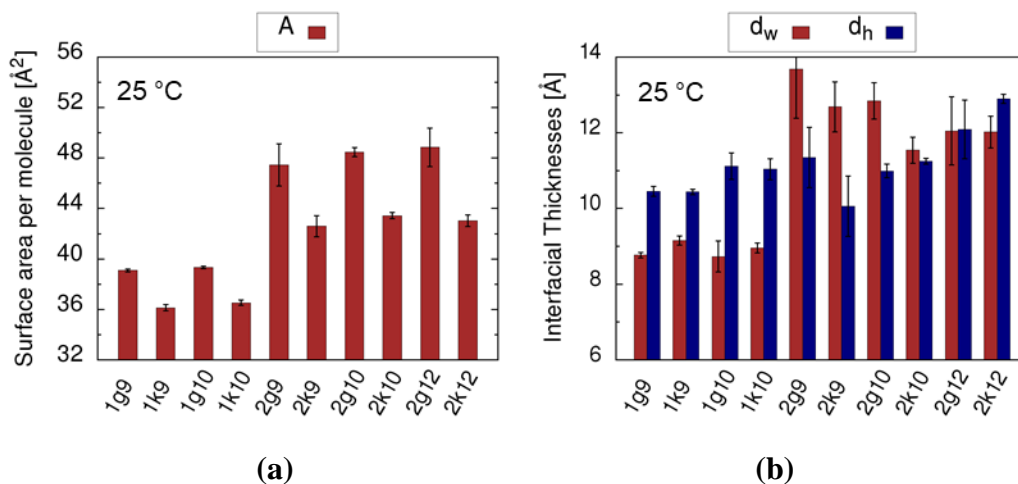


Fig. 22

(a) The surface area per molecule and (b) the interfacial thickness of water and heptane of the pure  $\alpha$ - and ( $\alpha$ ,  $\alpha$ -1 $\rightarrow$ 6)-alkylglucoside (represented by  $mgn$ ) and the  $\beta$ - and ( $\alpha$ ,  $\beta$ -1 $\rightarrow$ 4)-alkylglucoside (represented by  $mkn$ ) with varied hydrocarbon length at 25 °C, respectively.

#### 4.4.3 Heptane to Surfactant Ratio ( $hsr$ ) and Number Densities ( $hsnd, msnd^{-1}, hvnd$ )

With the same hydrocarbon length, the  $\beta$ - and ( $\alpha$ ,  $\beta$ -1 $\rightarrow$ 4)-alkylglucoside ( $mkn$ ) have significantly smaller heptane to surfactant ratio  $hsr$  and slightly smaller heptane surface number density  $hsnd$  than  $\alpha$ - and ( $\alpha$ ,  $\alpha$ -1 $\rightarrow$ 6)-alkylglucoside ( $mgn$ ) (**Fig. 23a** and **Fig. A14a**). Moreover, with the same hydrocarbon length, the  $mkn$  alkylglucoside have significantly smaller  $msnd^{-1}$  and  $hvnd$  than the  $mgn$  alkyl glucoside (**Fig. 23b** and **Fig. A14b**). These results suggest that in order to minimize the heptane transport rate, the  $\beta$ - and ( $\alpha$ ,  $\beta$ -1 $\rightarrow$ 4)-alkylglucoside are much better surfactants than  $\alpha$ - and ( $\alpha$ ,  $\alpha$ -1 $\rightarrow$ 6)-alkylglucoside (the structure in Glucopon) experimentally tested previously.

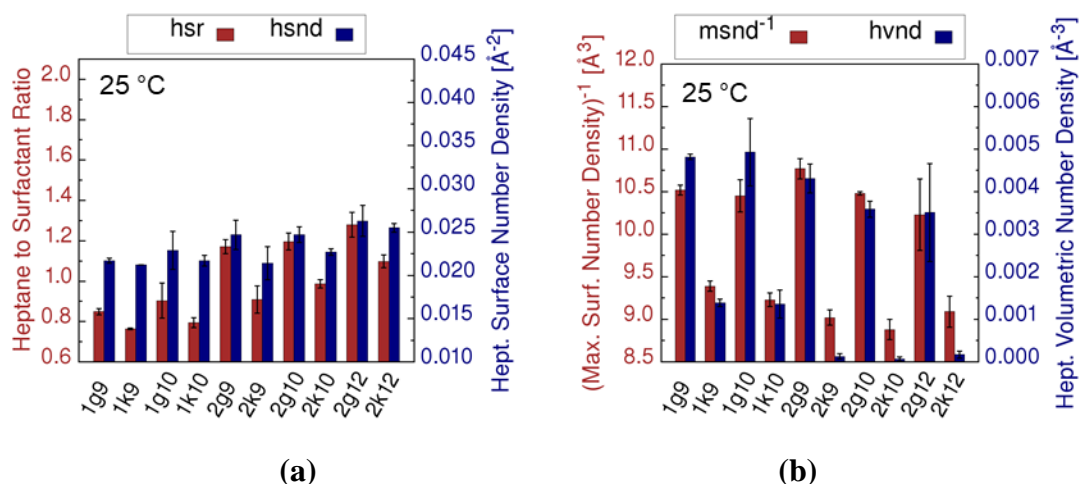


Fig. 23

(a) Heptane to surfactant ratio and the heptane surface number density and (b) inverse of maximum surfactant number density and heptane volumetric number density at maximum surfactant number density of the pure  $\alpha$ - and ( $\alpha$ ,  $\alpha$ -1 $\rightarrow$ 6)-alkylglucoside (represented by *mgn*) and the  $\beta$ - and ( $\alpha$ , $\beta$ -1 $\rightarrow$ 4)-alkylglucoside (represented by *mkn*) with varied hydrocarbon length at 25 °C, respectively.

#### 4.4.4 Intermolecular Hydrogen Bonds

As shown in **Fig. 24** and **Fig. A15**, with the same hydrocarbon length, the  $\beta$ - and ( $\alpha$ ,  $\beta$ -1 $\rightarrow$ 4)-alkylglucoside (*mkn*) have greater hydrogen bond number per molecule (*hbnm*) and the hydrogen bond number per Å<sup>2</sup> (*hbnA*) than the  $\alpha$ - and ( $\alpha$ ,  $\alpha$ -1 $\rightarrow$ 6)-alkylglucoside (*mgn*), which make them forming more stable surfactant monolayer, and better surfactant candidate for fire suppression.

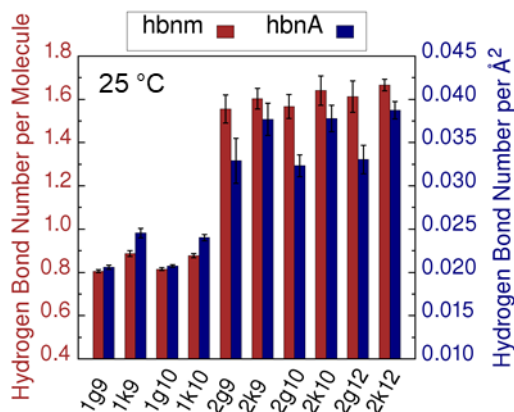


Fig. 24

Intermolecular hydrogen bond number per molecule and hydrogen bond number per Å<sup>2</sup> of varied types of the pure  $\alpha$ - and ( $\alpha$ , $\alpha$ -1 $\rightarrow$ 6)-alkylglucoside (represented by *mgn*) and the  $\beta$ - and ( $\alpha$ , $\beta$ -1 $\rightarrow$ 4)-alkylglucoside (represented by *mkn*) with varied hydrocarbon length at 25 °C.

## 4.5 Siloxane with Varied Head and Tail Group

### 4.5.1 Surfactant Chemical Structure

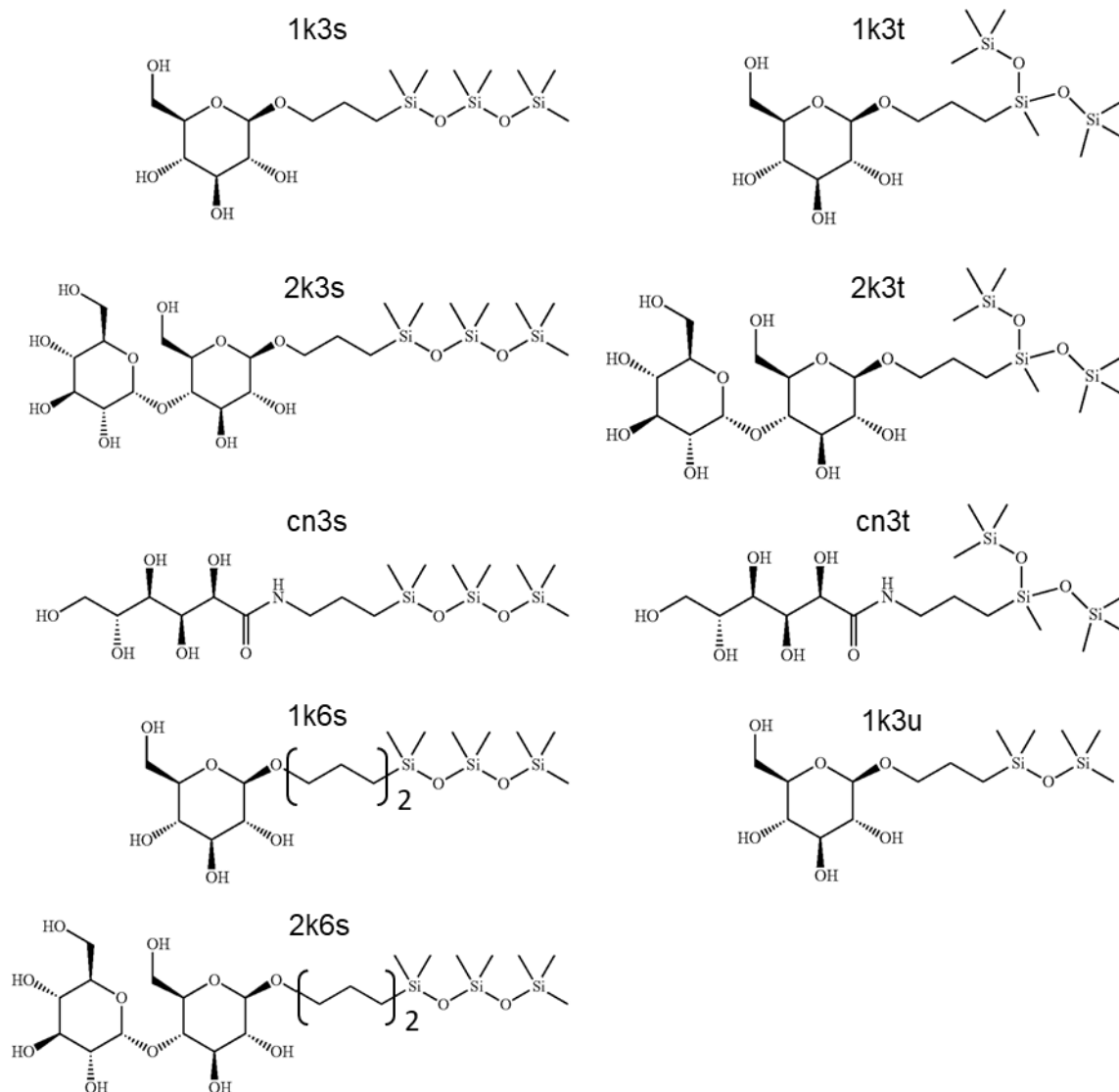


Fig. 25

Chemical structures surfactant with varied types of hydrophilic head group and hydrophobic tail.

The chemical structure of siloxane surfactant with varied head and tail groups are shown in **Fig. 25**. The MD simulations are performed on the pure siloxane surfactant with linear carbohydrate (*cn*) and cyclic carbohydrate, i.e. one glucoside (1k) or two glucosides (2k) with the  $\beta$ - and ( $\alpha,\beta$ -1 $\rightarrow$ 4)glucoside as the head group, and with a linear siloxane (3s,6s,3u) or a branched siloxane (3t) tail (at 25 °C and 60 °C). Among these structures, 1k3s, 1k3t, 2k3s, 2k3t, cn3t, and 1g3u are existing chemicals filed in patent (#US 9,687,686 B2), while the cn3s, 1k6s, and 2k6s are the artificial structure built and studied for comparison, understanding and optimization purpose.

#### 4.5.2 Surface Area per Molecule ( $A$ ) and Interfacial Thicknesses ( $d_w, d_h$ )

With the same head group (1k or 2k), 3u have the smallest surface area per molecule  $A$ . Siloxane with 6s tail have the smaller  $A$  than 3s, and 3t have the greatest  $A$ . With the same tail (3s or 3t), siloxane with 1g and  $cn$  head have similar  $A$ , and the values are smaller than siloxane with 2g (**Fig. 26a and Fig. A16a**). With the same head group (1k or 2k), siloxane with 6s tail have the smallest  $d_w$ . Siloxane with 3s and 3u have the slightly smaller  $d_w$  than 3t. With the same tail (3s or 3t), siloxane with 1k have the smallest  $d_w$ , followed by  $cn$ , and 2k have the greatest  $d_w$  (**Fig. 26b and Fig. A16b**). With the same head group (1k or 2k), siloxane with 6s tail have the greatest  $d_h$ , followed by 3s and 3t, and siloxane with 3u have the smallest  $d_h$ . With the same tail (3s or 3t), siloxane with 1k have the greater  $d_h$  than 2k and  $cn$ . The  $A$ ,  $d_w$  and  $d_h$  are generally slightly greater at 60 °C than 25 °C.

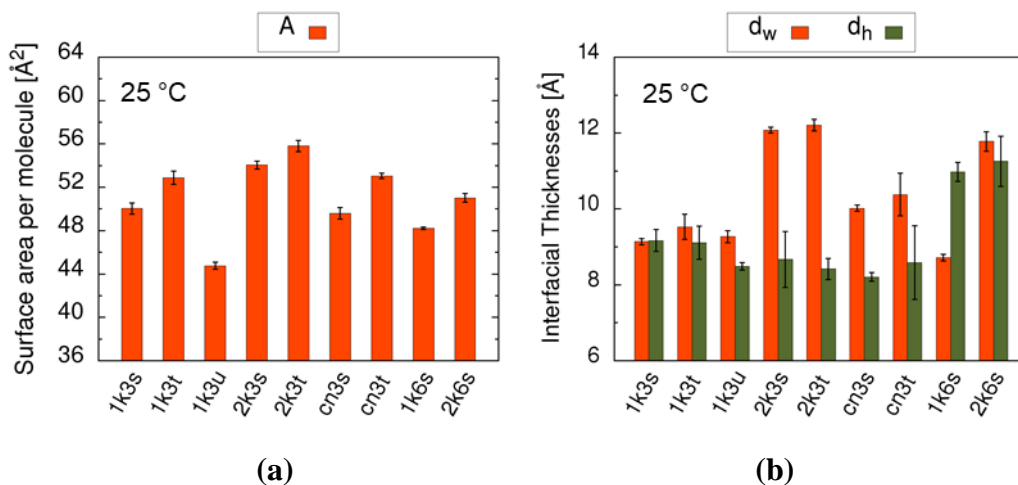


Fig. 26

(a) The surface area per molecule and (b) the interfacial thickness of water and heptane of varied types of siloxane surfactant at 25 °C, respectively.

#### 4.5.3 Heptane to Surfactant Ratio ( $hsr$ ) and Number Densities ( $hsnd, msnd^{-1}, hvnd$ )

With the same head group (1k or 2k), siloxane with 3u have the smallest heptane to surfactant ratio  $hsr$ , however, 3s, 3t, and 6s of  $hsr$  does not show clear tail dependence. With the same tail (3s or 3t), siloxane with  $cn$  have the smaller  $hsr$  than 1k and 2k at 25 °C (**Fig. 27a and Fig. A17a**). With the same head group (1k or 2k), siloxane with 3s and 3t have less  $hsnd$  than 6s. With the same tail (3s or 3t), siloxane with  $cn$  and 2k head groups have less  $hsnd$  than 1g at 25 °C. 1k3u have the smallest  $hsr$  and 2k3t have the smallest  $hsnd$  at 60 °C. 2k6s have the smallest  $msnd^{-1}$ , followed by 2k3t and 2k3s at both 25 °C and 60 °C. 2k6s, 2k3s and 2k3t also have the smallest  $hvnd$ , which make these three surfactant good candidate surfactant to minimize heptane transport rate (**Fig. 27b and Fig. A17b**).

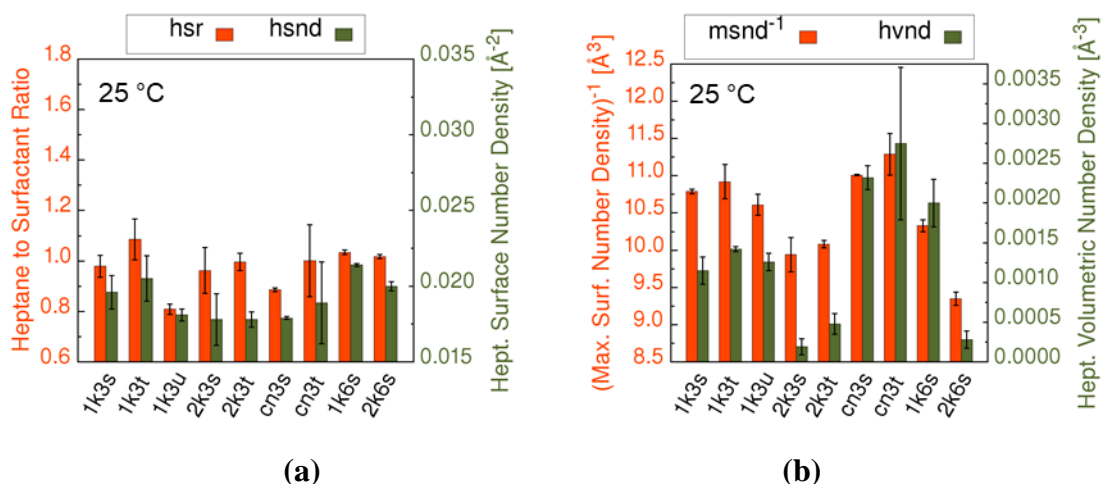


Fig. 27

(a) Heptane to surfactant ratio and the heptane surface number density and (b) inverse of the maximum surfactant number density and heptane volumetric number density at maximum surfactant number density of varied types of siloxane surfactant at 25 °C.

#### 4.5.4 Intermolecular Hydrogen Bonds

As shown in **Fig. 28** and **Fig. A18**, the siloxane 2k6s have the greatest hydrogen bond number per molecule (*hbnm*) and the hydrogen bond number per angstrom (*hbnA*), followed by 2k3s and 2k3t, which make them form more stable surfactant monolayer, and better surfactant candidate for fire suppression.

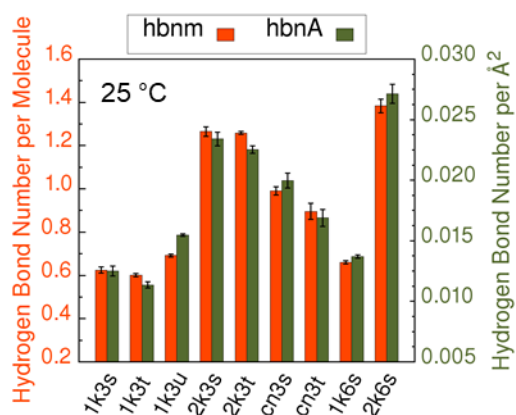


Fig. 28

Intermolecular hydrogen bond number per molecule and hydrogen bond number per  $\text{\AA}^2$  of varied types of siloxane surfactant at 25 °C.

### 4.6 Pure Hydrocarbon surfactant with varied charged head groups

#### 4.6.1 Surfactant Chemical Structure

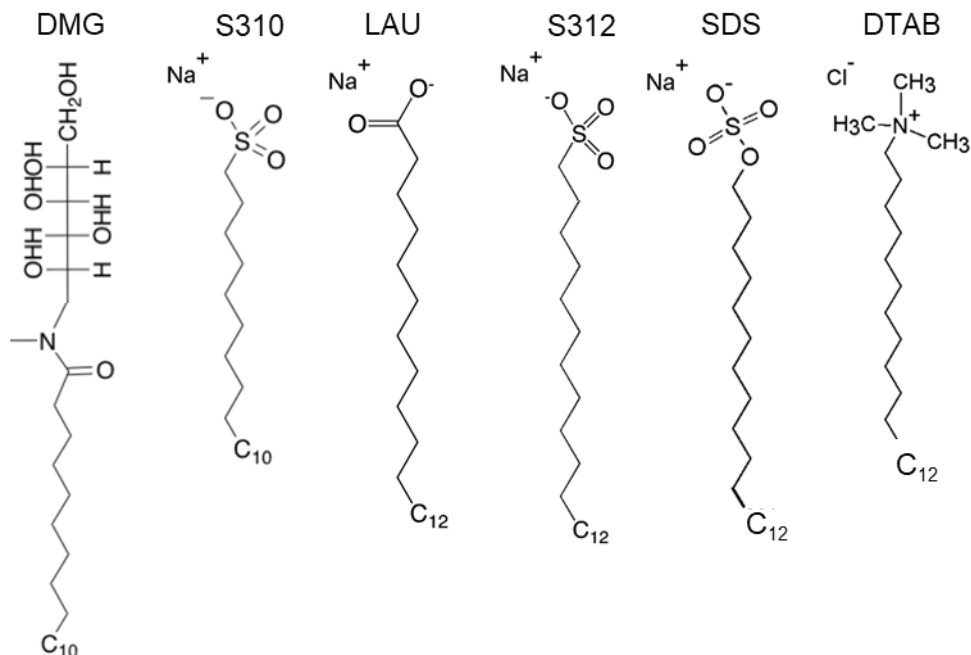


Fig. 29

Chemical Structure of hydrocarbon surfactant with varied charged head group, and hydrocarbon tail length of 10 and 12.

The chemical structure of hydrocarbon surfactant with varied charged head group are shown in **Fig. 29**. The MD simulations are performed on the pure hydrocarbon surfactant with neutral charge dmG, negative charged (s310, lau, s312 and sds) and positive charged dtab.

#### 4.6.2 Surface Area per Molecule ( $A$ ) and Interfacial Thicknesses ( $d_w$ , $d_h$ )

With hydrocarbon tail length of 10, the surfactant 1k10 ( $\beta$ -alkylglucoside) have the smallest surface area per molecule  $A$  and tightest packing (**Fig. 30a** and **Fig. A19a**). The surfactant s310 have the smallest  $d_w$  and dmG have the smallest  $d_h$ . With hydrocarbon tail length of 12, the surfactant 1g12 have the smallest surface area per molecule  $A$  and tightest packing (**Fig. 30b** and **Fig. A19b**). Please note that 1k12 is not simulated, otherwise, it would probably be the one that the smallest  $A$ . The surfactant lau have the smallest  $d_w$ , and lau and dtab have the smallest  $d_h$ . For both hydrocarbon tail length of 10 and 12, beside 2g head, the  $A$  of charged hydrocarbon surfactant are greater than the neutral ones. The values of  $A$ ,  $d_w$  and  $d_h$  at 60°C are generally slightly greater than the values at 25 °C as expected.

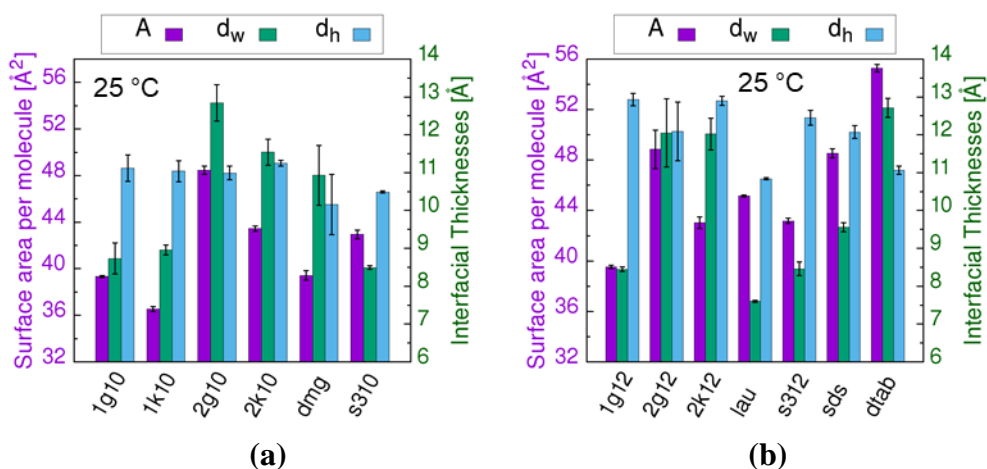


Fig. 30

The surface area per molecule and the interfacial thickness of water and heptane of varied types of hydrocarbon surfactant with the length of (a) 10 and (b) 12 at 25 °C, respectively.

#### 4.6.3 Heptane to Surfactant Ratio (*hsr*) and Heptane Surface Number Density (*hsnd*)

With hydrocarbon tail length of 10, the surfactants 1k10 and dmg have the smaller *hsr* than the rest surfactants at 25 °C (**Fig. 31a**), while 1k10, dmg and also s310 have smaller *hsnd* than the rest surfactants at 60 °C (**Fig. A20a**). 1k10, dmg and s310 have smaller *hsnd* than the rest surfactants. With hydrocarbon tail length of 12, the surfactants 1g12, lau and s312 have the smaller *hsr* than the rest surfactants, and lau have smallest *hsnd* (**Fig. 31b** and **Fig. A20b**).

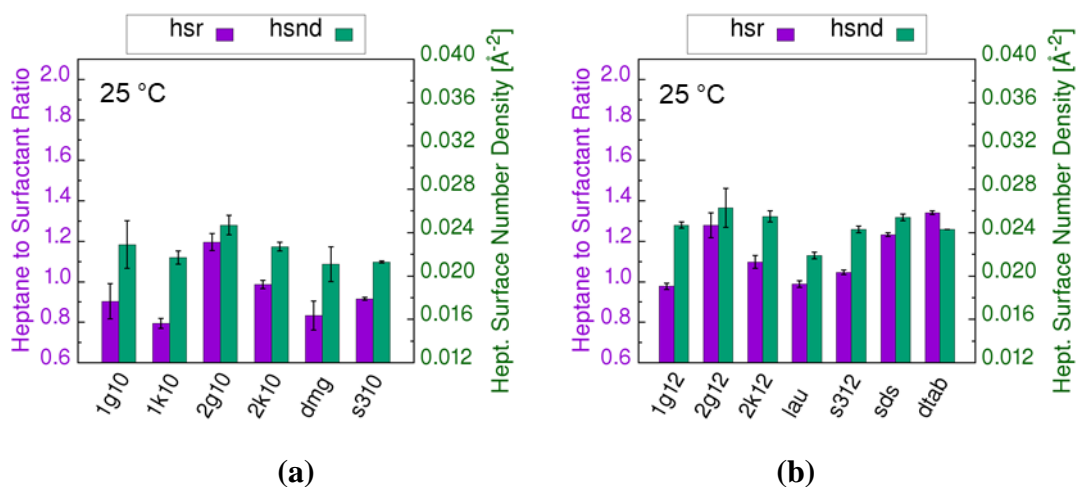


Fig. 31

Heptane to surfactant ratio in the interface and the heptane surface number density of varied types of hydrocarbon surfactant with the length of (a) 10 and (b) 12 at 25 °C.

#### 4.6.4 Volumetric Number Densities ( $msnd^{-1}$ and $hvnd$ )

With hydrocarbon tail length of 10, the surfactants 2k10 have the smallest  $msnd^{-1}$  and  $hvnd$ . Similarly with hydrocarbon tail length of 12, the surfactants 2k12 have the smallest  $msnd^{-1}$  and  $hvnd$  among the surfactants studied (**Fig. 32, A21**). The charged hydrocarbon surfactants s310, lau, s312, sds, and dtab have much greater  $msnd^{-1}$  and much higher  $hvnd$  than the neutral ones, which suggest a higher heptane transport rate of the charged hydrocarbon surfactants than the neutral ones.

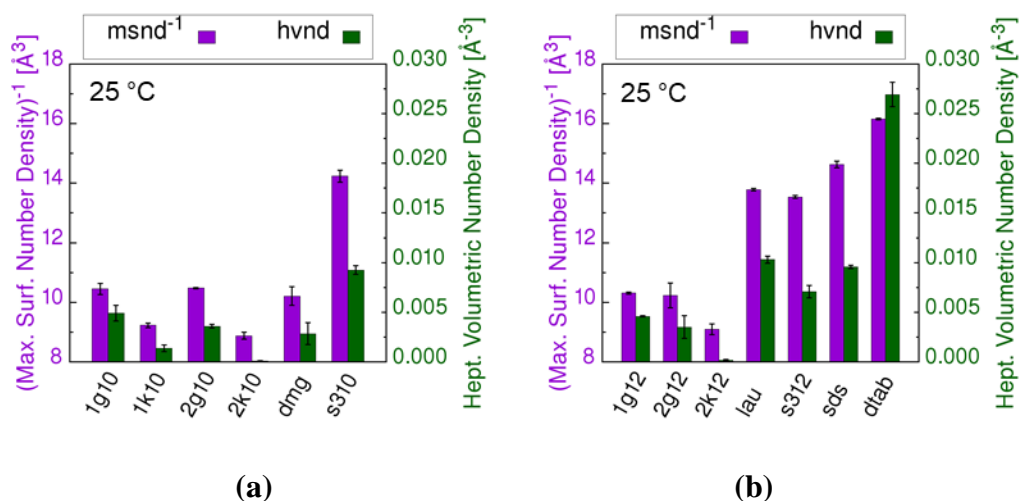


Fig. 32

Inverse of the maximum surfactant number density and heptane volumetric number density at maximum surfactant number density of varied type of hydrocarbon surfactant with length (a) 10 and (b) 12 at 25 °C.

### 4.7 Surfactant Mixtures with Varied Molecular (Molar) Fraction

#### 4.7.1 Surfactant Chemical Structure

The perfluorocarbon surfactant capstone (**Fig. 33**), polyoxyethylenated trisiloxane (**Fig. 2**), and alkylglucoside (**Fig. 2**) mixtures are simulated to study the component fraction dependence on the properties. The capstone is denoted as Ca, and the hydroxyl-capped polyoxyethylenated trisiloxane with oxyethylene length of 10 ( $X=OH$ ,  $n=10$ ) is denoted as H10. The pure perfluorocarbon, trisiloxane and alkylglucoside surfactants, the two-component Ca/1g9, Ca/2g9, H10/1g9, H10/2g9 with varied surfactant fractions are simulated at 25 °C. The H10/1g9/2g9 (1g9:2g9=3:7 mimicking Glucopon 225) with varied surfactant fractions are simulated at 25 °C and 60 °C.

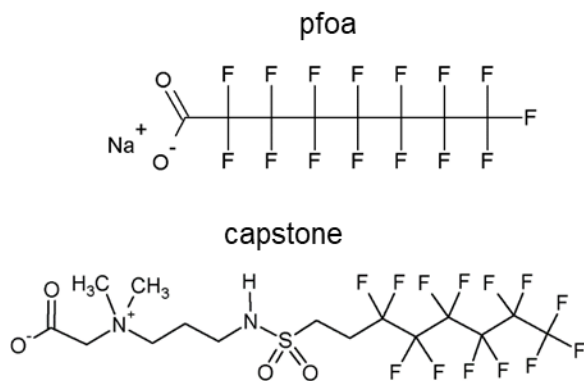


Fig. 33

Chemical Structure of perfluorocarbon surfactant pfoa and capstone.

#### 4.7.2 Surface Area per Molecule (A)

The surface area per molecules of two-component system capstone/1g9 and capstone/2g9 are shown in **Fig. 34**. The system with capstone fraction  $f = 0.0$  are the pure 1g9 and 2g9 monolayer, and  $f = 1.0$  is the pure capstone. The result show that capstone/1g9 shows a minimum at capstone fraction  $f$  around 0.5. The  $A$  of capstone/2g9 increases as  $f$  increases when  $f > 0.2$ . As  $f$  increases, the  $A$  of H10/1g9, H10/2g9, and H10/3g9 increases. When  $f > 0.4$ , the  $A$  of H10/2g9 and H10/3g9 are very similar. The surface area per molecules of three-component system H10/1g9/2g9 (1g9:2g9=3:7 mimicking g225, i.e. H10/g225) g225 are shown in **Fig. A22**. The fraction  $f = 0.0$  are the g225 monolayer, and  $f = 1.0$  is the pure trisiloxane. As  $f$  increases, the  $A$  of H10/1g9/2g9 increases.

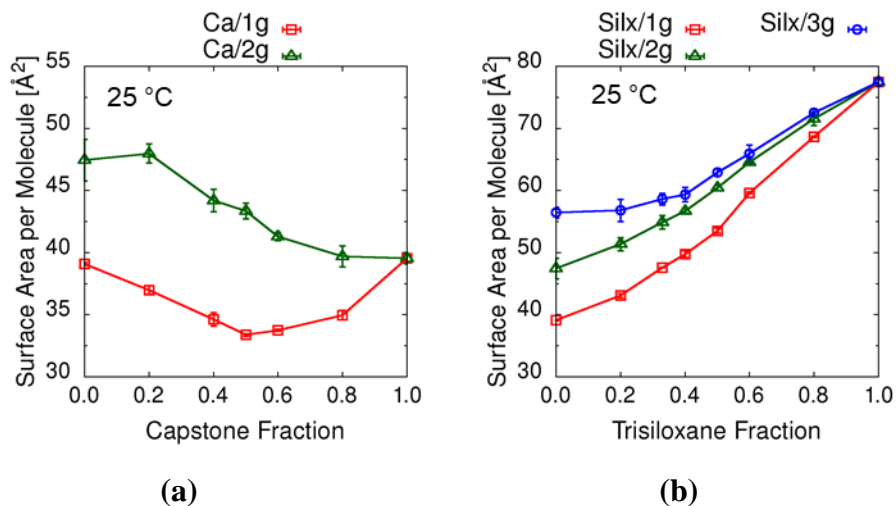


Fig. 34

The surface area per molecule of (a) capstone/1g9 and capstone/2g9 and (b) H10/1g9, H10/2g9 and H10/3g9 at 25°C as function of molecular fraction of capstone and H10, respectively.

### 4.7.3 Interfacial Thicknesses ( $d_w$ , $d_h$ )

The water interfacial thickness of Ca/2g9 shows a minimum for  $f$  between 0.4 and 0.6 (**Fig. 35a**). The heptane interfacial thickness of Ca/1g9 and Ca/1g9 show a minimum for  $f$  at 0.5 and 0.6 (**Fig. 35c**). While the water interfacial thickness of trisiloxane/alkylglucoside (H10/1g9, H10/2g9, H10/3g9) increases as  $f$  increase (**Fig. 35b, A23a**), and the heptane interfacial thickness do not show clear  $f$  dependence (**Fig. 35d, A23b**). The H10/1g9/2g9 systems generally have higher heptane interfacial thickness at 60°C than 25°C, and H10/1g9/2g9 at 60°C shows a minimum at  $f = 0.8$ .

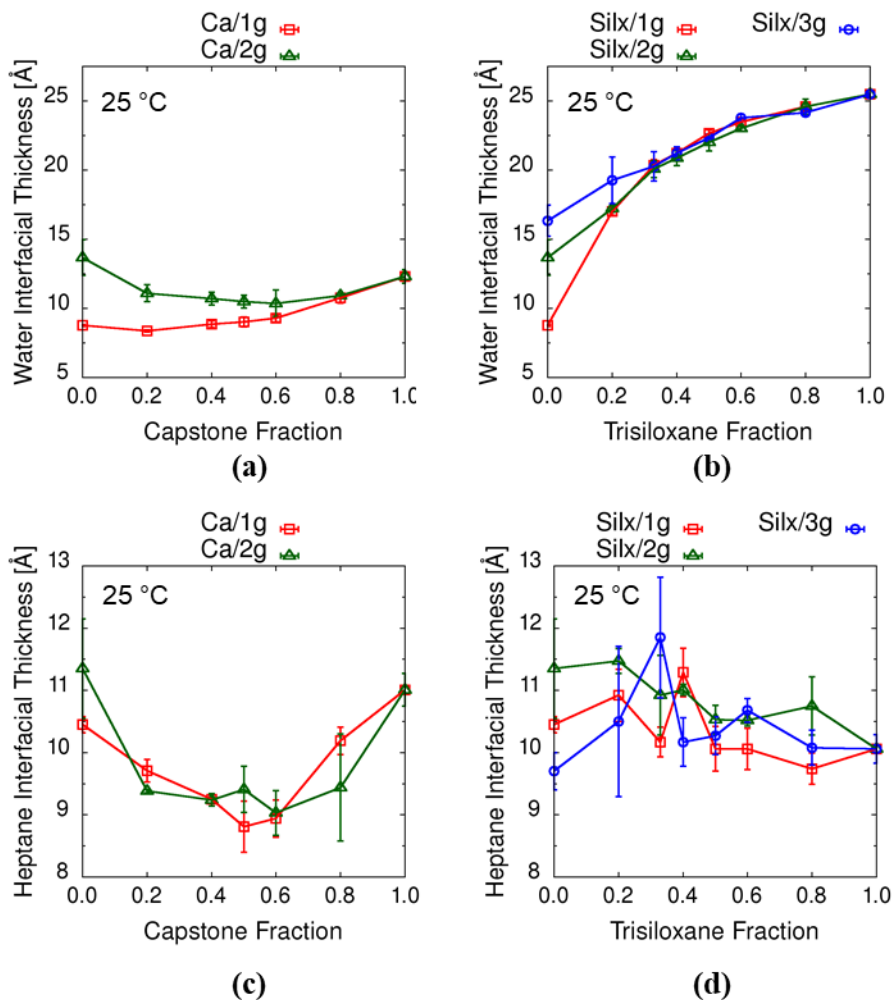


Fig. 35

The water interfacial thickness of (a) capstone/1g9 and capstone/2g9 and (b) trisiloxane/alkylglucoside (H10/1g9, H10/2g9, and H10/3g9) at 25°C as function of molecular fraction of capstone and H10, respectively. The heptane interfacial thickness of (c) capstone/1g and capstone/2g and (d) H10/1g9, H10/2g9 and H10/3g9 at 25°C as function of molecular fraction of capstone and H10, respectively.

#### 4.7.4 Heptane to Surfactant Ratio ( $hsr$ ) and Heptane Surface Number Density ( $hsnd$ )

The heptane to surfactant ratio ( $hsr$ ) of Ca/1g9 shows a minimum for  $f$  between 0.5 and 0.8 (**Fig. 36a**). The  $hsr$  of Ca/2g9 for  $f \geq 0.6$  is lower than  $f < 0.6$ . The  $hsr$  of trisiloxane/alkylglucoside increases as  $f$  increases. The  $hsr$  of H10/1g9 are lower than H10/2g9 and H10/3g9 (**Fig. 36b**). The heptane surface number density ( $hsnd$ ) of two-component capstone/alkylglucoside and trisiloxane/alkylglucoside systems at 25°C show similar trend as  $hsr$  (**Fig. A24**). The H10/1g9/2g9 shows a lower  $hsr$  and  $hsnd$  when  $f=0.4$  25°C, but increasing with  $f$  for 60°C. The  $hsr$  and  $hsnd$  of H10/1g9/2g9 is generally higher at 60°C than the values at 25°C (**Fig. A25**).

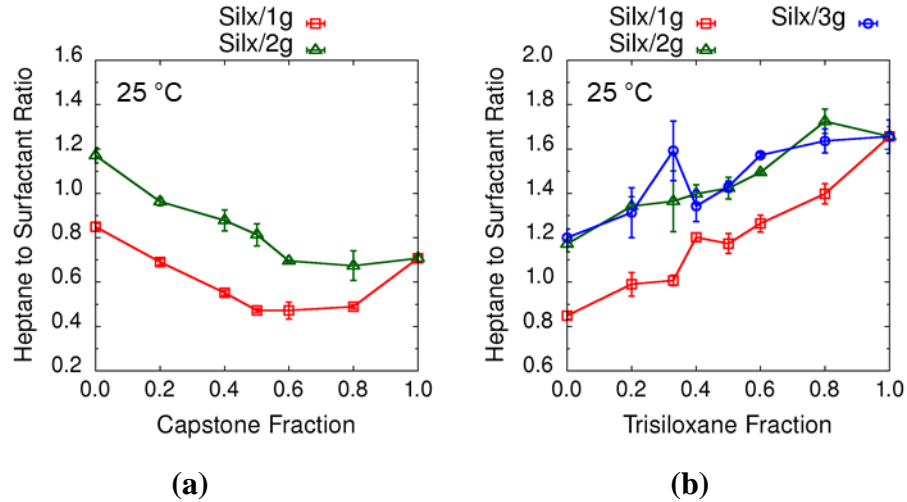


Fig. 36

The heptane to surfactant ratio of (a) capstone/1g9 and capstone/2g9 and (b) H10/1g9, H10/2g9, and H10/3g9 at 25°C as function of molecular fraction of capstone and H10, respectively.

#### 4.7.5 Volumetric Number Densities ( $msnd^{-1}$ and $hvnd$ )

As shown in **Fig. 37**, the inverse of the maximum surfactant number density ( $msnd^{-1}$ ) of Ca/1g9 and Ca/2g9 show a minimum at  $f=0.5$ . The  $msnd^{-1}$  of H10/1g9, H10/2g9 and H10/3g9 show a minimum at  $f=0.2$ . The heptane volumetric number density at  $msnd$  ( $hvnd$ ) of Ca/1g9 and Ca/2g9 decreases as  $f$  increases. The  $msnd^{-1}$  and  $hvnd$  of H10/1g9, H10/2g9 and H10/3g9 show a minimum at  $f=0.2$  or 0.33. For H10/1g9/2g9, the  $msnd^{-1}$  increases as  $f$  increases, while the  $hvnd$  show a minimum at  $f=0.4$  for 25°C and  $f=0.8$  for 60°C (**Fig. A26**).

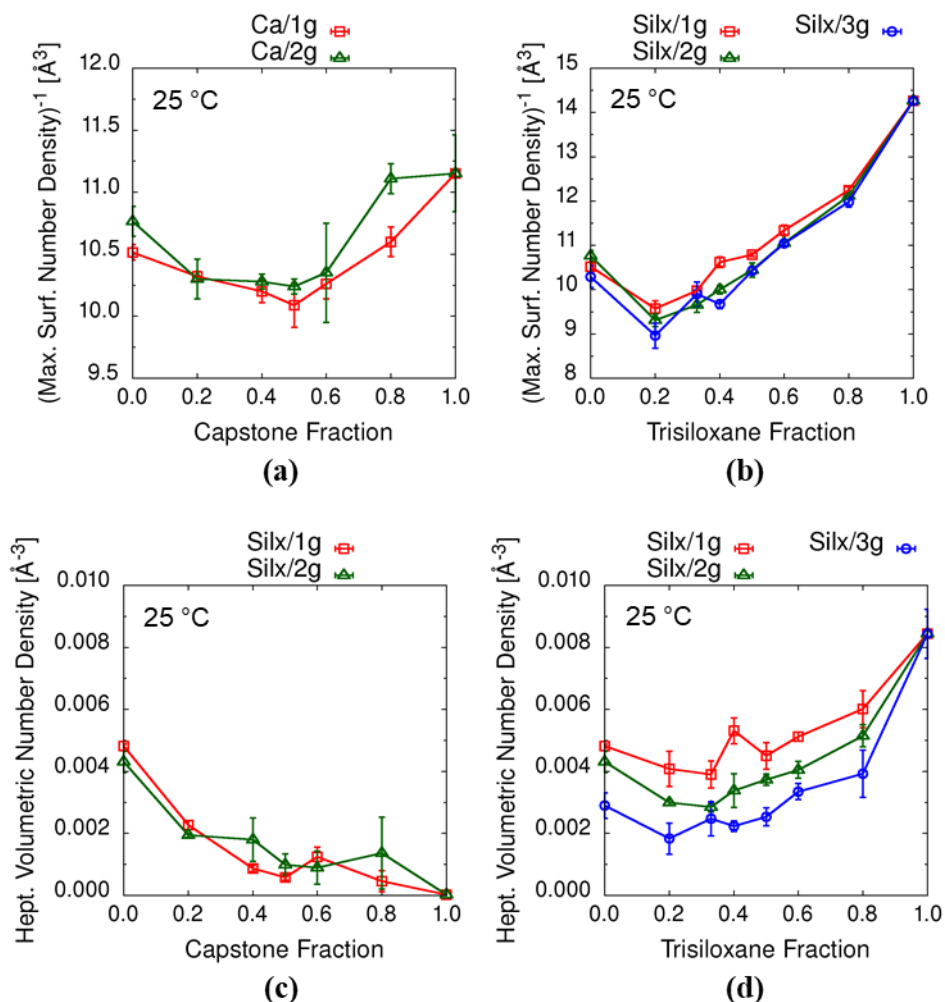


Fig. 37

The inverse of the maximum surfactant number density of (a) capstone/1g9 and capstone/2g9 and (b) H10/1g9, H10/2g9 and H10/3g9 at 25°C as function of molecular fraction of capstone and trisiloxane H10, respectively. The heptane volumetric number density at *msnd* of (c) capstone/1g and capstone/2g and (d) H10/1g9, H10/2g9 and H10/3g9 at 25°C as function of molecular fraction of capstone and H10, respectively.

#### 4.7.6 Intermolecular Hydrogen Bonds

The intermolecular hydrogen bond number per molecule (*hbnm*) and the hydrogen bond number per Å<sup>2</sup> (*hbna*) of Ca/1g9 show a maximum at capstone fraction  $f=0.2$ . The *hbnm* and *hbna* of Ca/2g9, H10/1g9, H10/2g9 and H10/3g9 decrease as  $f$  increase (Fig. 38, Fig. A27). Therefore, the Ca/g215 monolayer may be most stable at  $f=0.2$ . While as  $f$  increase, the stability of H10/g215 decreases.

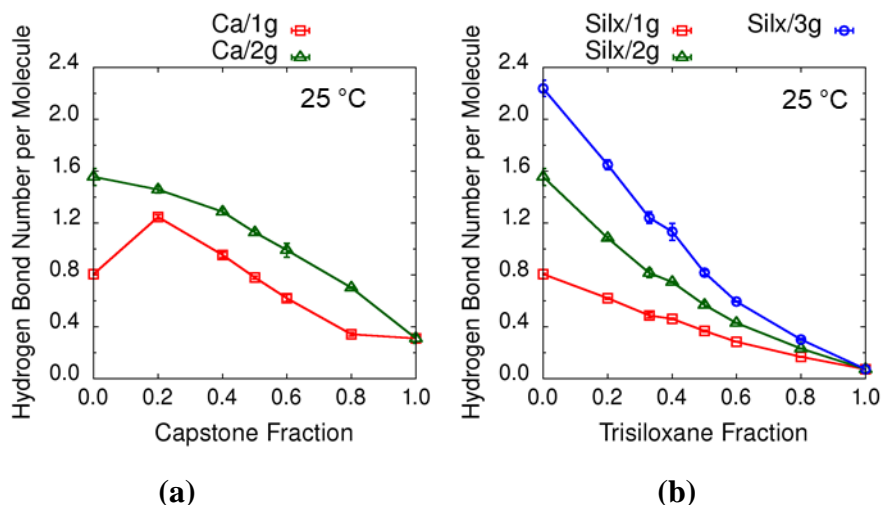


Fig. 38

Intermolecular hydrogen bond number per molecule of (a) capstone/1g9 and capstone/2g9 and (b) H10/1g9, H10/2g9 and H10/3g9 at 25°C as function of molecular fraction of capstone and H10, respectively.

## 4.8 Commercial Surfactants

### 4.8.1 Surfactant Chemical Structure

The perfluorocarbon surfactant pfoa and capstone (**Fig. 33**), polyoxyethylenated trisiloxane (**Fig. 2**), and alkylglucoside (**Fig. 2**) are simulated to mimic the commercial surfactants. The correlations of the commercial and simulated surfactant structures are shown **Table 1**. The M7 indicates the methoxyl-capped polyoxyethylenated trisiloxane with oxyethylene length of 7 ( $X=OCH_3$ ,  $n=7$ ). The H11 indicates the hydroxyl-capped polyoxyethylenated trisiloxane with oxyethylene length of 11 ( $X=OH$ ,  $n=11$ ). **Firstly**, the pure perfluorocarbon, trisiloxane and alkylglucoside surfactants are simulated. **Secondly**, Glucocon 215 is mimicked by simulate two-component 1g9 and 2g9 mixture with ratio 1g9:2g9=1:1, while Glucocon 225 is mimicked by simulate 1g9 and 2g9 mixture with ratio 1g9:2g9=3:7. The two-component capstone/1g9, capstone/2g9, trisiloxane/1g9 and trisiloxane/2g9 are also simulated. **Thirdly**, the three-component trisiloxane/1g9/2g9 (mimicking trisiloxane/g215 and trisiloxane/g225) are simulated.

Table 1. Commercial and the corresponding simulated surfactant nomenclatures. The oxyethylene lengths of commercial trisiloxane are based on experimental GPC data.

Commercial	Simulation
pfoa	pfoa
capstone	Ca
L77	M7
501w	M8
Gelest/SiH	H7
67A	H8
502w	H11

Gluc215	1g9:2g9=1:1
Gluc225	1g9:2g9=3:7

#### 4.8.2 Surface Area per Molecule (A)

As shown in **Fig.39a-b**, the pure capstone and 1g9 have lowest surface area per molecule (A). The pfoa (with 7 perfluorocarbon length) has greater A than capstone due to absence of hydrogen bonding in the head group (**Fig. 33**). The A of g215 is about the average of 1g9 and 2g9. The polyoxyethylenated trisiloxanes have much larger A than perfluorocarbon surfactants (pfoa and capstone) and alkylglucoside. For same oxyethylene length, the OCH<sub>3</sub>-capped trisiloxane (M7, M8) have slightly higher than OH-capped trisiloxane (H7, H8), respectively.

The two-component (trisiloxane/1g9 and trisiloxane/2g9) and three-component (trisiloxane/g215 and trisiloxane/g225) systems are simulated at 25°C and 60°C, while only two-component (Ca/1g9 and Ca/2g9) systems are simulated at 25°C. The Ca/g215e values are the pseudo three-component values estimated by averaging the two-component Ca/1g9 and Ca/2g9 values, as 1g9:2g9=1:1 for Glucopon 215. For comparison purpose, the H11/g215e values are also calculated to study the difference between true (H11/g215) and the pseudo (H11/g215e) three-component, in order to test the accuracy of Ca/g215e. The result shows that there is negligible difference between the A of H11/g215 and H11/g215e (**Fig.39c-d**).

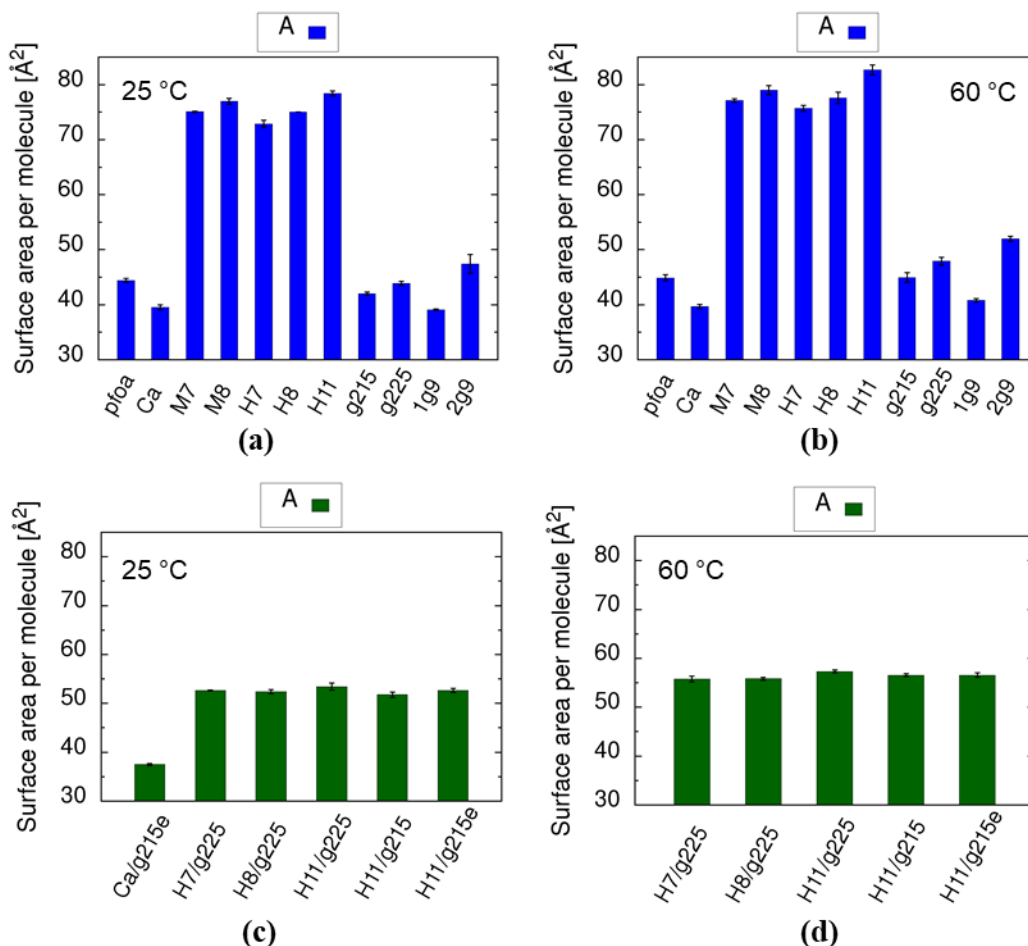


Fig. 39

The surface area per molecule of pure surfactant at (a) 25 °C and (b) 60 °C and surfactant with 1g9 and 2g9 as in Glucocon 225 and Glucocon 215 at (c) 25 °C and (d) 60 °C. The H11/g215e and Ca/g215e are the pseudo three-component values estimated by averaging the two-component H11/1g9 and H11/2g9 values, and Ca/1g9 and Ca/2g9 values, as 1g9:2g9=1:1 for Glucocon 215.

#### 4.8.3 Interfacial Thicknesses ( $d_w$ , $d_h$ )

As shown in **Fig. 40a-b**, for pure surfactant, the water interfacial thickness  $d_w$  of capstone is similar to g215 and g225, and it is better smaller than  $d_w$  of trisiloxanes (M7, M8, H7, H8, H11) as expected. When temperature changes from 25°C to 60°C, the  $d_w$  of fluorocarbon surfactants (pfoa, capstone), alkylglucoside hydrocarbon surfactants (g215, g225) slightly increase while the  $d_w$  of trisiloxanes slightly decrease. The variation of temperature has very small effect on  $d_w$ . When temperature changes from 25°C to 60°C, the  $d_h$  of fluorocarbon surfactants do not change, the  $d_h$  of hydrocarbon surfactants slightly increase (but the difference is within standard deviations), however, the  $d_h$  of trisiloxane surfactants increase significantly, which suggest that high temperature has more effect on the trisiloxane tails. For surfactant mixtures, the Ca/g215e has the smallest  $d_w$ ,  $d_h$ , and they are less than pure capstone and g215. Trisiloxane/alkylglucoside mixture show a similar trend as pure trisiloxane that the  $d_w$  slightly decrease while the  $d_h$  increase significantly (**Fig. 40c-d**).

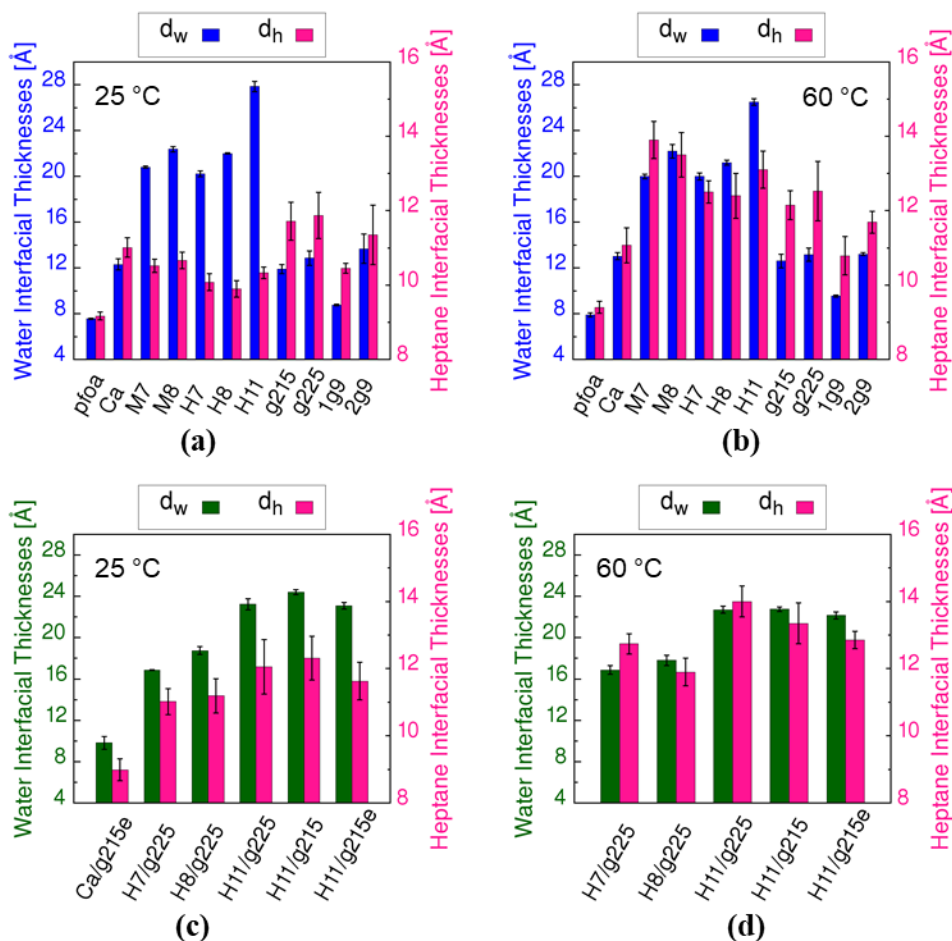


Fig. 40

The interfacial thickness of water and heptane of pure surfactant at (a) 25 °C and (b) 60 °C and surfactant with 1g9 and 2g9 as in Glucopton 225 at (c) 25 °C and (d) 60 °C. The H11/g215e and Ca/g215e are the pseudo three-component values estimated by averaging the two-component H11/1g9 and H11/2g9 values, and Ca/1g9 and Ca/2g9 values, as 1g9:2g9=1:1 for Glucopton 215.

#### 4.8.4 Heptane to Surfactant Ratio ( $hsr$ ) and Heptane Surface Number Density ( $hsnd$ )

As shown in **Fig. 41a-b**, for the heptane to surfactant ratio ( $hsr$ ), which is number of heptane per surfactant molecule, pfoa and capstone have smaller than alkylglucoside, and the trisiloxanes have the greatest  $hsr$ . The  $hsr$  of pure surfactants do not show temperature dependence. For the heptane surface number density ( $hsnd$ ), which is number of heptane per angstrom, pfoa and capstone are smallest, however, the  $hsnd$  of trisiloxane are smaller than alkylglucoside. The Ca/g215e has the smaller  $hsr$  and  $hsnd$  than trisiloxane/alkylglucoside. The mixture has much less  $hsr$  and slightly less  $hsnd$  than pure systems. The trisiloxane/alkylglucoside systems show higher temperature dependence than pure trisiloxane and pure alkylglucoside (**Fig. 41**).

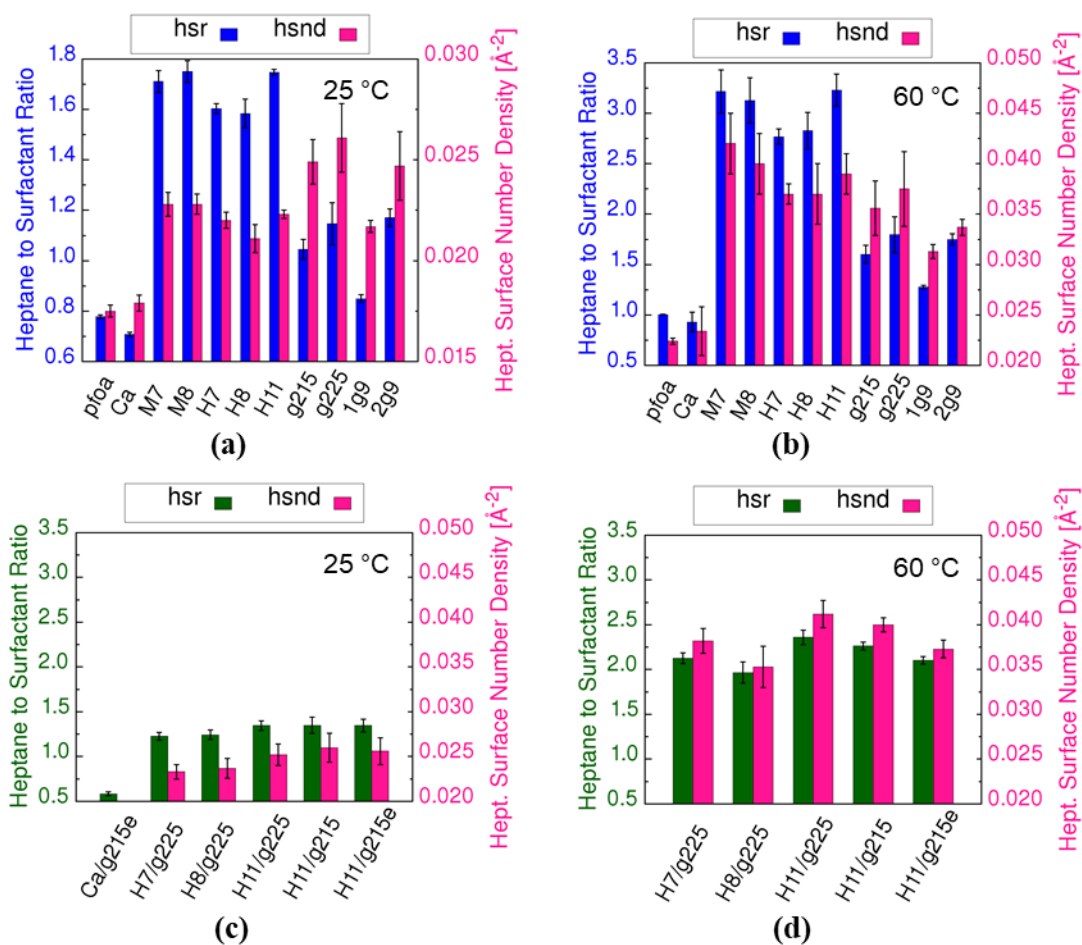


Fig. 41

The heptane to surfactant ratio and the heptane surface number density of pure surfactants at (a) 25 °C and (b) 60 °C and surfactant with 1g9 and 2g9 based on ratio in Glucocon 225 and 215 at (c) 25 °C and (d) 60 °C. The H11/g215e and Ca/g215e are the pseudo three-component values estimated by averaging the two-component H11/1g9 and H11/2g9 values, and Ca/1g9 and Ca/2g9 values, as 1g9:2g9=1:1 for Glucocon 215.

#### 4.8.5 Comparison of $msnd^{-1}$ and $hvnd$ to Experimental Heptane Diffusion Coefficient

The experimental heptane diffusion coefficient data in this report is for Glucocon 215 only. The simulated g215 is used when it is available, otherwise, the simulated g225 is used as the calculated heptane transport related properties ( $msnd^{-1}$  and  $hvnd$ ) of g215 and g225 are very similar as shown in **Fig. 42-43**.

The maximum surfactant number density ( $msnd$ ) describes the highest atomic number density of surfactant molecules in the monolayer, therefore the inverse of the maximum surfactant number density ( $msnd^{-1}$ ) describes the narrowest channel size in the monolayer, which is the upper limit that heptane molecule can pass through monolayer, and it is related to heptane transport rate. The heptane volumetric number density at  $msnd$  ( $hvnd$ ) is the heptane density at the narrowest channel. Both  $msnd^{-1}$  and  $hvnd$  may be related to the heptane transport rate. They are compared to

experimental heptane diffusion coefficient to have understand which properties describes heptane transport rate better.

For the surfactants with the same tail type, there is no preference on  $msnd^{-1}$  or  $hvnd$ . However, for surfactant with different tail type, the  $hvnd$  describe the heptane transport rate better than  $msnd^{-1}$ . For instance, as shown in **Fig. 42**, the capstone (Ca) has high  $msnd^{-1}$  and low  $hvnd$ , while g215 and g225 have low  $msnd^{-1}$  and high  $hvnd$ . We expect  $hvnd$  is more accurate because the  $msnd^{-1}$  does not include the lipophilicity of the surfactant tail. However, the tail hydrophobicity is demonstrated in  $hsr$ . Even though capstone has larger channel  $msnd^{-1}$ , the lipophobic perfluorocarbon tail repels the heptane away from the monolayer significantly decrease the source of the heptane that can be transport, i.e. lower  $hsr$ . The g215 and g225 with hydrophobic hydrocarbon tail attract heptane into the monolayer, which results in relatively high  $hsr$ . Based on our hypothesis, either low  $msnd^{-1}$  or low  $hsr$  is needed for low heptane transport rate, therefore, both capstone and Glucocon (g215, g225) have low heptane transport rate. The capstone have lower transport rate than Glucocon. Mover, the higher  $hsr$  of Glucocon results in lower stability than capstone.

The pfoa has much higher  $msnd^{-1}$  and  $hvnd$  than capstone, which suggest that the large and strong head group (due to hydrogen bonds) in the capstone is important to reduce the heptane transport (**Fig. 42**). There is no much difference between  $msnd^{-1}$  and  $hvnd$  of pure trisiloxanes, while the experimental heptane diffusion coefficient show clear difference. The experimental heptane diffusion coefficient of pure trisiloxane is not accurate which may be due to high heptane transport rate through foam affect the structure and stability of foam.

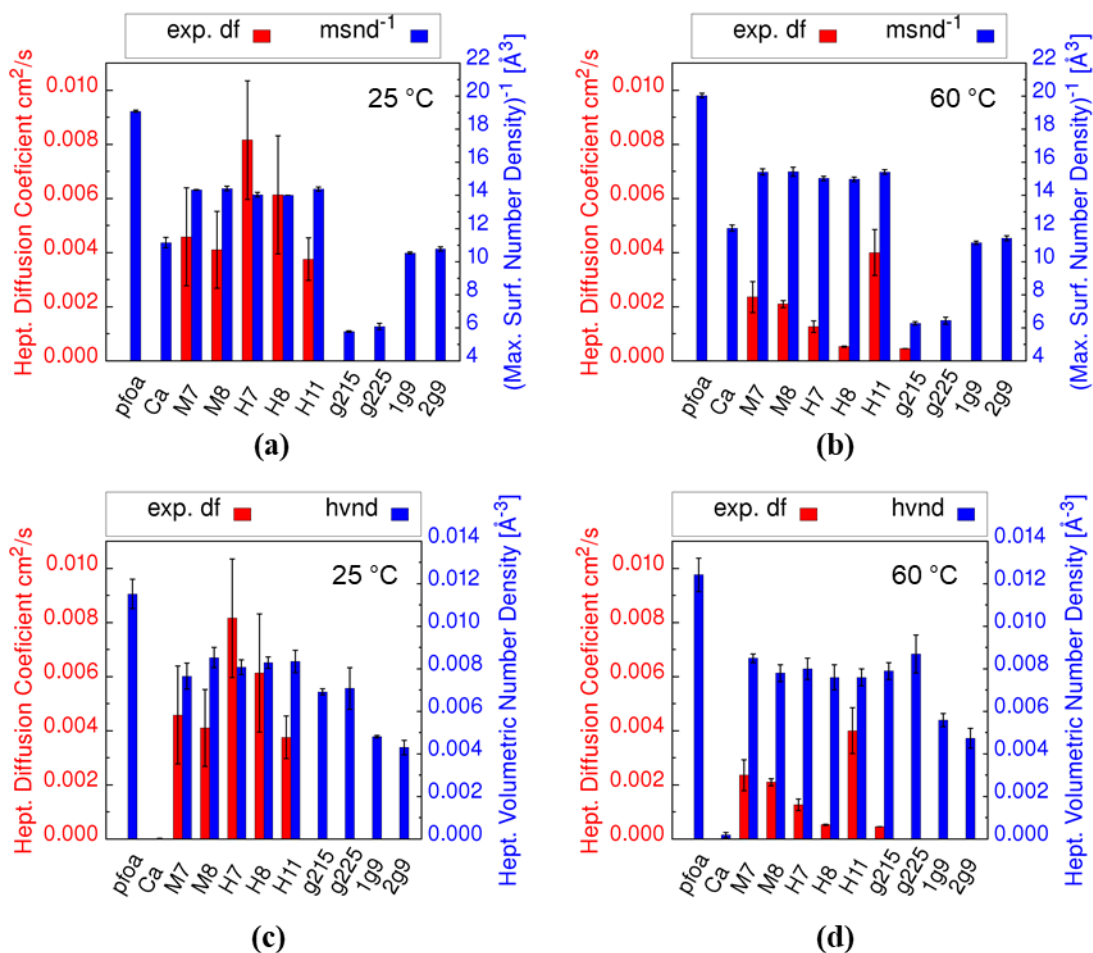


Fig. 42

Comparison of experimental diffusion coefficient data of surfactant with 1g9 and 2g9 based on ratio in Glucopton 225 and 215 to msnd<sup>-1</sup> at (a) 25 °C and (b) 60 °C and hvnd at (c) 25 °C and (d) 60 °C.

As shown in **Fig. 42-43**, as temperature changes 25°C from to 60°C, the msnd<sup>-1</sup> and hvnd of all pure and mixed surfactants increase slightly because agree with the slightly increasing surface area per molecule (**Fig. 39**) and increasing heptane interfacial thickness (**Fig. 40**). However, the experimental heptane diffusion coefficient of both pure and mixed trisiloxane/Glucopton decreases which suggests that the measurement is significantly by temperature, the dependence is much weaker for the mixture. The hvnd of H11/g225 and H11/g215 are slightly higher than H7/g225 and H8/g225, which agree with the trend in the experiment at 60°C (**Fig. 43d**). The g215 and g225 is stable in head group due to hydrogen bonding, but the tail is less stable due to high  $d_h$ , and intermediate  $hsr$ , but is has high hvnd thus high heptane transport rate.

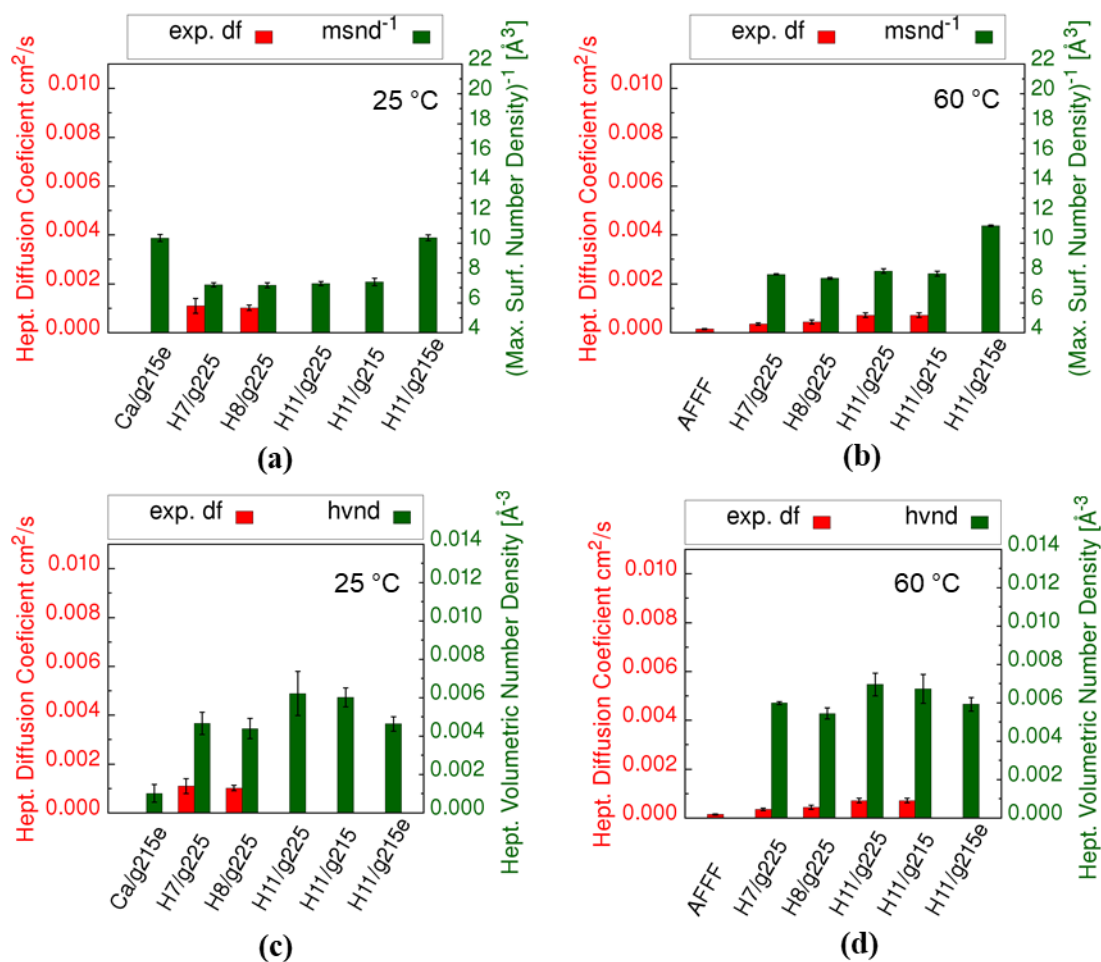


Fig. 43

Comparison of experimental diffusion coefficient data of surfactant with 1g9 and 2g9 based on ratio in Glucopon 225 and 215 to  $msnd^{-1}$  at (a) 25 °C and (b) 60 °C and  $hvnd$  at (c) 25 °C and (d) 60 °C. The H11/g215e and Ca/g215e are the pseudo three-component values estimated by averaging the two-component H11/1g9 and H11/2g9 values, and Ca/1g9 and Ca/2g9 values, as 1g9:2g9=1:1 for Glucopon 215.

#### 4.8.6 Comparison of Surfactants Packing

As shown in **Fig. 44** and **Fig. A28**, the packing of pure capstone is tightest and most ordered, and the 1g9 is packed tighter and more ordered than 2g9, while pure trisiloxane H10 has the loosest packing and it is much less ordered, which agree with the surface area per molecule  $A$  that the  $A$  of capstone is smallest, followed by 1g9 and 2g9, and trisiloxane H10 has the highest  $A$  (**Fig. 39**, **Fig. 3**). The pure capstone has the least penetration of heptane into the monolayer, followed by 1g9 and 2g9, while pure trisiloxane H10 has the most heptane penetration, which agree with  $hsr$  values shown in **Fig. 41a**. By mixing capstone with 1g9 with ratio 3:2, the Ca/1g9 and Ca/2g9 pack tighter and also have less heptane penetration than both pure capstone and 1g9. The packing of H10/1g9 and H10/2g9 and the heptane penetration is between pure H10 and 1g9, however, the heptane penetration is closer to 1g9 and 2g9, which agree with  $hsr$  values (**Fig. 41a**, **Fig. 6**).

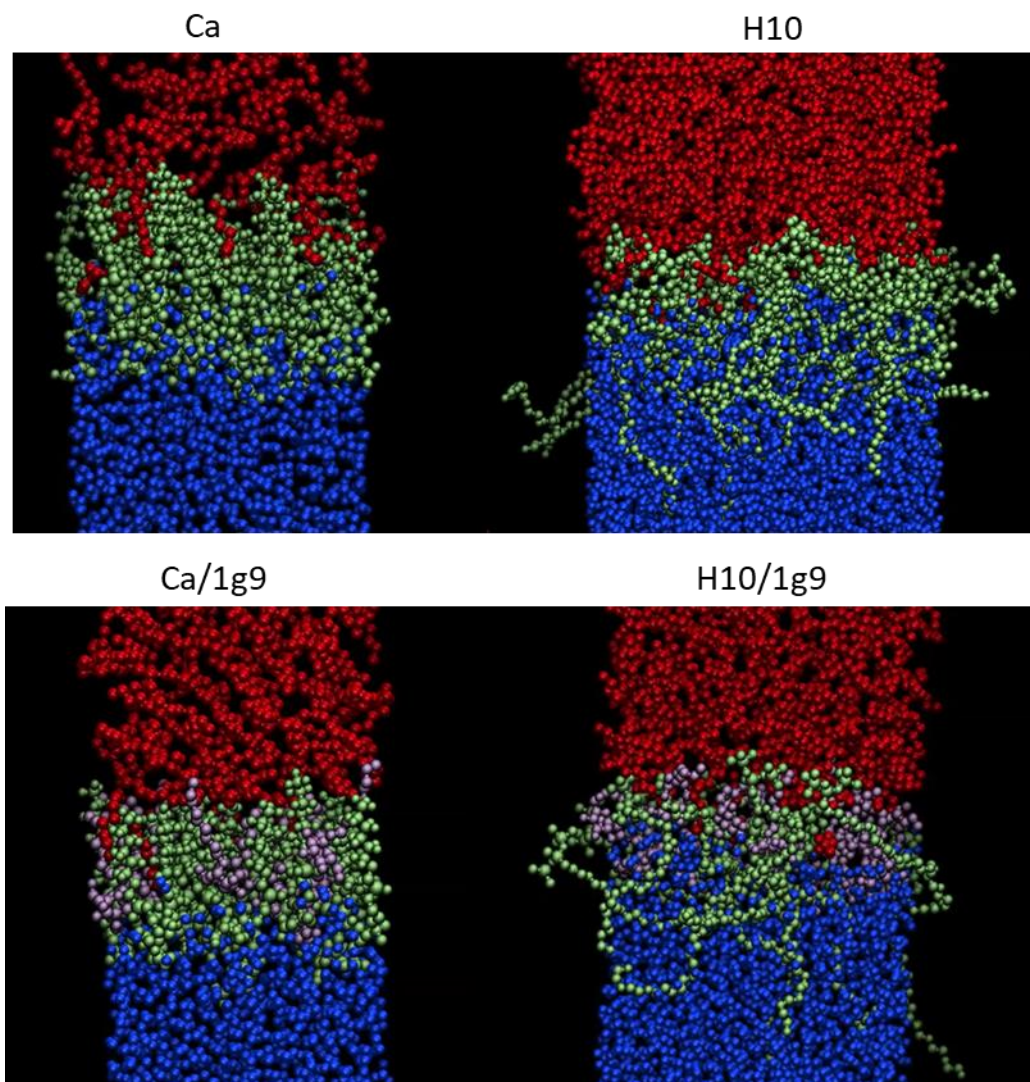


Fig. 44

The pure capstone, polyoxyethylenated trisiloxane H10 ( $X=OH$ ,  $n=10$ ), and two-component capstone/1g9 (with ratio 3:2), and H10/1g9 (with ratio 2:3) surfactant monolayer at the heptane/water interface system at the end of the MD simulations at 25 °C, respectively. (Water is shown in blue spheres, heptane is shown in red, capstone and trisiloxane surfactant are shown in green, and 1g9 is shown in pink spheres.) Only the top half in the  $z$  direction of the simulation setup are shown, the bottom half is a mirror image of top one.

## 5. CONCLUSION

For trisiloxane/1g9, trisiloxane/2g9, and trisiloxane/1g9/2g9, as trisiloxane oxyethylene length  $n$  increases, the surface area per molecule  $A$  increase and then level off when  $n \geq 8$ . The  $h_{sr}$  of the mixtures at  $n \leq 8$  are smaller than the ones at  $n \geq 9$ . The  $h_{vnd}$  of the mixtures increases dramatically

when  $n \geq 8$ . Therefore, to minimize fuel transport rate, the good trisiloxane candidate is to use  $n \leq 8$ . However, the  $hbnm$  of trisiloxane/2g9 are mostly higher when  $n \geq 13$ , which suggest that the monolayer may be more stable. Therefore, when using trisiloxane with single oxyethylene unit length, fuel transport rate and stability are trade off, and the optimization based on  $n$  is limited. One possible solution to mix the short and long oxyethylene length ( $n \leq 8$  and  $n \geq 13$ ).

By comparing the hydroxyl-capped (H) and methoxyl-capped (M) trisiloxane, the results show that hydroxyl-capped trisiloxane have smaller heptane interfacial thickness ( $d_h$ ), heptane to surfactant ratio ( $hsr$ ), and  $msnd^{-1}$  than and methoxyl-capped trisiloxane. Therefore, the hydroxyl-capped trisiloxane would be better choice.

For trisiloxane/alkylglucoside H11/1g and H11/2g, as alkyl glucoside hydrocarbon length  $n$  increases, the heptane surface number density  $hsnd$  for  $n \leq 6$  are greater than the values for  $n \geq 7$  and it shows a possible minimum at  $n$  around 8 for 25 °C. As the alkyl glucoside hydrocarbon length  $n$  increases, the maximum surfactants number density  $msnd$  increase first and then level off at  $n=9$ , and the heptane volumetric number density ( $hvnd$ ) at  $msnd$  decrease and level off as expected. The alkyl glucoside with hydrocarbon length  $n \geq 8$  have high  $hbnm$  and  $hbna$ , thus high monolayer stability. Therefore, the alkyl glucoside with hydrocarbon length  $n \geq 8$  would be better choice.

With the same hydrocarbon length, the  $\beta$ - and ( $\alpha, \beta-1 \rightarrow 4$ )alkyl glucoside (represented by  $mkn$ ) have significantly smaller surface area per molecule  $A$ , heptane to surfactant ratio  $hsr$ ,  $hvnd$  than the  $\alpha$ - and ( $\alpha, \alpha-1 \rightarrow 6$ )-alkylglucoside (represented by  $mgn$ ). Moreover, for  $mkn$ , the smaller hydrocarbon length have the slightly lower  $hsr$ , but also higher  $msnd^{-1}$  and  $hvnd$ . Therefore, intermediate value  $n=10$  may be best option.

Siloxane with 1g or  $cn$  head group with 3u or 6s tail have the smallest  $A$ . 1k3u have the smallest  $hsr$  and 2g3t have the smallest  $hsnd$  at 60 °C. 2k6s have the greatest  $msnd$ , followed by 2k3s and 2k3t at both 25 °C and 60 °C. 2k6s, 2k3s and 2k3t also have the smallest  $hvnd$ , which make these three surfactant good candidate surfactant to minimize heptane transport rate. The siloxane 2k6s have the greatest hydrogen bond number per molecule ( $hbnm$ ) and the hydrogen bond number per angstrom ( $hbna$ ), followed by 2k3s and 2k3t, which make them form more stable in the surfactant monolayer, and better surfactant candidate for fire suppression. (Or maybe we can try  $cn6s$ ,  $cn3u$  if it is feasible to prepare them experimentally).

The surfactants 1k10 and  $dmg$  have the smaller  $hsr$ , smaller  $hsnd$  than the rest surfactants. The 2k10 and 2k12 have much greater  $msnd$ , and much smaller  $hvnd$  than the charged hydrocarbon surfactants s310, lau, s312, sds, and dtab, which may suggest a neutral charged hydrocarbon surfactants have lower heptane transport rate than that of the charged ones.

By comparing the interfacial properties with varied capstone or trisiloxane H10 to alkylglucoside (1g9, 2g9) fraction, we conclude that capstone/alkylglucoside has minimum  $d_h$  and minimum  $msnd^{-1}$  when capstone fraction  $f=0.5$ , and capstone/1g9 has maximum  $hbnm$  when  $f=0.2$ . The H10/alkylglucoside has minimum  $msnd^{-1}$  when trisiloxane H10 fraction  $f=0.2$ .

By studying the commercial surfactants, we conclude that two Glucocon-based hydrocarbon surfactants (g215 and g225) have very similar interface properties. Among the commercial surfactant, capstone and capstone/g215e have the minimum  $hvnd$  which agree with the experimental heptane diffusion rate of AFFF. Among the pure trisiloxane and trisiloxane/alkylglucoside studied, the H8 and H8/g225 have the minimum  $d_h$ ,  $hsr$  and also  $msnd^{-1}$

<sup>1</sup> and *hvnd*, which agree with the experimental results that pure H8 has the minimum heptane diffusion coefficient.

## 6. FUTURE WORK

The surfactant in the monolayer forms are studied here. The solubility of the free surfactants that our lab mates concern is beyond the scope of the MD simulation on the interface. We present many results on the effect of the surfactant structures on the monolayer properties. If it is possible, I hope that there will be more available experimental data in the future to test the results mentioned here.

## 7. ACKNOWLEDGEMENTS

We would like to thank the Strategic Environmental Research and Development Program (SERDP) of the U.S. Department of Defense (DoD) for supporting this work via grants WP2739 and WP18-1592. We also would like to thank the US Office of Naval Research for funding this work through the Naval Research Laboratory Base Program. We would like to thank the DoD for providing High Performance Computational resources; the simulations were performed on Thunder clusters of Air Force Research Laboratory (AFRL) DoD Supercomputing Resource Center. We also would like to thank our teammate Arthur Snow and Nickolaus Weise for performing the GPC measurement to determine the oxyethylene length of the commercial trisiloxane, and Katherine M. Hinnant for measuring and providing the experimental data of the heptane diffusion coefficient.

## 8. PERSONNEL

Xiaohong Zhuang<sup>1,2</sup>, and Ramagopal Ananth<sup>2</sup>

<sup>1</sup>American Society for Engineering Education Postdoctoral Associate

<sup>2</sup>Chemistry Division, U.S. Naval Research Laboratory, Washington, DC 20375, United States

## 9. REFERENCES

- [1] S. Achilefu, C. Selve, M.J. Stebe, J.C. Ravey, J.J. Delpuech, Monodisperse perfluoroalkyl oxyethylene nonionic surfactants with methoxy capping - synthesis and phase-behavior of water surfactant binary-systems, *Langmuir*, 10 (1994) 2131-2138.
- [2] L. Hsiao, H.N. Dunning, P.B. Lorenz, Critical micelle concentrations of polyoxyethylated non-ionic detergents, *Journal of Physical Chemistry*, 60 (1956) 657-660.
- [3] M.J. Rosen, A.W. Cohen, M. Dahanayake, X.Y. Hua, Relationship of structure to properties in surfactants .10. Surface and thermodynamic properties of "2-dodecyloxypoly(ethenoxyethanol)s, C12H25(OC2H4)xOH, in aqueous-solution, *Journal of Physical Chemistry*, 86 (1982) 541-545.

## 10. APPENDIX A

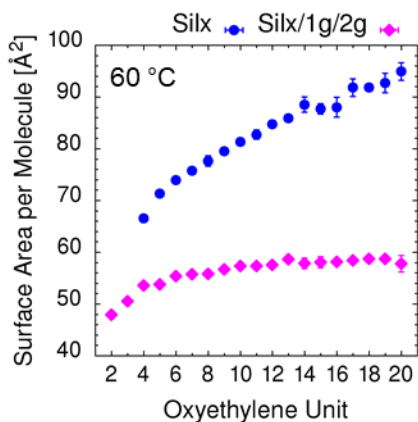


**Fig. A1.** The surface area per molecule of pure trisiloxane and trisiloxane/1g9/2g9 at the heptane/surfactant-monolayer/water interface at 60 °C as function of trisiloxane oxyethylene length.

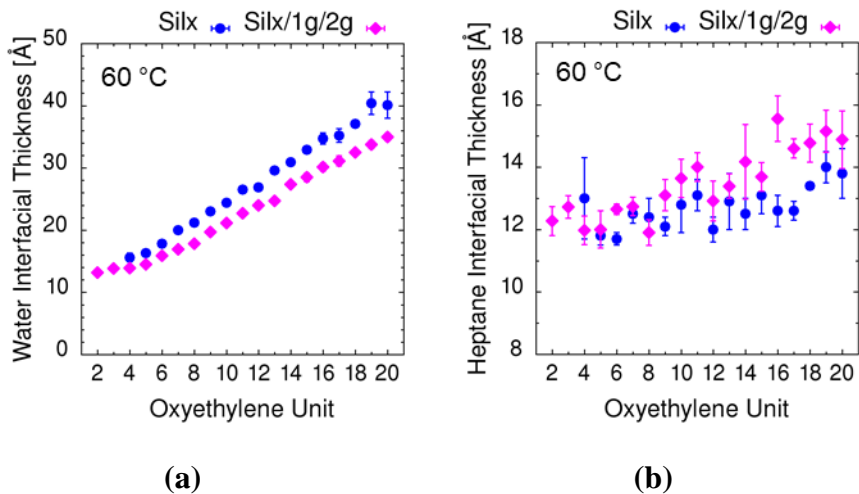
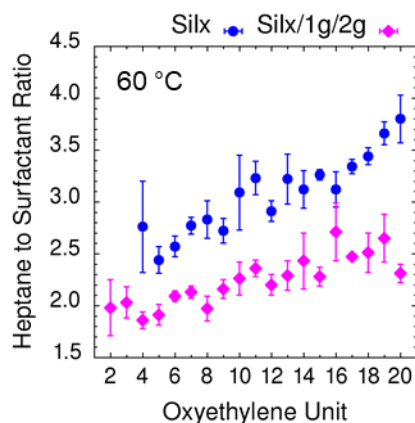
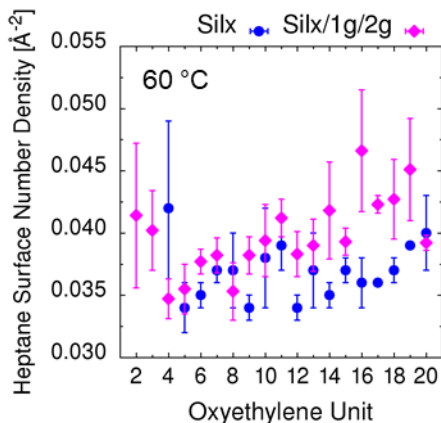


**Fig. A2.** The interfacial thickness of (a) water (b) heptane of pure trisiloxane and trisiloxane/1g9/2g9 at the heptane/surfactant-monolayer/water interface at 60 °C as function of trisiloxane oxyethylene length.

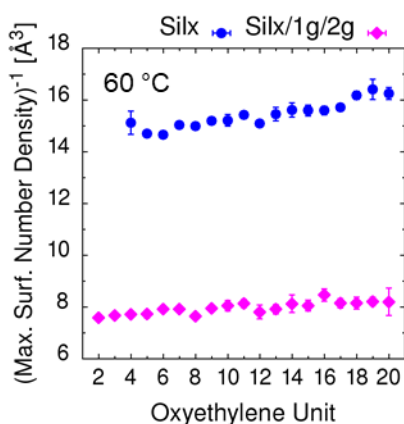


(a)

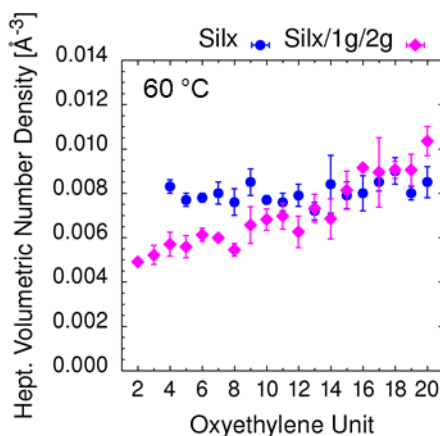


(b)

**Fig. A3** (a) Heptane to surfactant ratio and (b) the heptane surface number density at 60 °C as function of trisiloxane oxyethylene length.



(a)



(b)

**Fig. A4** (a) Inverse of maximum surfactant volumetric number density ( $msnd^{-1}$ ) (b) the heptane volumetric number density ( $hvnd$ ) at maximum surfactant number density at 60 °C as function of trisiloxane oxyethylene length.

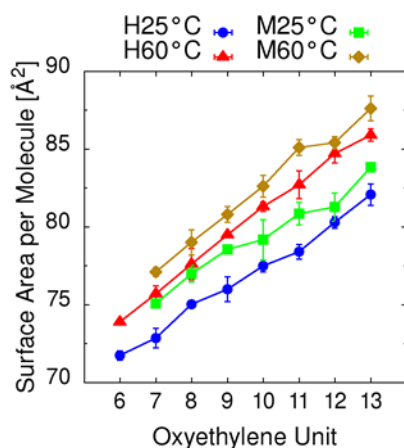


**Fig. A5** The surface area per molecule of pure hydroxyl-capped (H) and methoxyl-capped (M) polyoxyethylenated trisiloxanes at 25 °C and 60 °C as function of trisiloxane oxyethylene length.

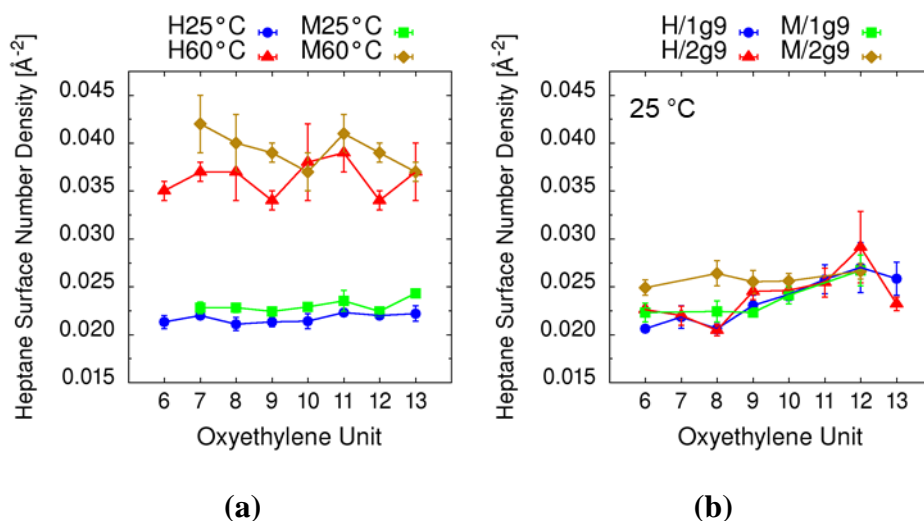


**Fig. A6** The heptane surface number density of (a) pure hydroxyl-capped (H) and methoxyl-capped (M) trisiloxane at 25 °C and 60 °C and (b) trisiloxane/1g9 and trisiloxane/2g9 at 25 °C as function of trisiloxane oxyethylene length.

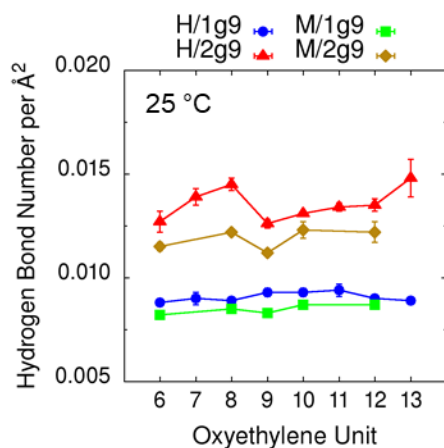


**Fig. A7** Intermolecular hydrogen bond number per molecule of hydroxyl-capped (H) trisiloxane/alkylglucoside and methoxyl-capped (M) trisiloxane/alkylglucoside at 25 °C as function of trisiloxane oxyethylene length.

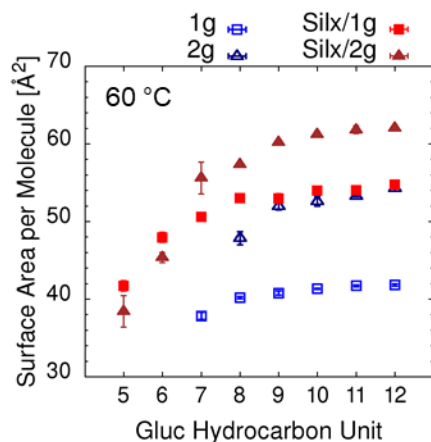


**Fig. A8** The surface area per molecule of pure alkylglucoside, trisiloxane/alkylglucoside (H11/1g and H11/2g) at the heptane/surfactant-monolayer/water interface at 60 °C as function of alkylglucoside hydrocarbon ( $\text{CH}_2$ ) length.

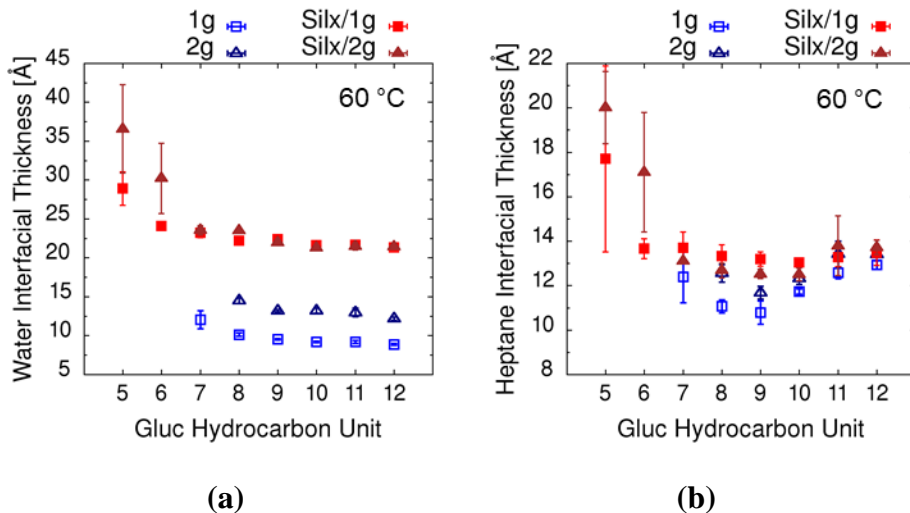


**Fig. A9** (a) The interfacial thickness trisiloxane/alkylglucoside (H11/1g and H11/2g) at the heptane/surfactant-monolayer/water interface at 60 °C as function of alkyl glucoside hydrocarbon length.

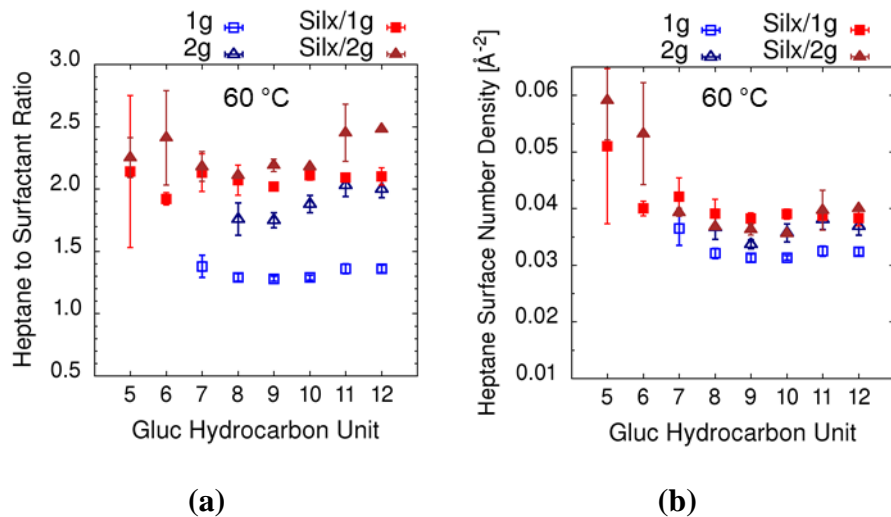


**Fig. A10** (a) Heptane to surfactant ratio and (b) The heptane surface number density of pure glucoside, trisiloxane/alkylglucoside (H11/1g and H11/2g) at 60 °C as function of alkyl glucoside hydrocarbon length.

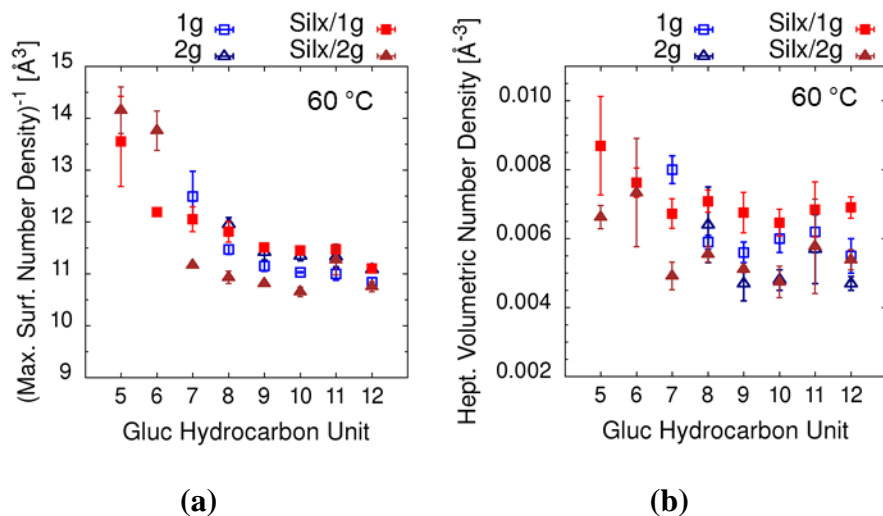


**Fig. A11** (a) Inverse of the maximum surfactant volumetric number density and (b) heptane volumetric number density at maximum surfactant number density of pure glucoside, trisiloxane/alkylglucoside (H11/1g and H11/2g) at 60 °C as function of alkyl glucoside hydrocarbon length.

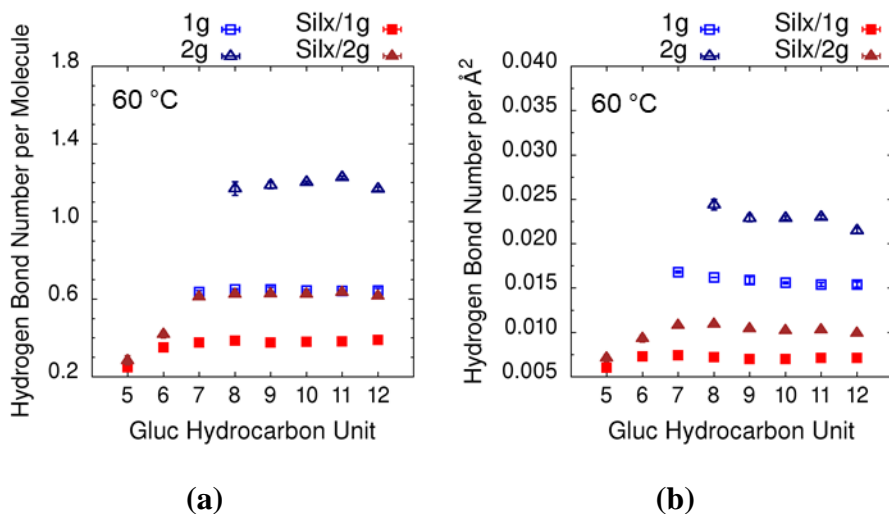


**Fig. A12** (a) Intermolecular hydrogen bond number per molecule and (b) Intermolecular hydrogen bond number per angstrom of pure glucoside, trisiloxane/alkylglucoside (H11/1g and H11/2g) at 60 °C as function of alkyl glucoside hydrocarbon length.

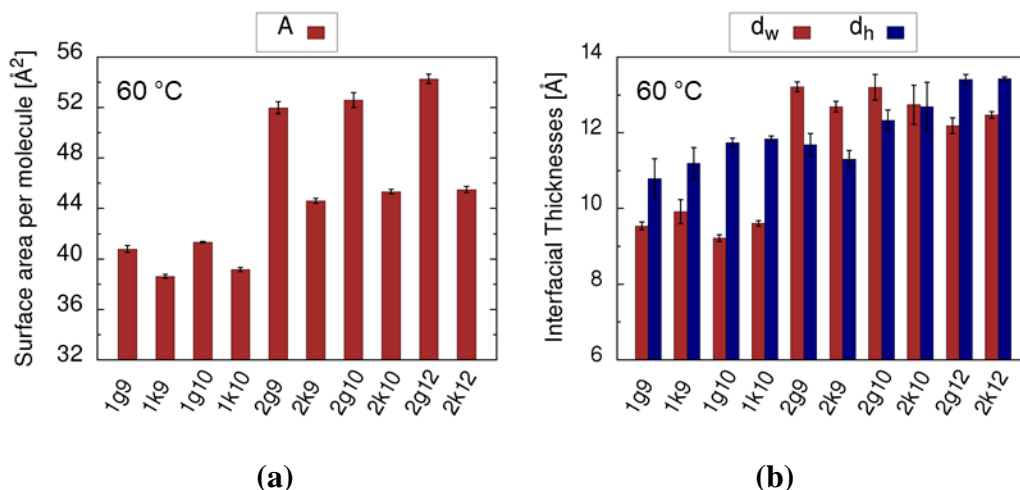


**Fig. A13** (a) The surface area per molecule and (b) the interfacial thickness of water and heptane of the pure  $\alpha$ - and  $(\alpha, \alpha-1 \rightarrow 6)$ -alkylglucoside (represented by  $mgn$ ) and the  $\beta$ - and  $(\alpha, \beta-1 \rightarrow 4)$ -alkylglucoside (represented by  $mkn$ ) with varied hydrocarbon length at 60 °C, respectively.

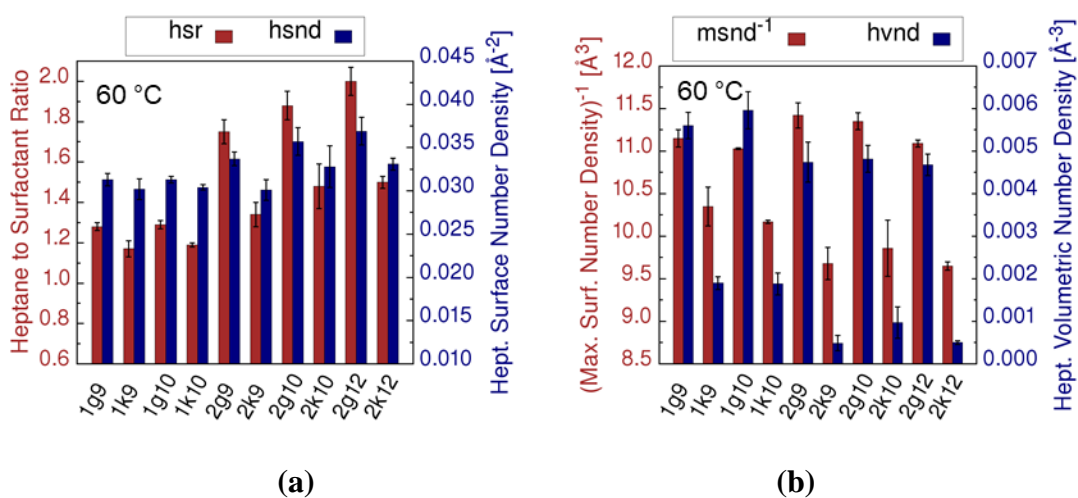


**Fig. A14** (a) Heptane to surfactant ratio and the heptane surface number density and (b) inverse of maximum surfactant volumetric number density and heptane volumetric number density at maximum surfactant number density of the pure  $\alpha$ - and  $(\alpha, \alpha-1 \rightarrow 6)$ -alkylglucoside (represented by  $mgn$ ) and the  $\beta$ - and  $(\alpha, \beta-1 \rightarrow 4)$ -alkylglucoside (represented by  $mkn$ ) with varied hydrocarbon length at 60 °C, respectively.

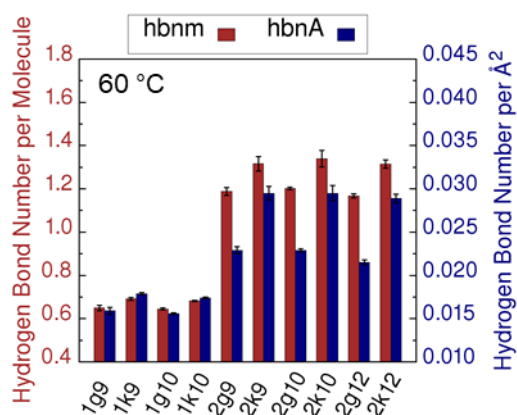


**Fig. A15** Intermolecular hydrogen bond number per molecule and hydrogen bond number per Å<sup>2</sup> of varied types of the pure  $\alpha$ - and ( $\alpha,\alpha$ -1 $\rightarrow$ 6)-alkylglucoside (represented by *mgn*) and the  $\beta$ - and ( $\alpha,\beta$ -1 $\rightarrow$ 4)-alkylglucoside (represented by *mkn*) with varied hydrocarbon length at 60 °C.

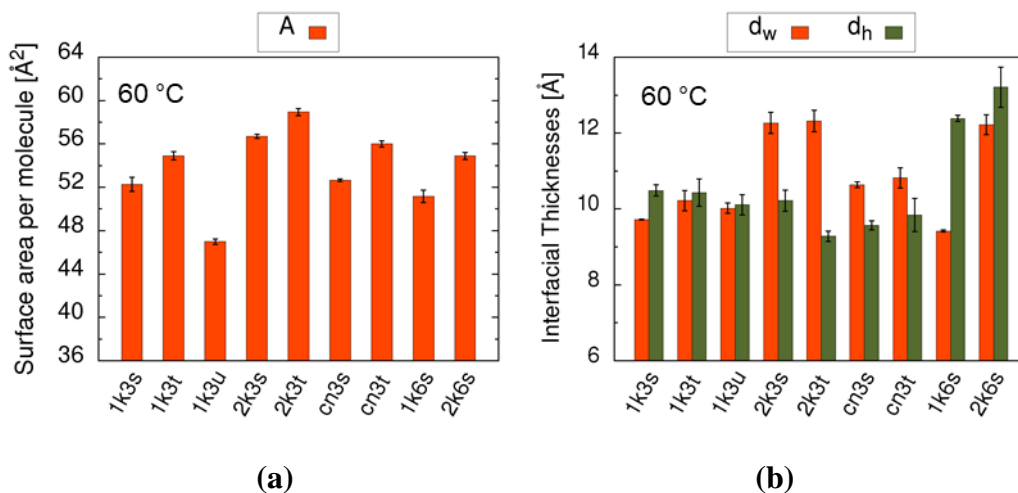


**Fig. A16** (a) The surface area per molecule and (b) the interfacial thickness of water and heptane of varied types of siloxane surfactant at the heptane/surfactant-monolayer/water interface at 60 °C, respectively.

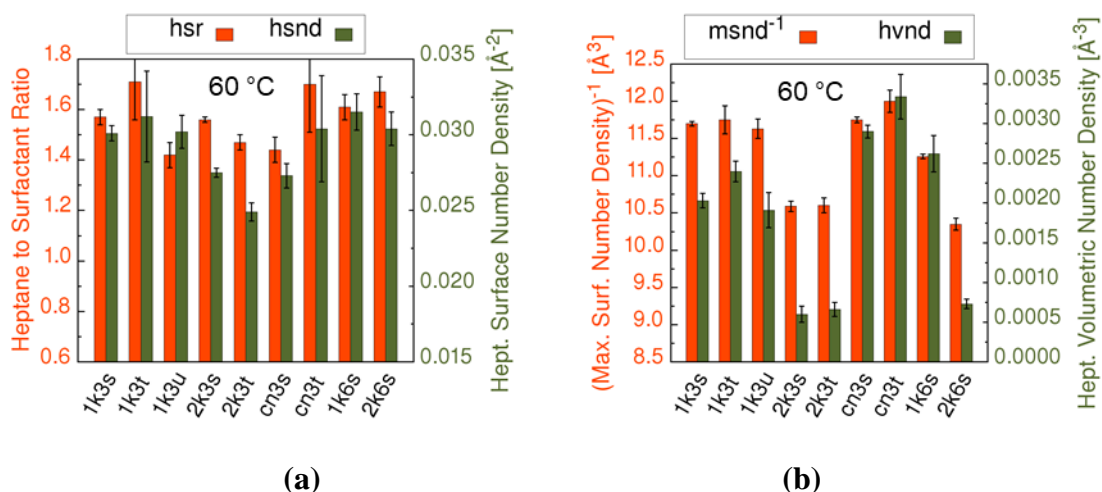


**Fig. A17** (a) Heptane to surfactant ratio in the interface and the heptane surface number density and (b) inverse of the maximum surfactant volumetric number density and heptane volumetric number density at maximum surfactant number density of varied types of siloxane surfactant at 60 °C.

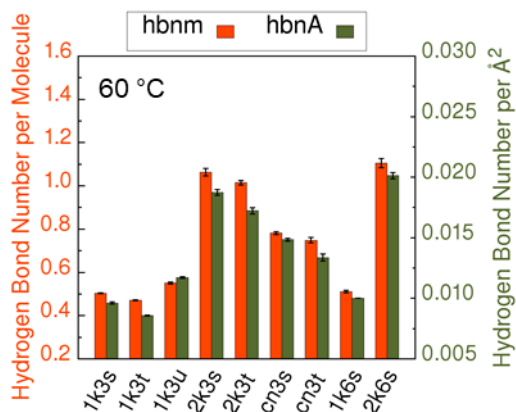


**Fig. A18** Intermolecular hydrogen bond number per angstrom of varied types of siloxane surfactant at the heptane/surfactant-monolayer/water interface at 60 °C.

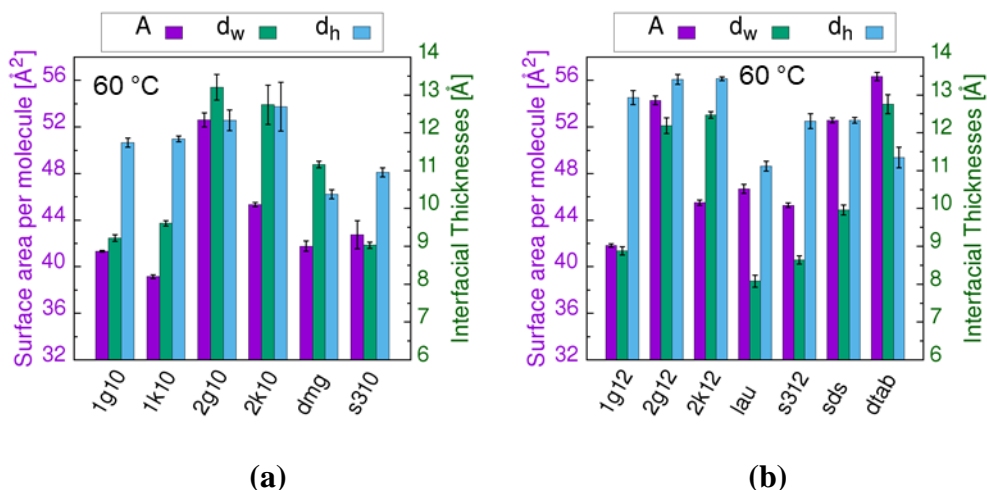


**Fig. A19** The surface area per molecule and the interfacial thickness of water and heptane of varied type of hydrocarbon surfactant with length (a) 10 and (b) 12 at the heptane/surfactant-monolayer/water interface at 60 °C, respectively.

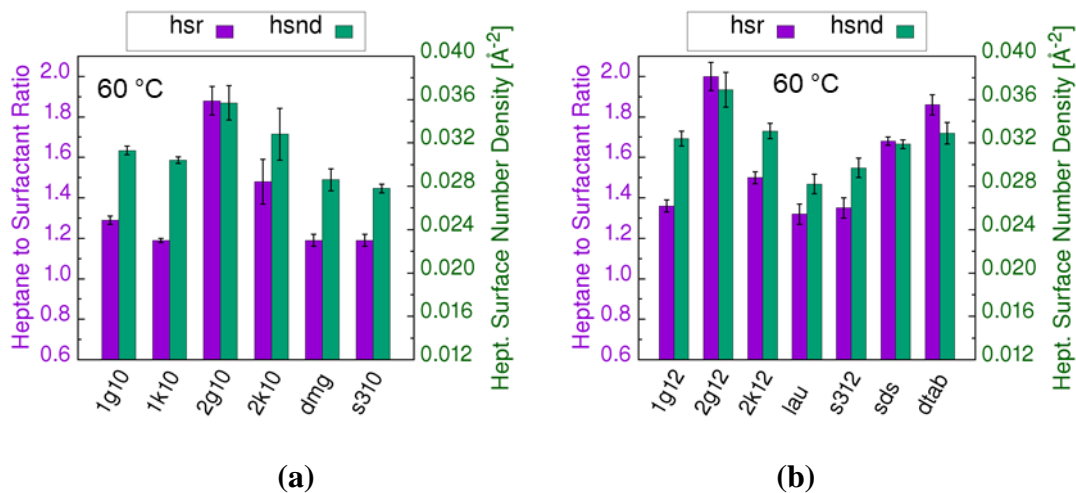


**Fig. A20** Heptane to surfactant ratio in the interface and the heptane surface number density of varied type of hydrocarbon surfactant with length (a) 10 and (b) 12 at 60 °C.

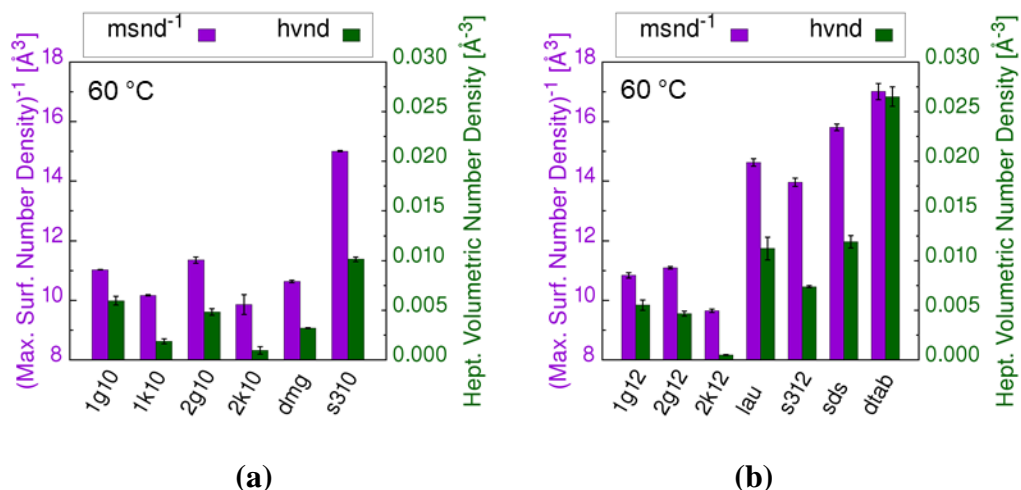


**Fig. A21** Inverse of the maximum surfactant volumetric number density ( $msnd^{-1}$ ) and heptane volumetric number density at maximum surfactant number density ( $hvnd$ ) of varied type of hydrocarbon surfactant with length (a) 10 and (b) 12 at 60 °C.

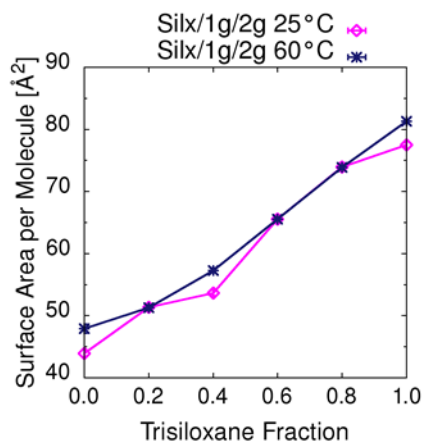


**Fig. A22** Surface area per molecule of H10/1g9/2g9 (1g9:2g9=3:7 mimicking Glucopton 225, i.e. H10/g225) at 25 °C and 60 °C as function of molecular fraction of H10.

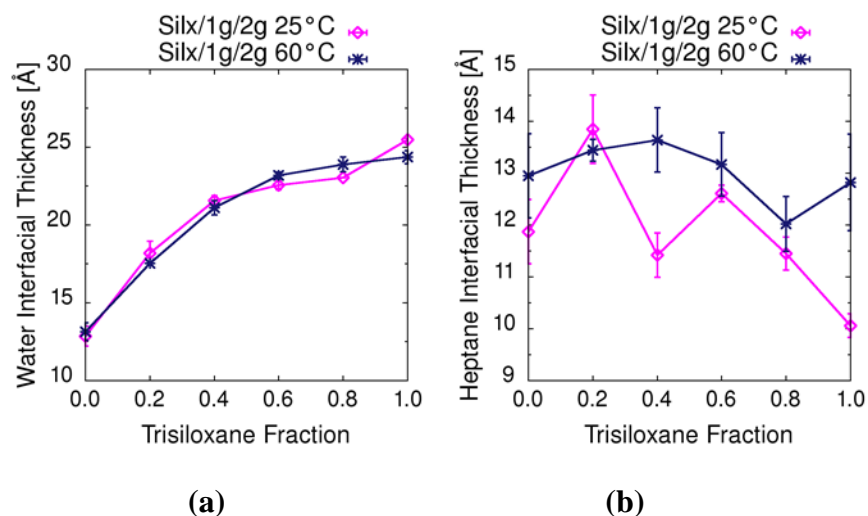


**Fig. A23** (a) Water interfacial thicknesses and (b) heptane interfacial thickness of H10/1g9/2g9 (1g9:2g9=3:7 mimicking Glucopon 225, i.e. H10/g225) at 25°C and 60°C as function of molecular fraction of H10.

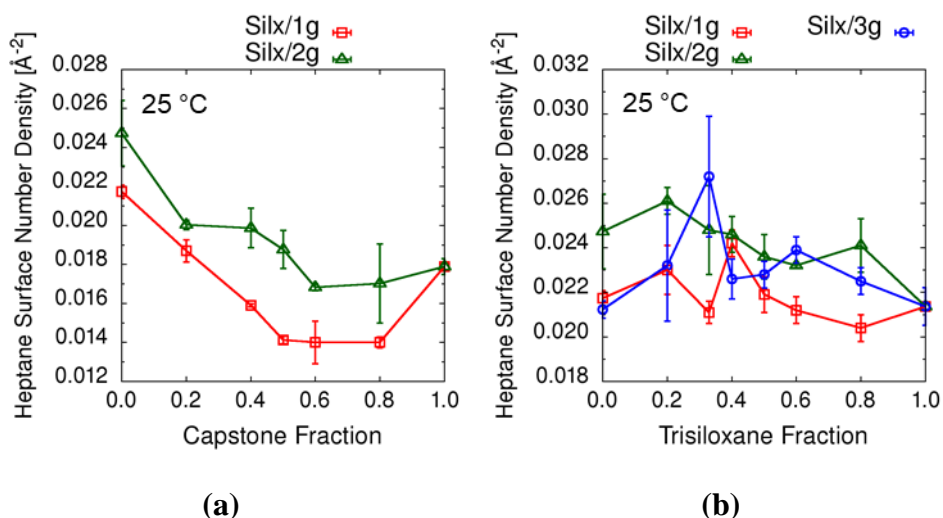


**Fig. A24** The heptane surface number density of (a) capstone/1g9 and capstone/2g9 and (b) trisiloxane/alkylglucoside (H10/1g9, H10/2g9, and H10/3g9) at 25°C as function of molecular fraction of capstone and H10, respectively.

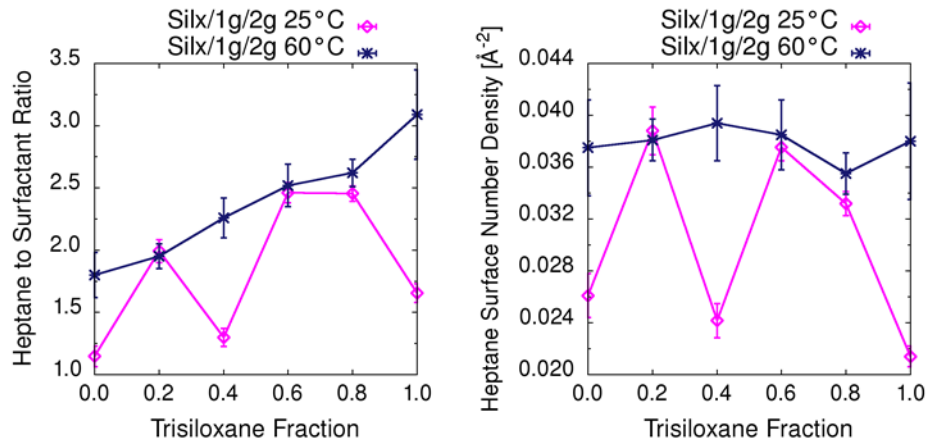


**Fig. A25** Heptane to surfactant ratio (*hsr*) and heptane surface number density (*hsnd*) of H10/1g9/2g9 (1g9:2g9=3:7 mimicking Glucocon 225, i.e. H10/g225) at 25°C and 60°C as function of molecular fraction of H10.

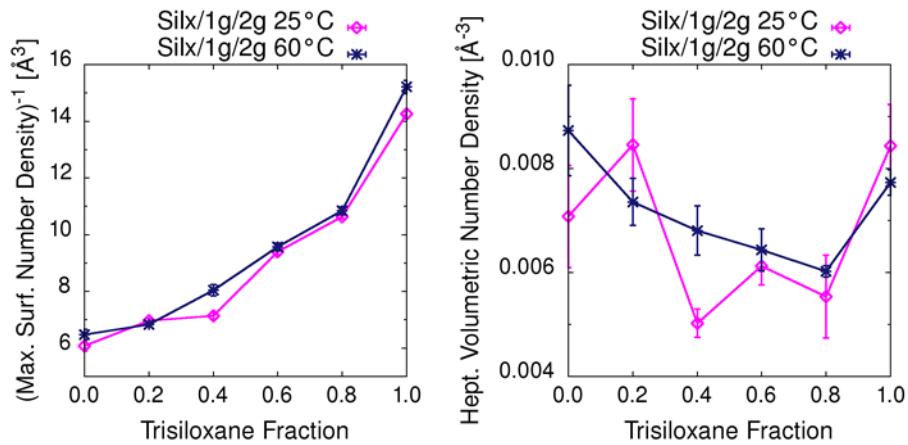


**Fig. A26** Inverse of the maximum surfactant volumetric number density ( $msnd^{-1}$ ) and heptane volumetric number density ( $hvnd$ ) of H10/1g9/2g9 (1g9:2g9=3:7 mimicking Glucocon 225, i.e. H10/g225) at 25°C and 60°C as function of molecular fraction of H10.

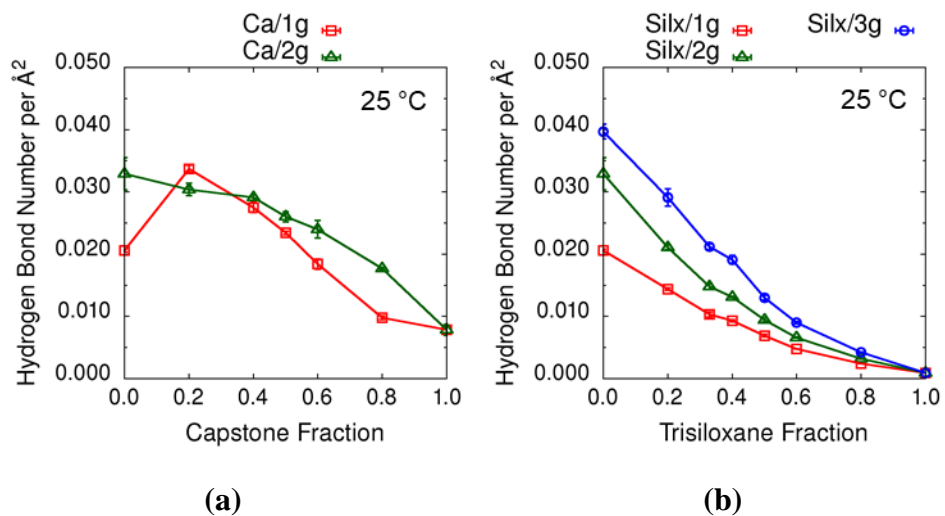


**Fig. A27** Intermolecular hydrogen bond number per angstrom of (a) capstone/1g<sup>9</sup> and capstone/2g<sup>9</sup> and (b) H10/1g<sup>9</sup>, H10/2g<sup>9</sup> and H10/3g<sup>9</sup> at 25 °C as function of molecular fraction of capstone and H10, respectively.

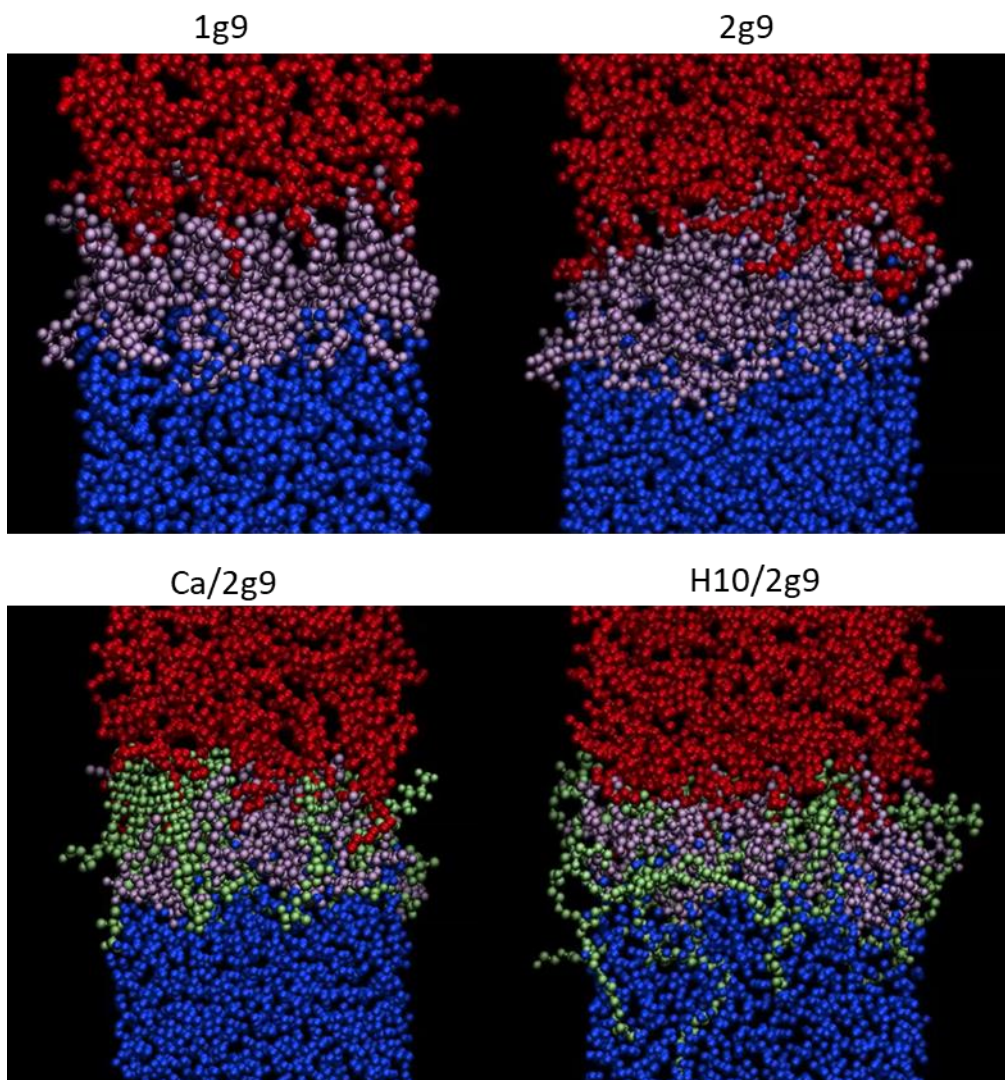


**Fig. A28** The pure alkyl glucoside 1g9 and 2g9 , and two-component capstone/2g9 (with ratio 3:2), and H10/2g9 (with ratio 2:3) surfactant monolayer at the heptane/water interface system at the end of the MD simulations, respectively. (Water is shown in blue spheres, heptane is shown in red, capstone and trisiloxane surfactant are shown in green, and 1g9 and 2g9 is shown in pink spheres.) Only the top half in the  $z$  direction of the simulation setup are shown, the bottom half is a mirror image of top one.